

University of Alberta

The role of genetically defined lamina VII spinal interneurons in generating the locomotor rhythm

by

Jason Dyck

A thesis submitted to the Faculty of Graduate Studies and Research
in partial fulfillment of the requirements for the degree of

Doctor of Philosophy

Centre for Neuroscience

©Jason Dyck
Fall 2011
Edmonton, Alberta

Permission is hereby granted to the University of Alberta Libraries to reproduce single copies of this thesis and to lend or sell such copies for private, scholarly or scientific research purposes only. Where the thesis is converted to, or otherwise made available in digital form, the University of Alberta will advise potential users of the thesis of these terms.

The author reserves all other publication and other rights in association with the copyright in the thesis and, except as herein before provided, neither the thesis nor any substantial portion thereof may be printed or otherwise reproduced in any material form whatsoever without the author's prior written permission.

ABSTRACT

Locomotor activity in mammals is generated by neural networks known as central pattern generators (CPGs), which are comprised of interneurons located in the ventral regions of the spinal cord. Recently, molecular genetic characterization of transcription factor expression at early embryonic time points has led to the identification of a handful of genetically-distinct interneuronal populations in the central nervous system. This work has provided valuable insight into the structure and mechanism of function of the locomotor CPG. Of particular interest is the dI6 interneuronal population. These cells originate in the dorsal neural tube, but migrate ventrally during embryogenesis to reside in lamina VII of the postnatal spinal cord. Although it has been suggested that these cells are functionally similar to the neighbouring V0 population and play a role in coordinating left-right alternation during locomotion, dI6 cells have not been physiologically characterized, and as such their role in the locomotor CPG is currently unknown.

In the present work I examine the function of the dI6 cells during fictive locomotion. In part one of this thesis, I describe a novel *in vitro* fictive locomotor preparation that I developed in order to target neurons located close to the central canal for whole cell recording while leaving the locomotor CPG functionally intact. In the second part of this thesis, this preparation was used to make electrophysiological recordings from dI6 interneurons and investigate their function during fictive locomotion. My results indicate that the dI6 neurons are an electrophysiologically diverse population with the majority oscillating rhythmically during fictive locomotion. Analysis of their intrinsic membrane properties suggest that they are likely involved in generating rhythmic, locomotor-like activity in the mammalian spinal cord.

TABLE OF CONTENTS

Chapter 1 - General Introduction

1.1 Introduction	1
1.2 Historical evidence for the presence of the locomotor CPG	2
1.3 Preparations used to study the locomotor CPG	4
1.4 Location of key elements of the locomotor CPG.	5
1.5 Conceptual models of locomotor CPG	7
1.6 Pacemaker cells: A potential population of first-order component of the locomotor CPG	11
1.7 Efforts to identify rhythm generating neurons.	12
1.8 Incorporating molecular genetics to study the locomotor CPG.	14
1.9 Genetically-defined neuronal populations capable of generating the locomotor rhythm.	16
1.10 Conclusions	23
1.11 References	25

Chapter 2 - Whole cell recordings from visualized neurons in functionally intact spinal cord

2.1 Introduction	40
2.2 Methods	43
2.3 Results	48
2.4 Discussion	52

2.5 References	57
----------------	----

Chapter 3 - Functional characterization of dI6 interneurons in the neonatal mouse spinal cord

3.1 Introduction	68
3.2 Methods	71
3.3 Results	75
3.4 Discussion	81
3.5 References	86

Chapter 4 - General discussion and conclusions

4.1 Development of a novel in-vitro preparation	102
4.2 dI6 neurons contribute to rhythm generation in the locomotor CPG	104
4.3 Limitations of this work	105
4.4 Future Directions	108
4.5 Where do dI6 neurons fit into the current model of the locomotor CPG?	111
4.6 References	114

LIST OF TABLES

Table 1. Summary of genetically defined interneuronal populations

38

LIST OF FIGURES

Chapter 1:

Figure 1-1. In-vitro isolated spinal cord preparation	35
Figure 1-2. Models of the locomotor CPG	36
Figure 1-3. Transcription factors expressed in spinal cell populations	37

Chapter 2:

Figure 2-1. Schematic of modified in-vitro preparation	62
Figure 2-2. Electroneurograms recorded from modified in-vitro preparation	63
Figure 2-3. Imaging of GFP labelled interneurons	64
Figure 2-4. Recording from rhythmically active interneurons in modified in-vitro preparation	65

Chapter 3:

Figure 3-1. Transcriptional profile of labeled neurons in Dbx1CreRosa26EFP mouse	92
Figure 3-2. Intrinsic oscillations in LC dI6 neurons	94
Figure 3-3. Firing patterns of oscillatory dI6 neurons during fictive locomotion	95
Figure 3-4. Non-linear membrane properties in LC dI6 neurons	96
Figure 3-5. Oscillations in TC dI6 neurons are voltage insensitive	97
Figure 3-6. TC dI6 neurons receive highly rhythmic drive potentials	98
Figure 3-7. Rhythm generating schematic of the locomotor CPG	100

Chapter 4:

Figure 4-1. LC dI6 neurons display voltage dependent firing frequency activity patterns	119
Figure 4-2. LC, but not TC, dI6 neurons display hyperpolarizing induced (I _h) currents	120

Figure 4-3. Activity pattern of LC dI6 neuron during deletion in fictive

locomotion

121

Figure 4-4. Hybrid model of the locomotor CPG

122

LIST OF ABBREVIATIONS

5-HT	5-hydroxytryptamine
B-GAL	Beta-galactosidase
aCSF	Artificial cerebrospinal fluid
AP	Action Potential
BMP	Bone morphogenic protein
CIN	Commissural interneuron
CPG	Central pattern generator
Cm	Membrane capacitance
CNQX	6-cyano-7-nitroquinoxaline-2,3-dione
Cre	Cre recombinase
r-aCSF	Recording artificial cerebrospinal fluid
d-aCSF	Dissection artificial cerebrospinal fluid
Dbx1	Developing brain homeobox protein 1
DTA	Diphtheria toxin A
ENG	Electroneurogram
FRA	Flexor reflex afferent
EFP	Enhanced fluorescent protein
EGFP	Enhanced green fluorescent protein
Evx1	Even-skipped homeobox 1
EM	Membrane potential
FE	Flexor-extensor

Hb9	Homeobox-9
GFP	Green fluorescent protein
IR-DIC	Infrared differential interference contrast
I-V	Current-voltage
LDP	Locomotor drive potential
LC	Loosely coupled
MLR	Mesencephalic locomotor region
NMDA	N-Methyl-D-aspartic acid
PBS	Phosphate buffered saline
PF	Pattern forming
PIC	Persistent inward current
PMI	Pre-motor interneuron
RG	Rhythm generating
Rm	Membrane resistance
Rs	Series resistance
SCI	Spinal cord injury
SD	Standard deviation
Shh	Sonic hedgehog
TC	Tightly coupled
TeNT	Tetanus toxin
TTX	Tetrodotoxin
UBG	Unit burst generator

YFP Yellow fluorescent protein

VR Ventral root

Wt1 Wilms tumor-1

**Chapter 1 -
General Introduction**

1.1 Introduction

Swallowing, breathing, and walking are all examples of rhythmic motor behaviours that are generated by neural circuits. When circuits such as these are capable of generating rhythmic output endogenously (i.e. without rhythmic sensory or central input) they are referred to as central pattern generators (CPGs). Work presented in this thesis is focused on the mammalian spinal locomotor CPG, which generates the basic rhythmic activity underlying walking.

Why study the locomotor CPG? In addition to providing a better understanding of the general organization and oscillatory mechanisms underlying neural networks throughout the CNS, identifying interneuronal components and determining how they interact to generate locomotor outputs will be a beneficial step in developing strategies towards restoring function after spinal cord injury (SCI). Stem cell transplant and rehabilitative training have emerged as some of the most promising treatments (Thuret et al. 2006), however such approaches have resulted in relatively minor progress in repairing the injured spinal cord. Perhaps it is not surprising that we do not know how to repair a spinal cord after injury considering that we do not know how the intact spinal cord generates normal locomotor activity. For this reason, it is imperative to be able to identify the spinal interneuron populations that make up the locomotor CPG and better understand its connectivity and function.

1.2 Historical evidence for the presence of the locomotor CPG.

Attempts to understand how the mammalian spinal cord generates and coordinates locomotor behaviour began more than 100 years ago. Even in these early years it was recognized

that the brain was not essential for the production of locomotor-like activity, as reports of stepping-like movements in spinalized animals had been made (Freusberg, 1874). What was unclear, however, was whether such stepping movements were the result of peripheral inputs or an intrinsic property of the spinal cord. Among the first to address this question was Charles Sherrington, as he studied extensively the stepping movements in spinalized animals. Sherrington showed that following spinal cord transection, brief episodes of reflex stepping could be produced which closely resembled normal stepping movements (Sherrington, 1910). Although he acknowledged that the spinal cord likely contributes to rhythm generation, Sherrington favoured a model in which locomotion was largely the result of cyclical rhythmic input from proprioceptive afferents activated during stepping movements.

It was not long after Sherrington's original publication that his sensory-based model of locomotion was disputed, ironically by one of his own students. In 1911, Graham Brown reported rhythmic alternation between ankle flexor and extensor nerves in a spinalized cat in which both hind limbs were deafferented (Brown, 1911). The fact that locomotor activity persisted despite the lack of afferent input is direct evidence that stepping movements in spinalized animals are not simply a series of stereotypic reflexes. Instead, Brown's findings were the first evidence that neural circuits within the spinal cord were sufficient for generating the locomotor rhythm. Brown's observations lead to the conceptualization of his half-centre model of the locomotor CPG, which will be reviewed in detail later in this thesis (Section 1.5A).

1.3.Preparations used to study the locomotor CPG.

Decerebrate cat preparation.

One of first approaches to provide substantial insight into the neural control of locomotion was the decerebrate cat preparation. With this preparation, the cortices are removed and a dorsoventral transection of the brainstem is made, just rostral to the superior colliculus (Orlovsky et al., 1999). Locomotor activity can be elicited by electrical stimulation of a small region of the pons (pedunculopontine and cuneiform nuclei) referred to as the mesencephalic locomotor region (MLR; Shik et al., 1966). MLR stimulation can be used to generate overground walking in a decerebrate cat, in which locomotor activity can be monitored through electromyogram (EMG) recordings. Alternatively, MLR stimulation can be used as a means to induce fictive locomotion, where the hindlimbs are paralyzed and locomotor activity is recorded from peripheral nerves. As opposed to other *in vitro* models used to study the locomotor CPG (see below), the decerebrate cat preparation has the advantage of providing information in the fully mature and intact nervous system. As such, this preparation has been used extensively to investigate how reflexes modulate locomotion (reviewed in Pearson et al., 1998) and, when paired with intracellular recordings, has allowed for identification of interneurons which are part of the locomotor CPG (see section 1.5A; Jankowska et al., 1967).

In vitro fictive locomotor preparation.

The neonatal rodent *in vitro* isolated spinal cord preparation (Figure 1-1) has been an invaluable tool for the study of the locomotor CPG. In this preparation, the spinal cord of a neonatal

rat or mouse is isolated and kept alive in a bath containing oxygenated artificial cerebrospinal fluid (aCSF). By applying various neuroactive substances, such as NMDA and 5HT, rhythmic activity, which resembles locomotion, can be generated (Kudo and Yamada, 1987; Smith and Feldman, 1987). Suction electrodes attached to flexor related (i.e. L2) and extensor related (i.e. L5) ventral roots are used to record alternating bursts of ENG activity between ipsilateral flexor and extensor nerves as well contralateral flexor (or contralateral extensor) nerves. Recently this preparation has been used to provide a great deal of information on the locomotor CPG via experiments on various transgenic mouse models (see later sections).

1.4. Location of key elements of the mammalian locomotor CPG.

It stands to reason that in order to study the structure and mechanism of function of the locomotor CPG it is necessary to know where its component interneurons are located. The following section will address this question by identifying critical boundaries within the neonatal rodent spinal cord in which the locomotor CPG is contained.

The mammalian locomotor CPG is located ventromedially.

One approach that has been used to identify the boundaries of the locomotor CPG is to progressively transect the spinal cord in several planes (i.e. rostro-caudal, dorso-ventral, and medio-lateral) and determine whether fictive locomotion can still be elicited. Using such an approach, multiple laboratories have demonstrated that locomotor activity persists as long as a portion of the spinal cord caudal to T12 and rostral to L6 remain intact (Cowley and Schmidt, 1997; Kjaerulff and Kiehn, 1996), suggesting that the key components reside within these spinal segments. Lesions to

the dorsal spinal cord (above the central canal) indicate that it is not required for the generation of locomotor activity as fictive locomotion persists following its removal (Kjaerulff and Kiehn, 1996; Antri et al., 2011). This is not to say that the dorsal spinal cord does not play an important role in overground locomotion, but rather that the basic locomotor rhythm in-vitro can be generated independently of dorsal neurons. Finally, lesion studies also indicate that the locomotor CPG resides in more medial regions (i.e. laminae VII, VIII, and X) rather than in the lateral edges of the spinal cord (Kjaerulff and Kiehn, 1996). The findings from the lesion studies are supported by the use of activity-dependent markers (such as c-fos staining) to label neurons which that are active during locomotion (Dai et al, 2005). Results of such studies indicate that the majority of neurons active during fictive locomotion are located in laminae VII, VIII and X.

Components of the locomotor CPG are distributed in a rostral-caudal gradient.

There is compelling evidence that rostral segments of the spinal cord are more rhythmogenic than caudal segments. Ablation of interneurons in L1 or L2 of the adult rat spinal cord via kainate injection severely impairs overground locomotion, whereas kainate injection to more caudal segments had little effect (Magnuson et al., 2005). Similar conclusions have been drawn in the isolated spinal cord preparation using a split bath approach. Selective addition of 5HT and NMDA to rostral regions (L1 and L2) of the lumbar cord results in rhythmic locomotor activity in both rostral and caudal segments (Cazalets, et al. 1995). Conversely, selectively applying these agents to caudal segments only (L5 and L6) produces tonic activity in caudal regions of the spinal cord. Furthermore, when the lumbar spinal cord is separated into short pieces consisting of a few spinal segments, locomotor activity is much more robust in the isolated rostral segments (T12-L1)

than in isolated caudal segments (L4-L6; Kjaerulff and Kiehn, 1996). It is possible that a gradient of neuronal receptors involved in initiating locomotion (such as 5HT receptors) could also account for differences in rhythmogenic capacity (Liu and Jordan, 2005).

1.5. Conceptual models of locomotor CPG.

Based on the experimental findings described above, several conceptual models of the locomotor CPG have been developed over the years. These models propose mechanisms by which the basic locomotor rhythm is generated in the spinal cord, while also explaining how this rhythm can be shaped to produce meaningful overground walking. The following section is not an exhaustive review of all models of the locomotor CPG, but rather describe three of the most influential.

Half Centre Model.

Based on his observation that stepping patterns could be elicited in spinal animals lacking afferent input, Brown theorized that two groups of interneurons (i.e. half centres) exist in the spinal cord, and that these two half centres mutually inhibit one another (Brown, 1911; Figure 1-2A). According to this model, one half centre excites all extensor motoneurons while the opposing half centre excites all flexor motoneurons. Alternating activity between flexor and extensor half centres occurs when the inhibitory connection between them fatigues, releasing the inactive half centre from inhibition. Brown's model was capable of explaining the simple alternation between flexor and extensor muscles observed in spinal animals.

The first experimental findings in support of Brown's half centre model came from intracellular interneuron recordings from the cat lumbar spinal cord during fictive locomotion (Jankowska et al., 1967). These authors identified a group of neurons that were activated during a specialized form of afferent-induced fictive locomotion known as flexion reflex afferent (FRA) stimulation. Such recordings indicated the presence of two interneuron populations that were organised in a reciprocal inhibitory manner. Specifically, one group of neurons were activated by ipsilateral FRA stimulation and a second group were activated by contralateral FRA stimulation. The mutual inhibitory connections between these groups was demonstrated by the observation that activating one group of neurons with ipsilateral FRA stimulation could be abolished by simultaneously stimulating the contralateral FRA.

Despite this experimental support for Brown's half centre model, it is unable to account for the complex activity patterns of certain muscles during overground locomotion. For example activity in certain muscles, such as the hip flexor semitendinosus which is active during both the swing (flexion) and stance (extension) phase of walking, can not be accounted for in the half-centre model. Furthermore, this model cannot explain changes to the locomotor pattern that occur during more difficult tasks, such as backwards walking. The fact that these complex activity patterns persist following deafferentation (Gillner and Zangger, 1974) rules out the possibility that sensory afferents are simply altering the basic flexor/ extensor pattern generated by a half centre model.

Unit burst generator model.

The next major model of the locomotor CPG to be put forth was born out of an attempt to explain the aforementioned complex muscle patterns that Brown's model could not explain.

Grillner and Zangger (1974) proposed that the locomotor CPG consisted of multiple half centre modules, which they coined unit burst generators (UBGs; Figure 1-2B). According to their theory, muscles around each joint are controlled by separate UBGs, which are tightly coupled during normal locomotion, but could be differentially modulated by descending commands. Unlike Brown's model, this theory removes the requirement of synchronous activation of all flexor muscles followed by the synchronous activation of all extensor muscles.

Some of the cellular components of the UBG model have now been identified. Using an *in-vitro* lamprey spinal cord preparation, Grillner has shown that the rhythmic undulations that the lamprey uses to swim are generated by a chain of oscillators located in each spinal segment (or myotome; Grillner et al. 1988). Each individual oscillator is sufficient to produce rhythmic activity in a given myotome. Yet, under normal circumstances, individual oscillators are coupled to neighbouring oscillators to generate a propagating wave of rhythmic activity. One could easily imagine how a similar scenario could exist in the mammalian locomotor CPG, and allow for coupling between muscles around the neighbouring hip, knee and ankle joints.

Two layer model.

Building upon the unit burst generator model, Lafreniere-Roula and McCrea (2005) recently proposed a two-layer model of the locomotor CPG. They hypothesize that the basic timing of the locomotor rhythm is generated by a clock-like network, which in turn activates a separate network to distribute this rhythm to the appropriate motor pools. The authors refers to these two circuits as the rhythm generating (RG) and pattern forming (PF) layers, respectively (Figure 1-2C). The

separation between these two layers differs from the connectivity proposed in the unit burst generator model where the circuitry that generates the rhythm and pattern are one and the same.

Evidence to support the two-layer model of the locomotor CPG comes from experiments using the decerebrate cat fictive locomotor preparation, where authors describe the occurrence of missing burst of activity (so called deletions or dropouts) in the fictive motor pattern (Lafreniere-Roula and McCrea, 2005). Interestingly, the authors found that following a deletion, the timing of bursts was often maintained (events referred to as non-resetting deletions). In other words, the burst of activity immediately following a deletion would sometimes occur at the expected time point had the deletion not occurred (based on the average period of prior bursts), indicating that the timing of the locomotor rhythm was being maintained during the deletion. This observation supports the theory that there is a separation in the circuitry that generates the rhythm and the circuitry that directly activates motoneuron pools.

Deletions are not simply the result of a motoneuron excitability being low and failing to fire. Since deletions can be simultaneously seen across numerous motoneuron pools acting around several joints, elements upstream of the motoneurons must be affected. Experiments performed in the same preparation during a similar behaviour, fictive scratch, argue against the theory that rhythmicity during a deletion could be maintained by the contralateral spinal cord. Since fictive scratch requires only ipsilateral spinal cord circuitry, maintenance of rhythmic activity during a deletion requires a separation of the rhythm generating and pattern forming layers. The authors propose that a similar organization could also underly deletions occurring during fictive locomotion (Lafreniere-Roula and McCrea, 2005).

To date, the neurons which comprise the RG and PF networks have not been identified. Preliminary studies aimed at this have utilized computer models, which have been able to reproduce the fictive locomotor pattern (including non-resetting deletions; McCrea and Ryback, 2008). Results from this work have indicated that neurons that make up the rhythm generating layer rely on persistent sodium currents as a means of intrinsic bursting.

1.6 Pacemaker cells: A potential population of first-order component of the locomotor CPG.

As mentioned in the previous section, determining which interneurons are part of the locomotor CPG has historically proven difficult. A logical first step towards this goal is to identify which cells initiate rhythmic activity and subsequently determine their synaptic targets. Such an approach provides a systematic way to determining the connectivity of the vast number of intermingled cells which make up the locomotor CPG. Thus far however, the identification of cells which initiate the locomotor rhythm, so called pacemaker or rhythm generating neurons, has been elusive. In order to facilitate the discovery of such neurons, it is beneficial to identify some of the key properties and characteristics that they should possess. Recently, Brownstone and Wilson (2008) put forth a set of criteria they believe to be required if a cell is to be involved in rhythm generation. They postulate that generating neurons should be glutamatergic, located in the ventromedial lumbar spinal cord, not make direct contacts onto motoneurons, rhythmically active during locomotion, and possess membrane properties necessary for intrinsic oscillations (i.e. conditional bursting; see Wilson and Brownstone, 2008).

At this time, it is also worth acknowledging the possibility that pacemaker neurons may not be solely responsible for generating the locomotor rhythm. It is possible that rhythmic activity in

the locomotor CPG is generated by emergent network properties. In this scenario, no specific group of neurons act as conditional bursters, but rather recurrent synaptic connections between groups of excitatory interneurons are responsible for rhythm generation. Until a population of interneurons which meet most of the above criteria are found and shown to be necessary for rhythm generation, a network driven model of rhythm generation can not be ruled out.

1.7 Efforts to identify rhythm generating neurons.

Over the past few decades several groups have attempted to identify cells that are involved in generating the locomotor rhythm. Using a juvenile (P7-14) rat spinal cord slice preparation, Hochman et al. (1994) were among the first to identify spinal interneurons with conditional bursting properties within the ventromedial spinal cord. These authors found that voltage dependent oscillations could be induced in a small group of neurons when exposed to high concentrations of NMDA (20-100 μ M), and that these oscillations persisted when the neurons were synaptically isolated with tetrodotoxin (TTX). While an interesting finding, it is difficult to determine whether these results are physiologically relevant given that such high concentrations of NMDA (20-100 μ M) were used to induce oscillations in these cells. In fact, these concentrations of NMDA are 4 to 20 times what is normally used to induce locomotion in the brainstem-spinal cord *in vitro* preparation. Furthermore, there is no way to correlate these oscillations to locomotor output as the recordings were done in a spinal cord slice preparation. Nonetheless, this study opened the door to the possibility of intrinsic bursting neurons being present in the mammalian spinal cord, and capable of initiating the locomotor rhythm.

In a similar study, Kiehn et al. (1996) observed rhythmic oscillations (or plateau potentials) in spinal interneurons located near the central canal. However, in this study fictive locomotion was induced using lower (5-7 μ M) concentration of NMDA. Furthermore, recordings were performed in an whole spinal cord preparation in which the locomotor CPG was functionally intact. Kiehn et al. (1996) found that many of these oscillatory neurons possessed intrinsic conductances that contributed to their plateau potential and discovered that a persistent inward current (PIC) could be observed in many oscillating neurons. Interestingly, in only a small number of cells did oscillations persist when the preparation was synaptically isolated (with TTX). Thus it remained unclear whether persistent sodium currents were essential for intrinsic bursting in these cells.

In both of the aforementioned studies only a small fraction of the total number of rhythmically active neurons recorded were intrinsic bursters. It was unclear whether this low number was an experimentally induced artefact or an accurate representation of the small number of pacemaker neurons in the locomotor CPG. Recently this question was addressed by Tazaret et al. (2008) who examined the effect of calcium concentration in the extracellular solution on the emergence of pacemaker properties in spinal interneurons. The authors found that the removal of extracellular calcium resulted in the emergence of intrinsic pacemaker properties in 75% of lamina VIII spinal interneurons. In these cells, the appearance of such pacemaker properties were paralleled by an increase a sodium-dependent PIC that was riluzole sensitive. Based on these findings it was concluded that persistent sodium currents were up-regulated when extracellular calcium was removed. However, given that calcium-free aCSF is an artificially induced condition, one could argue that the emergence of pacemaker properties in these cells is unlikely to have physiological significance. It is therefore possible that enhancement of persistent sodium currents

could enhance bursting properties in spinal interneurons, which would then initiate the locomotor rhythm. In agreement with such a theory is the finding that several neuromodulators known to be involved in initiation of the locomotor rhythm (i.e. dopamine and 5HT) have been shown to also enhance persistent sodium currents (Gorelova and Yang, 2000; Harvey et al. 2006).

1.8 Incorporating molecular genetics to study the locomotor CPG.

Thus far a major obstacle that has hindered efforts aimed at identifying cells with a given function during locomotion (such as rhythm generation) has been the fact that neurons with a variety of functions are intermingled within the mammalian spinal cord. Recent advances in molecular genetic techniques have provided insights into the developmental processes underlying patterning of the spinal cord (Tanabe and Jessell, 1996) and demonstrated that spinal neurons can be divided into a handful of families based on transcription factor expression. It has since been shown that properties such as neurotransmitter phenotype (Cheng et al. 2005; Mizuguchi et al. 2006; Pillai et al. 2007) and axonal projection patterns (Betley et al. 2009) are ultimately regulated by complement of transcription factors that they express. This has led to the hypothesis that neurons within a given genetic background will share similar characteristics and similar functions during behaviours such as locomotion.

Development of the spinal cord.

Patterning of the ventral spinal cord results from the opposing actions of morphogens secreted from the ventral (sonic hedgehog; Shh) and dorsal (bone morphogenic proteins; BMPs) aspects of the developing neural tube (Yamada et al., 1991). Shh and BMPs diffuse through the

developing spinal cord in opposing directions, setting up an overlapping concentration gradient. These morphogens act to regulate gene expression (i.e. transcription factors) in progenitor cells located in the ventricular zone (Tanabe and Jessell, 1996). Since activation (or repression) of each of these transcription factors requires a different threshold concentration, the opposing actions and overlapping concentration gradients of Shh and BMP ensure that sharp boundaries of gene expression are created. These boundaries result in the creation of discrete progenitor domains in ventricular zone neurons, which ultimately lead to discrete neuronal populations in the postnatal spinal cord.

Genetically-defined neuronal populations generated in the spinal cord.

Based on the unique complement of transcription factors, molecular biologists have recently been able to identify eleven distinct populations of spinal neurons (dI1-dI6, V0-V3, VMN; Tanabe and Jessell, 1996) in the spinal cord. These populations can first be detected by approximately embryonic day 9 (E9) and by E13 they have begun migrating towards their final positions in the spinal cord (Figure 1-3). During this journey, each class of neurons expresses a unique complement of transcription factors which allows them to be identified.

Recently, the intrinsic properties of each of these genetically defined populations as well as the function during locomotor activity have been investigated. Since the locomotor CPG is located in the ventral spinal cord, most work has been performed on the interneuron populations that take up ventral positions postnatally. This includes the V0, V1, V2 and V3 cells in addition to the dI6 population which originates in the dorsal neural tube but migrate ventrally during development. Electrophysiological and anatomical investigations of many of the ventral genetically-defined

neuronal populations has identified the basic characteristics of several populations (see Table 1 for summary), including neurotransmitter phenotype and axonal projection pattern. While it may be an oversimplification to ascribe one property to a single population, this classification has provided a framework around which further hypotheses (regarding the function of each population) can be tested. As more detailed genetic markers for each population become available, each genetic population is being divided into more homogenous subpopulations.

1.9 Genetically-defined neuronal populations capable of generating the locomotor rhythm.

As mentioned in previous sections, neurons responsible for rhythm generation are postulated to be localized in lamina VII and VIII of the spinal cord, excitatory in nature and project their axons ipsilaterally (Brownstone and Wilson, 2008). To this point, no single genetically-defined neural population has been identified that acts as the sole rhythm generator, however, many meet some of the aforementioned criteria (Brownstone and Wilson, 2008). The fact that locomotor-like rhythms persist after selectively silencing or removing each the V0, V1, V2 and V3 populations (Lanuza et al., 2004, Gosgnach et al., 2006, Crone et al., 2008., Zhang et al., 2008) raises the possibility that rhythm generation could be a shared function amongst numerous populations.

In the following sections, the potential role that genetically-defined populations play in locomotor rhythm generation will be discussed. This discussion will focus only on those populations located in regions known to be critical for rhythm generation (i.e. lamina VII, VIII, and X of the thoraco-lumbar spinal cord). The rhythm generating role of two genetically-defined populations of neurons (V1 and V2b) will not be addressed here, as both of these populations have been shown to be exclusively inhibitory (Lundfald et al., 2007; Sapir et al., 2004). It has been

suggest that inhibition is not required for rhythmogenesis (Bracci et al., 1996), meaning that it is unlikely that these cells contribute to rhythm generation. Furthermore, many V1 interneurons directly innervate motoneurons and are situated adjacent to motoneuron pools (Sapir et al., 2004), making them unlikely candidates to contribute to rhythm generation. Therefore, the following section will focus on the rhythm generating role of V0, V2a (a subset of the V2 population that is excitatory), V3, and dI6 populations, as well as a small population of interneurons referred to as Hb9 neurons.

Hb9 interneurons.

In addition to the V0-V3 and dI1-dI6 populations mentioned previously, a small population of interneurons that express the transcription factor Hb9 has recently been described. Unlike the other genetically-defined populations, the embryonic origin of Hb9 interneurons is unclear, as they unexpectedly share similar genetic markers as motoneurons (Arber et al., 1999). Despite their obscure origin, this relatively small population of interneurons has been extensively studied and well characterized. These neurons are clustered around the central canal, are exclusively glutamatergic, and have ipsilaterally projecting axonal projections (Hinkley et al., 2004; Wilson et al., 2005). All of these properties make this population prime candidates to contribute to locomotor rhythm generation.

Accordingly, Hb9 neurons display many intrinsic properties that are consistent with rhythm generation. Whole cell recordings from Hb9-positive neurons in both the hemisected (Hinkley et al., 2004) and spinal cord slice (Wilson et al., 2005) preparations demonstrate that these cells are highly rhythmic and fire in phase with the ipsilateral ventral root in the same segment (i.e. the local

ventral root). Such oscillations persist in Hb9 neurons when the cell is synaptically isolated with TTX, indicating that these cells are conditional bursters (Wilson et al., 2005). Furthermore, many of these cells display intrinsic membrane properties that could support such oscillations, such as post-inhibitory rebound (Wilson et al. 2005) and a sodium-dependent persistent inward current (PIC; Ziskind-Conhaim et al. 2008).

Despite these observations, many questions still remain regarding the role of Hb9 interneurons in initiating locomotion. First of all, these cells are distributed only in the lower thoracic and upper lumbar spinal cord (T11-L3; Hinkley et al. 2004). No Hb9 interneurons are located in the lower lumbar region of the spinal cord, yet L4 and L5 segments of the isolated spinal cord can generate rhythmic activity (Kjaerulff and Kiehn, 1996). Furthermore, even in the rostral lumbar cord, there are so few Hb9 neurons (2-3 per 100 μ m) that it is unlikely that they alone are sufficient to generate the locomotor rhythm. There has also been some question regarding the nature of the intrinsic bursting properties in these cells. The frequency of oscillations in isolated Hb9 neurons decreases (instead of increasing) as the cell is depolarized (Wilson et al., 2005). This contradicts the voltage dependent bursting properties which are commonly associated with pacemaker cells in other rhythmic networks (Del Negro et al., 2002; Tazerart et al., 2008). In addition, calcium imaging experiments demonstrate that although Hb9 interneurons fire rhythmically during fictive locomotion, they lag behind the onset of the local ventral root burst (Kwan et al., 2009). If Hb9 neurons were solely responsible for initiating locomotor activity, one would expect oscillations in these cells to proceed the ventral root. Unfortunately, the role of Hb9 neurons in generating locomotor activity can not be directly tested by the elimination of all Hb9-

expressing cells, as there is currently no method to silence these interneurons without also silencing motoneurons (and thus losing locomotor output).

V0 Interneurons.

The V0 population is located in located lamina VII and VIII of the postnatal spinal cord, the region in which we would expect to find rhythm generating cells. V0 interneurons were initially divided into two subpopulations (ventral V0v and dorsal V0d). While both V0v and V0d neurons express the transcription factor Dbx1, the two populations can be distinguished by the expression of Evx1, which is specific to V0d neurons (Pierani et al., 2001). Initial characterization of these cells demonstrated that they project axons commissurally (Pierani et al., 2001), are primarily inhibitory (Lanuza et al., 2004) and active during locomotion (Lanuza et al., 2004). Selective knock-out studies demonstrate that this population of interneurons is responsible for maintaining left-right alternation during fictive locomotion, an essential characteristic of locomotor behaviour (Lanuza et al., 2004).

While 70% of V0 interneurons are inhibitory, the role of excitatory V0 cells is unknown. A recent study demonstrated that a small subpopulation (~5%) of excitatory V0 cells (V0c) do not have properties of pacemaker cells and are likely not involved in rhythm generation (Zagoraïou et al., 2009). Further studies are needed to address whether there are additional populations of ipsilaterally projecting V0 neurons which may contribute to rhythm generation. However, as of yet, there has not been a way to identify and target the 30% of glutamatergic V0 interneurons in live tissue and determine (through whole cell recording) whether these neurons possess pacemaker-like properties.

Recently, inspiratory pacemaker neurons which originate from Dbx1 progenitor cells were identified (Gray et al., 2010) in the respiratory CPG, which is located in the ventro-lateral medulla. Interestingly, these Dbx1-derived pacemaker neurons are ipsilaterally projecting and glutamatergic, which raises the possibility that excitatory V0 cells may play a similar role in the locomotor CPG. However, the fact that locomotor activity persists when the V0 population is selectively removed (Dbx1^{-/-} mouse; Lanuza et al., 2004) provides strong evidence that this population is not solely responsible for initiating locomotor activity.

V2 Interneurons.

The V2 interneuron population can be broken down into two main subpopulations, referred to as the V2a and V2b populations (Lundfald et al., 2007). As mentioned previously, I will not discuss the V2b population here as they are exclusively inhibitory. At first glance, it would appear that the V2a cells would be prime candidates to be included in a rhythmogenic network, given that they are located in laminae VII and VIII, excitatory, and ipsilaterally projecting (Lundfald et al. 2007). In spite of this, arresting V2a neuronal activity using the Chx10-DTA mouse line reveals no change in burst duration or amplitude during fictive locomotion. Interestingly, the only phenotype seen is synchronous bursting on the left and right side of the spinal cord as the speed of locomotion increases (Crone et al., 2009). Anatomical tracing of the axonal projections of V2a interneurons revealed that these cells make connections onto commissural interneurons, including many Evx1-positive V0 neurons (Crone et al., 2008). Based on this data, the authors proposed that V2a interneurons maintain left right alteration at higher speeds by recruiting a V0-mediated inhibitory commissural pathway.

The specific role of the V2a neurons in the locomotor rhythm generation is therefore unclear. While many V2a neurons display intrinsic properties that potentially support intrinsic bursting, it has been suggested that these cells are not likely to contribute to rhythm generation (Dougherty et al. 2010; Zhong et al., 2010) due to the lack of a related locomotor phenotype and the fact that V2a neurons have been shown to be electrophysiologically heterogeneous. Such a claim is perhaps premature, given that experiments to test whether these cells act as conditional bursters (i.e. synaptic isolation experiments) were not performed.

V3 Interneurons.

In comparison to other genetic populations, relatively little is known about the function of the V3 interneurons. These cells derive from progenitors that express the transcription factor *Sim1*, are exclusively glutamatergic, and the majority directly contact contralateral motoneurons (Zhang et al. 2008). Of particular interest with respect to rhythm generation are the small proportion of V3 neurons (~15%) that are ipsilaterally projecting. Given that these cells are located in laminae VII and VIII, it is plausible that this subset of V3 interneurons play a role in generating locomotor activity.

One of the difficulties in understanding the function of these cells lies in the fact that the locomotor phenotype in the absence of V3 cell activity is not as clear as it is in the absence of other cell populations (i.e. V0 or V1 interneurons). The activity in V3 interneurons has been blocked by selective expression of either Tetanus toxin light chain (TeNT), or the allatostatin receptor. In both situations, the stability of fictive locomotor activity was greatly diminished upon silencing of V3 cell activity. Using the *Sim1*-TeNT approach, 30% of the mice were unable to generate normal

locomotor activity when drug concentration were matched to control mice. In the preparations where locomotor activity could be generated, the rhythm was unstable and erratic, often with periods where the rhythm was dramatically slowed. Similarly, unbalanced rhythms were seen in which the allatostatin receptor system was used to selectively and reversibly silence V3 interneurons in the neonate and the adult.

As a result of this work, V3 neurons are not considered candidates to participate in rhythm generation. However, these conclusions may be hasty. The extent to which V3 interneurons are completely silenced (rather than slightly hyperpolarized) via the allatostatin approach in the whole spinal cord preparation is unclear. With the TeNT approach, output from all V3 cells is abolished. However, since this occurs at an early embryonic time point, it is possible that compensatory mechanisms occur.

Finally, whole cell recordings to assess the intrinsic membrane properties of V3 interneurons indicates that these cells do not possess intrinsic oscillatory properties. However, the study in question targets only the “lamina VIII” or “ventral” V3 neurons that were monosynaptically coupled to motoneurons. It is highly unlikely that last order interneurons would contribute to rhythm generation, thus it is not surprising that these cells lack intrinsic oscillatory properties. Further experiments are required to determine whether the more dorsally located V3 interneurons share the same membrane properties.

dI6 Interneurons.

Although they do not originate in the ventral aspect of the developing neural tube, dI6 interneurons migrate ventrally during development and settle in lamina VII and VIII of the post

natal spinal cord (Goulding et al., 2002). Based solely on their settling position, these cells are appealing candidates to contribute to locomotor rhythm generation. Up to this point in time, only preliminary steps have been made to characterize this cell population. Unpublished data indicate that dI6 neurons represent a mixed inhibitory and excitatory population and likely contain both ipsilateral and contralateral projecting neurons (Goulding, 2009). Initial studies indicate that these cells are closely related to the V0 cell population, as both groups derive from Dbx2 progenitors (Lanuza et al., 2004). Interestingly, when V0 cells are removed during development (i.e. in the $Dbx^{-/-}$ mouse) there is an increase in the number of dI6 neurons, which may account for the commissural inhibitory input remaining in the $Dbx^{-/-}$ mouse (Lanuza et al., 2004).

dI6 neurons remain the only ventrally located interneuron population that has not been well characterized. In this thesis, I will investigate the activity pattern of these cells during fictive locomotion as well as their intrinsic membrane properties in order to assess their potential role in rhythm generation. This work is an important step in identifying which genetically-defined populations contribute to rhythm generator and ultimately how rhythmic activity is produced in the locomotor CPG

1.10 Conclusions.

Much has been discovered over the last century about the neural control of locomotion, and the organization of the mammalian locomotor CPG. This network is now known to be distributed throughout the lumbar spinal cord and capable of generating endogenous rhythmic activity without either sensory or descending inputs. Although the mechanism of function of the CPG remains unclear, it appears that there is a separation between the network which generates the rhythm and

the network which transmits this activity to motoneuron pools. The identity of the specific neurons responsible for generating the locomotor rhythm (so called pacemaker neurons) has proven difficult, however recent advances in molecular genetics has allowed the function of discrete interneuronal populations that share many intrinsic properties to be investigated.

Only one genetically defined interneuron population in the ventral spinal cord of the postnatal mouse has yet to be examined; the dl6 neurons. Given that these neurons are located in a region known to be critical for rhythm generation, it is possible that at least a portion of the neurons are actively involved in initiating locomotor activity. If not, it is possible that emergent network properties (rather than a single rhythm generating population) are responsible for rhythm generation. Either way, the characterization of this neuronal population will greatly add to our understanding of the structure and mechanism of the locomotor CPG.

The work to be presented in this thesis is divided into two parts. First, a I describe a preparation that I devised which was essential to visually identify and record from dl6 interneurons in the functionally intact spinal cord. Secondly, I use this preparation to record from dl6 interneurons record intrinsic membrane properties from this population and test the hypothesis that these neurons play a vital role in the initiation of locomotion.

1.11 References:

Antri M, Mellen N, Cazalet J (2011) Functional organization of locomotor interneurons in the ventral lumbar spinal cord of the newborn rat. *PLoS One*. 6:e20529

Arber S, Han B, Mendelsohn M, Smith M, Jessell TM, and Sockanathan S (1999) Requirement for the homeobox gene Hb9 in the consolidation of motor neuron identity. *Neuron* 23:659–674

Betley JN, Wright CV, Kawaguchi Y, Erde'lyi F, Szabo' G, Jessell TM, Kaltschmidt JA (2009) Stringent specificity in the construction of a GABAergic presynaptic inhibitory circuit. *Cell* 139:161–74.

Bouvier J, Thoby-Brisson M, Renier N, Dubreuil V, Ericson J, Champagnat J, Pierani A, Chedotal A, Fortin G (2010) Hindbrain interneurons and axon guidance signaling critical for breathing. *Nature Neuroscience* 13:1066-74.

Bracci E, Ballerini L, Nistri A (1996) Localization of Rhythmogenic Networks Responsible for Spontaneous Bursts Induced by Strychnine and Bicuculline in the Rat Isolated Spinal Cord. *J Neurosci*. 16:7063-7076

Brown TG (1911). The intrinsic factors in the act of progression in the mammals. *Proc. Roy. Soc.* 84: 308.

Brownstone, R and Wilson, J. (2008). Strategies for delineating spinal locomotor rhythm-generating networks and the possible role of Hb9 interneurons in rhythmogenesis. *Brain research reviews*. 57:64-76

Cazalets JR, Borde M, Clarac F (1995) Localization and organization of the central pattern generator for hindlimb locomotion in newborn rat. *J. Neurosci*. 15:4943–51

Cheng L, Samad OA, Xu Y, Mizuguchi R, Luo P, Shirasawa S, Goulding M, Ma Q (2005) Lbx1 and Tlx3 are opposing switches in determining GABAergic versus glutamatergic transmitter phenotypes. *Nat Neurosci* 8:1510–5.

Cowley KC, Schmidt BJ. (1997) Regional distribution of the locomotor pattern-generating network in the neonatal rat spinal cord. *J. Neurophysiol*. 77:247–59

Crone SA, Quinlan KA, Zagoraiou L, Droho S, Restrepo CE, Lundfald L, Endo T, Setlak J, Jessell TM, Kiehn O, Sharma K (2008) Genetic ablation of V2a ipsilateral interneurons disrupts left-right locomotor coordination in mammalian spinal cord. *Neuron* 60:70–83.

Crone SA, Zhong G, Harris-Warrick R, Sharma K (2009) In mice lacking V2a interneurons, gait depends on speed of locomotion. *J Neurosci* 29:7098 –7109.

Dai X, Noga BR, Douglas JR, Jordan LM (2005) Localization of spinal neurons activated during locomotion using the c-fos immunohistochemical method. *J. Neurophysiol.* 93:3442–52

Del Negro CA, Koshiya N, Butera RJ & Smith JC (2002) Persistent sodium current, membrane properties and bursting behaviour of pre-Botzinger complex inspiratory neurons in vitro. *J Neurophysiol* 88:2242–2250.

Dougherty K, Kiehn O (2010) Firing and cellular properties of V2a interneurons in the rodent spinal cord. *J Neurosci* 30:24 –37.

Freusberg A (1874) Reflexbewegungen beim Hunde. *Pflügers Arch.* 9, 358–391.

Gosgnach S, Lanuza GM, Butt SJ, Saueressig H, Zhang Y, Velasquez T, Riethmacher D, Callaway EM, Kiehn O, Goulding M (2006) V1 spinal neurons regulate the speed of vertebrate locomotor outputs. *Nature* 440:215-219.

Gorelova NA, Yang CR (2000) Dopamine D1/D5 receptor activation modulates a persistent sodium current in rat prefrontal cortical neurons in vitro. *J Neurophysiol* 84:75– 87.

Goulding M (2009) Circuits controlling vertebrate locomotion: moving in a new direction. *Nat Rev Neurosci* 10:507-518

Goulding M, Lanuza G, Sapir T, Narayan S. (2002). The formation of sensorimotor circuits. *Curr Opin Neurobiol.* 12:508-515.

Goulding M, Pfaff SL. (2005). Development of circuits that generate simple rhythmic behaviors in vertebrates. *Curr Opin Neurobiol.* 15:14-20.

Gray P, Hayes J, Ling G, Llona I, Tupal S, Picardo M, Ross S, Hirata T, Corbin J, Eugén J, and Del Negro (2010) Developmental Origin of PreBotzinger Complex Respiratory Neurons. *J Neurosci* 44:14883-14895

Grillner S, Zangger P (1979) On the central generation of locomotion in the low spinal cat. *Exp. Brain Res.* 34:241–61

Grillner, S., Buchanan, J.T., Lansner, A (1988) Simulation of the segmental burst generating network for locomotion in lamprey. *Neurosci. Lett.* 89:31–35.

Guertin, P (2009) The mammalian central pattern generator for locomotion. *Brain Research Reviews* 62:45-56.

Harvey PJ, Li X, Li Y, Bennett DJ (2006) 5-HT₂ receptor activation facilitates a persistent sodium current and repetitive firing in spinal motoneurons of rats with and without chronic spinal cord injury. *J Neurophysiol* 96:1158–1170.

Hinckley CA, Hartley R, Wu L, Todd A, Ziskind-Conhaim L (2005) Locomotor-like rhythms in a genetically distinct cluster of interneurons in the mammalian spinal cord. *J. Neurophysiol.* 93:1439–49

Hochman S, Jordan LM, MacDonald JF (1994) N-methyl-d-aspartate receptor-mediated voltage oscillations in neurons surrounding the central canal in slices of rat spinal cord. *J. Neurophysiol.* 72:565–77

Jankowska, E., Jukes, M.G., Lund, S., Lundberg, A (1967) The effect of DOPA on the spinal cord. 6. Half-centre organization of interneurones transmitting effects from the flexor reflex afferents. *Acta Physiol. Scand.* 70:389–402

Jessell TM, Kiehn O, Sharma K (2008) Genetic ablation of V2a ipsilateral interneurons disrupts left-right locomotor coordination in mammalian spinal cord. *Neuron* 60:70–83.

Kiehn O, Johnson BR, Raastad M (1996) Plateau properties in mammalian spinal interneurons during transmitter-induced locomotor activity. *Neuroscience* 75:263–73

Kjaerulff O, Barajon I, Kiehn O (1994) Sulphorhodamine-labeled cells in the neonatal rat spinal cord following chemically induced locomotor activity in vitro. *J. Physiol.* 478(Pt. 2):265–73

Kjaerulff O, Kiehn O (1996) Distribution of networks generating and coordinating locomotor activity in the neonatal rat spinal cord in vitro: a lesion study. *J. Neurosci.* 16:5777–94

Kudo N, Yamada T (1987) N-methyl-D-aspartate induced locomotor activity in a spinal cord hind limb muscle preparation of the newborn studied in vitro. *Neurosci Lett* 75:43–48.

Kwan AC, Dietz SB, WebbWW, Harris-WarrickRM (2009) Activity of Hb9 interneurons during fictive locomotion in mouse spinal cord. *J Neurosci* 29:11601–11613.

Lafreniere-Roula, M., McCrea, D.A (2005) Deletions of rhythmic motoneuron activity during fictive locomotion and scratch provide clues to the organization of the mammalian central pattern generator. *J. Neurophysiol.* 94:1120–1132.

Lanuza GM, Gosgnach S, Pierani A, Jessell TM, GouldingM (2004) Genetic identification of spinal interneurons that coordinate left-right locomotor activity necessary for walking movements. *Neuron* 42:375–386.

Liu J, Jordan LM. (2005) Stimulation of the parapyramidal region of the neonatal rat brainstem produces locomotor-like activity involving spinal 5-HT₇ and 5-HT_{2A} receptors. *J. Neurophysiol.* 94:1392–404

Lundfald L, Restrepo CE, Butt SJ, Peng CY, Droho S, Endo T, Zeilhofer HU, Sharma K, Kiehn O (2007) Phenotype of V2-derived interneurons and their relationship to the axon guidance molecule EphA4 in the developing mouse spinal cord. *Eur J Neurosci* 26:2989–3002.

Magnuson DS, Lovett R, Coffee C, Gray R, Han Y (2005) Functional consequences of lumbar spinal cord contusion injuries in the adult rat. *J. Neurotrauma* 22:529–43

McCrea, D.A., Rybak, I.A (2008) Organization of mammalian locomotor rhythm and pattern generation. *Brain Res. Rev.* 57:134–146.

Mizuguchi R, Kriks S, Cordes R, Gossler A, Ma Q, Goulding M (2006) *Ascl1* and *Gsh1/2* control inhibitory and excitatory cell fate in spinal sensory interneurons. *Nat Neurosci* 9:770–8.

Orlovsky G, Deliagina T, and Grillner (1999) Neuronal control of locomotion. From mollusc to man. Oxford University Press. Oxford, NY. pg. 164.

Pearson K, Misiaszek J, Fouad K (1998) Enhancement and resetting of locomotor activity by muscle afferents. *Ann N Y Acad Sci.* 860:203-15.

Pierani A, Moran-Rivard L, Sunshine MJ, Littman DR, Goulding M, Jessell TM (2001) Control of interneuron fate in the developing spinal cord by the progenitor homeodomain protein Dbx1. *Neuron* 29:367–384.

Pillai A, Mansouri A, Behringer R, Westphal H, Goulding M (2007) Lhx1 and Lhx5 maintain the inhibitory neurotransmitter status of interneurons in the dorsal spinal cord. *Development* 134:357–66.

Pumain R, Heinemann U (1981) Extracellular calcium and potassium changes in mammalian neocortex. *Adv Biochem Psychopharmacol* 29:53–58.

Rabe N, Gezelius H, Vallstedt A, Memic F, Kullander K (2009) Netrin-1-Dependent Spinal Interneuron Subtypes Are Required for the Formation of Left-Right Alternating Locomotor Circuitry. *J Neurosci* 29:15642-15649

Sapir T, Geiman EJ, Wang Z, Velasquez T, Mitsui S, Yoshihara Y, Frank E, Alvarez FJ, Goulding M. (2004) Pax6 and engrailed 1 regulate two distinct aspects of renshaw cell development. *J Neurosci* 24:1255–64.

Saueressig H, Burrill J, Goulding M (1999) Engrailed-1 and netrin-1 regulate axon pathfinding by association interneurons that project to motor neurons. *Development* 126:4201–12.

Sherrington CS (1910) Flexion-reflex of the limb, crossed extension-reflex, and reflex stepping and standing. *J. Physiol.* 40:28–12

Shik M, Severin F, Orlovsky G (1966) Control of walking and running by means of electrical stimulation of the mid-brain. *Biophysics.* 11:756-765

Smith JC, Feldman JL (1987) In vitro brainstem-spinal cord preparations for study of motor systems for mammalian respiration and locomotion. *J Neurosci Methods* 21:321–333

Tanabe and Jessell (1996). Diversity and Pattern in the Developing Spinal Cord. *Science* 274:1115-1123

Tazerart S, Vinay L, Brocard F (2008) The persistent sodium current generates pacemaker activities in the central pattern generator for locomotion and regulates the locomotor rhythm. *J Neurosci* 28:8577– 8589.

Thuret S, Moon LD, Gage FH (2006) Therapeutic interventions after spinal cord injury. *Nat Rev Neurosci* 7:628-643.

Yamada T, Placzek M, Tanaka H, Dodd J, Jessell TM (1991) Control of cell pattern in the developing nervous system: polarizing activity of the floor plate and notochord. *Cell* 64:635-647

Wilson JM, Hartley R, Maxwell DJ, Todd AJ, Lieberam I, Kaltschmidt JA, Yoshida Y, Jessell TM, Brownstone RM (2005) Conditional rhythmicity of ventral spinal interneurons defined by expression of the Hb9 homeodomain protein. *J Neurosci* 25: 5710–5719

Zagoraiou L, Akay T, Martin JF, Brownstone RM, Jessell TM, Miles GB (2009) A cluster of cholinergic premotor interneurons modulates mouse locomotor activity. *Neuron* 64:645– 662.

Zhang Y, Narayan S, Geiman E, Lanuza GM, Velasquez T, Shanks B, Akay T, Dyck J, Pearson K, Gosgnach S, Fan CM, Goulding M (2008) V3 spinal neurons establish a robust and balanced locomotor rhythm during walking. *Neuron* 60:84 –96.

Zhong G, Droho S, Crone S, Dietz S, Kwan AC, Webb WW, Sharma K, Harris-Warrick RM (2010) Electrophysiological characterization of the V2a interneurons and their locomotor-related activity in the neonatal mouse spinal cord. *J Neurosci* 30:170 –182.

Ziskind-Conhaim L, Wu L, Wiesner EP (2008) Persistent sodium current contributes to induced voltage oscillations in locomotor-related Hb9 interneurons in the mouse spinal cord. *J Neurophysiol* 100:2254 –2264.

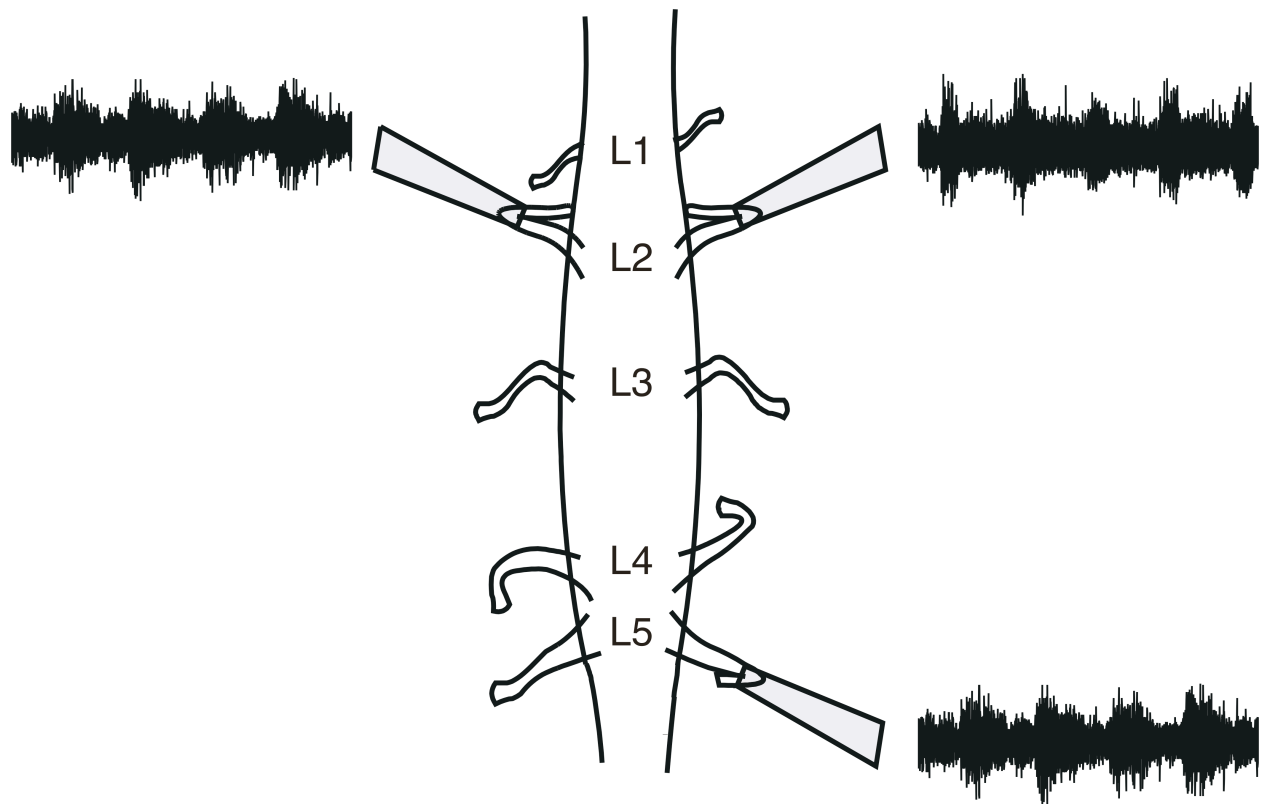


Figure 1-1. In-vitro isolated spinal cord preparation. Suction electrodes record activity from L2 and L5 ventral roots. Pharmacological excitation with 5HT and NMDA generates rhythmic fictive locomotor activity, which is marked by alternation between the left and right flexors (i.e. L2 vs L2) as well as ipsilateral flexor and extensors (L2 vs L5).

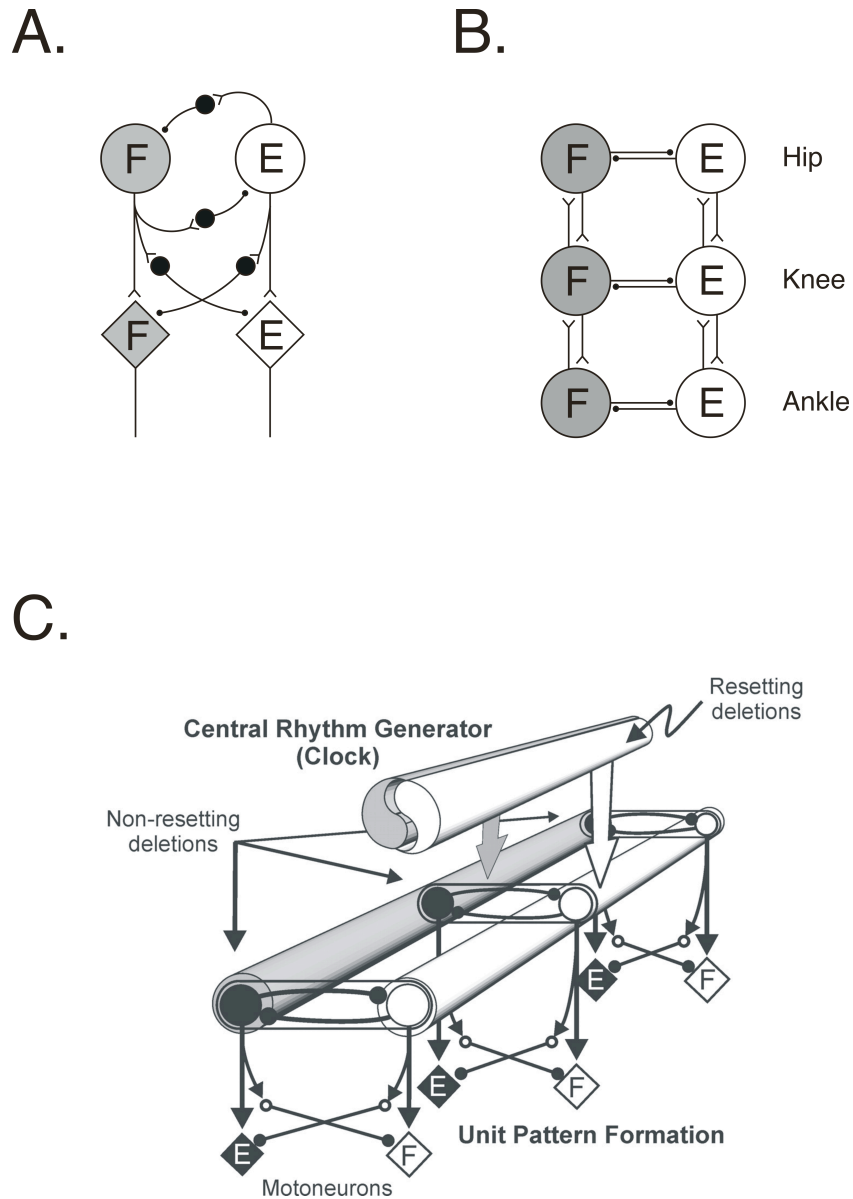


Figure 1-2. Proposed models of the locomotor CPG. A. Brown's original half centre model developed to explain simple alternation between flexor and extensor muscles in an isolated spinal cord. B. Grillner's unit burst generator model consisting of individual oscillators for each joint (hip, knee, and ankle). C. McCrea's two layer model consisting of a rhythm generating network (i.e. clock) and an pattern forming network. (figure taken from Lafreniere-Roula et al. 2005).

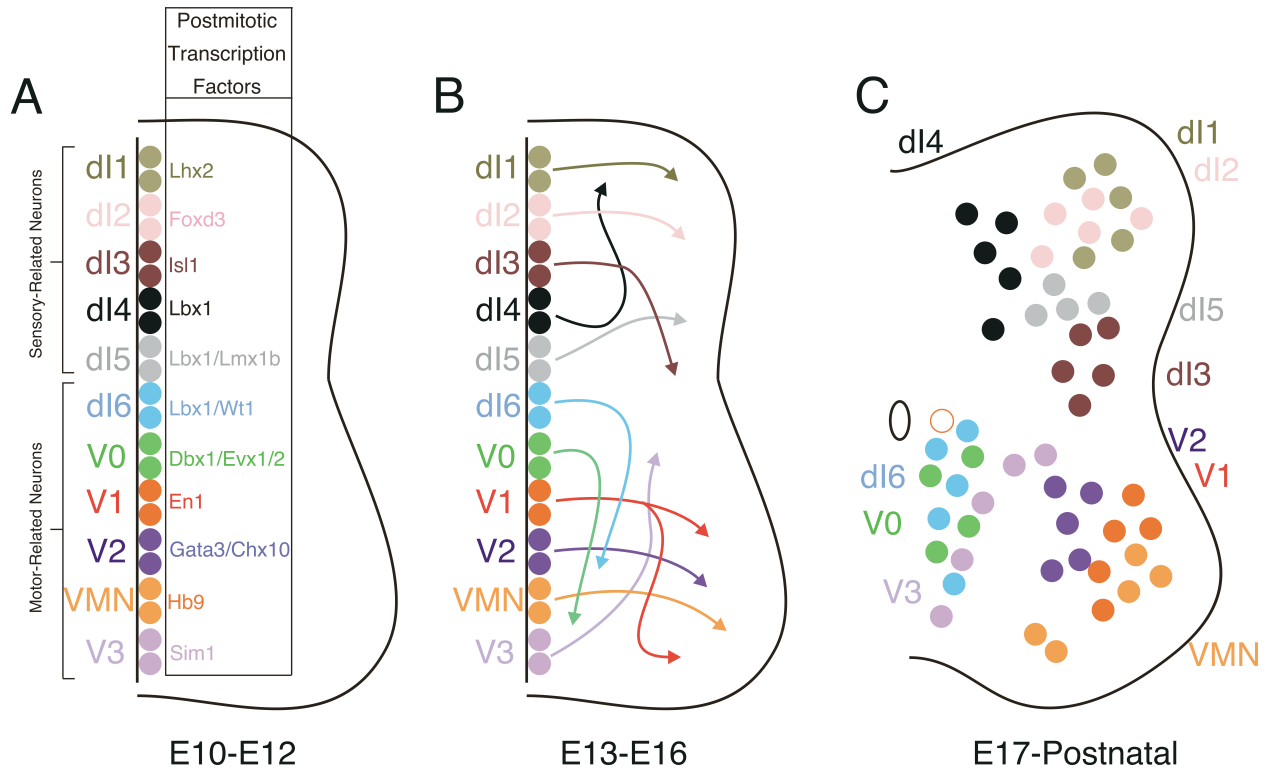


Figure 1-3. A. Transcription factors expressed in spinal cell populations (dI1-V3) at progenitor stage (embryonic day 9;E9) and postmitotic stage (E11). B. From E13-E16 cells migrate towards settling positions. C. Just before birth, cell populations reach their final positions in the spinal cord where they remain throughout adulthood.

Table 1. Summary of genetically defined interneuronal populations

Cell Population	Subpopulations	Neurotransmitter Phenotype	Axonal Projection	Knockout Phenotype	Primary Reference
dI6		Some cells inhibitory	Some cells commissural	Not determined	Goulding (2009) Rabe et al. (2010)
V0	V0 _D	Inhibitory/Excitatory	Primarily commissural	Loss of left-right coordination	Pierani et al. (2001) Lanuza et al (2004) Zagoraïou et al. (2009)
	V0 _v	Inhibitory/Excitatory	Primarily commissural		
		V0 _{C/G}	Excitatory		
V1		Inhibitory	Ipsilateral	Slow rhythm	Saueressig et al. (1999) Gosgnach et al. (2006)
V2	V2a	Excitatory	Ipsilateral	Left-right synchrony at high speed	Lundfald et al. (2007) Crone et al. (2008) Crone et al. (2009) Dougherty et al. (2010) Zhong et al (2010)
	V2b	Inhibitory	Primarily ipsilateral	Not determined	Lundfald et al. (2007) Lanuza et al. (2007) Zhang et al. (2010)
V3		Excitatory	Ipsilateral and Commissural	Unbalanced rhythm	Zhang et al. (2008)
Hb9		Excitatory	Ipsilateral	Not determined	Hinkley et al. (2005) Wilson et al (2005) Kwan et al. (2009)

Chapter 2 -

Whole cell recordings from visualized neurons in inner laminae of the functionally intact spinal cord.¹

¹ A version of this chapter has been published. Dyck and Gosgnach 2009. J Neurophysl. 102: 590-597.

2.1 Introduction

The manner in which specific neurons are interconnected to produce physiological outputs has long been a fundamental issue for neuroscientists, particularly those studying neural circuits. One neural circuit in which connectivity has proven elusive is the mammalian locomotor central pattern generator (i.e. the locomotor CPG). It was first proposed that a neural network was responsible for the specific pattern of motoneuron firing resulting in locomotor muscle synergies almost a century ago (Brown, 1911). In the years since, there has been a great deal of study attempting to identify component interneurons of this circuit as well as patterns of connectivity (see Kiehn, 2006 for review). Traditional methods aimed at studying the locomotor CPG have employed *in vivo* and *in vitro* techniques to identify and characterize single interneurons based on their electrophysiological characteristics, and used anatomical tracing techniques to determine their projection patterns. These approaches have been effective in providing detailed network structure of locomotor circuits in non-mammalian species (Grillner, 2003; Roberts et al. 1998). Despite this, the large number of cells in the mammalian spinal cord, coupled with the fact that neurons of a similar function are intermingled with others of different functions, makes the task of recording from a significant number of functionally homogeneous neurons extremely difficult.

Recently, the identification of discrete neuronal populations in the central nervous system (CNS), via molecular genetic characterization of gene and transcription factor expression at early embryonic time points, has led to optimism that an understanding of the structure and function of the locomotor CPG is attainable (Tanabe and Jessell, 1996; Goulding et al. 2002). Since gene and transcription factor expression determine neuronal characteristics such as cell fate, channel

composition, axonal projection pattern and neurotransmitter phenotype, it stands to reason that populations of neurons with a similar genetic lineage will share many properties, and perhaps have an analogous function in locomotion (Goulding et al. 2002). Molecular genetic techniques have been used to silence, ablate, and label (via expression of reporter proteins) populations of neurons in the ventral spinal cord and show that they have specific functional roles in the production of locomotor activity (Lanuza et al. 2004; Gosgnach et al. 2006; Crone et al. 2008; Zhang et al. 2008). Despite this progress, there have been few investigations focusing on the intrinsic membrane properties of any of the genetically-defined neuronal populations. These types of studies are key to furthering our understanding of how the locomotor CPG functions since the behavioural outputs generated by the CPG are reliant on the intrinsic membrane properties of its component interneurons (Harris-Warrick, 2002).

The scarcity of these types of studies is, at least in part, due to the lack of an appropriate preparation for the targeting of labeled interneurons with a recording electrode. While it is feasible to visually identify and record from genetically-labeled neurons located in superficial laminae since they are visible through the surface of the spinal cord (Nishimaru et al. 2006), a major impediment to the aforementioned experiments is that the core of the locomotor CPG is located in the ventromedial aspect of the lumbar spinal cord close to the central canal (Kjaerulff and Kiehn, 1996). Due to the depth of these neurons (200 μ m-300 μ m from the ventral surface of the spinal cord in the neonatal mouse), those expressing reporter proteins cannot be visualized nor targeted with a recording electrode in the intact preparation. It has therefore been necessary to devise alternative techniques to study these neurons. Thus far two techniques have been used. The first is the spinal

cord slice technique in which a 200 μ m-300 μ m coronal section of the lumbar spinal cord is cut, and labeled neurons close to the cut surface are visible and can be recorded (Wilson et al. 2007). The second is the hemisect technique in which a midsagittal section of the spinal cord (Kiehn et al. 1996) allows labeled cells located close to the midline to be targeted for recording (Hinckley et al. 2005, Hinckley et al. 2006). Since the locomotor CPG has been shown to be distributed throughout the ventromedial aspect of the lower thoracic and lumbar spinal cord and interneurons that coordinate bilateral alternation of the CPG send axons through the ventral commissure, neither of these techniques are ideal as they both involve a complete cut of the spinal cord and substantial damage to this neural circuit.

Here we describe a method which enables the visualization of neurons that express reporter proteins while leaving neuronal connectivity between the left and right side of the spinal cord, as well as all tissue rostral to the recorded neuron, intact. Since the ventral portion of the spinal cord is unlesioned, connectivity between different components of the CPG, as well as connectivity between brainstem centres that initiate locomotor activity and the CPG, remain intact and can be mapped. Since the size and the location of the notch can vary, this technique allows for the electrophysiological and anatomical investigation of neurons and neural networks throughout the CNS.

2.2 Materials and Methods

Animals and preparation

All animal procedures were in accord with the Canadian Council on Animal Care (CCAC) and approved by the Animal Welfare Committee at the University of Alberta. Experiments were performed on 31 neonatal mice aged postnatal day 0 (P0) - postnatal day 4 (P4). The mice used in these experiments resulted from a cross between the *Dbx1^{Cre}* strain, which express the Cre recombinase in the *Dbx1* locus (gift from Dr. Martyn Goulding, Salk Institute for Biological Studies, La Jolla, CA) and the *ROSA26^{EGFP}* reporter strain (Jackson Labs; Srinivas et al. 2001) which have EGFP cDNAs inserted into the *ROSA26* locus, preceded by a loxP-flanked stop sequence. PCR was used to genotype offspring. Those that were both Cre and EGFP positive expressed EGFP in a population of interneurons close to the central canal. A portion of these cells are V0 interneurons which are located in lamina VIII throughout the rostral-caudal extent of the spinal cord (Pierani et al. 2002), and are involved in producing appropriate left-right alternation during locomotion (Lanuza et al. 2004). Mice were anesthetized via inhalation of isoflurane (4% delivered with 95% O₂-5% CO₂). After evisceration, the brainstem-spinal cord was dissected out in a bath containing oxygenated, ice-cold dissecting artificial cerebrospinal fluid (d-aCSF) containing (in mM) 111 NaCl, 3.08 KCl, 11 glucose, 25 NaHCO₃, 1.18 KH₂PO₄, 3.7 MgSO₄, 0.25 CaCl₂ (pH of 7.4, osmolarity 280-300 mOsm). Next, the dorsal roots were cut away using fine microscissors to allow for easy access to the ventral roots with a suction electrode which would be used to monitor fictive locomotor activity. A thin strip of agarose (4%, 20 mm length x 1.75 mm width x 1.75 mm height) was glued (Roti Coll 1, Carl Roth) to the ventral midline of the spinal cord, along its length, taking care to avoid the ventral roots (Figure 2-1A). The strip of agarose was

then glued to a second platform of 4% agarose (3 cm length x 1 cm width x 0.75 cm-1 cm height) that was cut along its length at a 1-2 degree angle resulting in the caudal end of the brainstem/spinal cord being positioned higher than the rostral end (Figure 2-1B, 2-1C). The entire preparation (situated dorsal side up, ventral side glued to agarose block) was transferred to a vibratome (Leica VT1200S, Leica Microsystems) sectioning chamber containing oxygenated d-aCSF. The sectioning window of the blade was specified to span from the first (L1) to the sixth (L6) lumbar segments of the spinal cord and was lowered until it just made contact with the dorsal surface of the L6 segment. Using a sapphire etched blade (Leica Microsystems), 200–300 μm were cut away from the dorsal spinal cord in 50 μm increments at a speed of 0.10 mm/s with a blade displacement of 1.95 mm to create a notch (Figure 2-1C). Sectioning continued until the dorsal aspect of the central canal was visible using a dissecting microscope (Figure 2-1D). Following sectioning, the agarose platform was carefully cut away and the preparation was situated dorsal side up on a coverslip in a plexi-glass recording chamber and held in place via nylon threads stretched over a platinum wire flattened into a horseshoe shape.

Electrophysiological Recording

The recording chamber containing the preparation was moved onto the stage of an upright microscope (Zeiss Axioskop 2 FS fitted with a GFP filter [490 nm] and infrared differential interference contrast [IR-DIC] optics) and constantly perfused with room temperature, oxygenated recording aCSF (r-aCSF) containing (in mM): 111 NaCl, 3.08 KCl, 11 glucose, 25 NaHCO₃, 1.18 KH₂PO₄, 1.25 MgSO₄, 2.52 CaCl₂ (pH of 7.4, osmolarity 280-300 mOsm). The notch that had been made in the cord was situated under the objective lens. Using brightfield and a low power (4x)

objective, bipolar suction electrodes (A-M Systems Inc.) were positioned on two or three of the flexor-related (second lumbar i.e. L2) and extensor-related (fifth lumbar i.e. L5) ventral roots on either side of the spinal cord and suction was applied with a 5cc syringe. Fictive locomotor activity was induced by bath application of 10 μ M 5-hydroxytryptophan (5-HT) and 5 μ M N-Methyl-D-Aspartate (NMDA) (both from Sigma-Aldrich). Electroneurogram (ENG) recordings were obtained from the ventral roots via the suction electrodes, amplified (20,000x) and band pass filtered (100Hz-1kHz) with custom made equipment (R&R Designs).

For patch clamp recordings, patch electrodes (tip resistance: 3–5 M Ω) were pulled from borosilicate glass (Harvard Apparatus) and filled with internal solution containing (in mM): K-gluconate, 138; Hepes, 10; CaCl₂, 0.0001; GTP-Li, 0.3; ATP-Mg, 5 (pH adjusted to 7.2, osmolarity 290-305 mOsm). Liquid junction potential was calculated to be ~12mV. Em values were not corrected for the liquid junction potential since the extent to which the contents of the cells had been completely replaced with the pipette solution was unclear. In some cases either Lucifer Yellow (1%, Sigma-Aldrich) or Neurobiotin (0.2%, Vector Labs) were added to the patch electrode to allow for intracellular labeling. A micromanipulator (MPC-385, Sutter Instruments) was used to position the electrode over the notch and lower it into the tissue. GFP+ cells were identified using the 40x objective, a GFP filter, and a live image video camera (IR-1000, Dage-MTI). An IR-DIC filter was used to target these cells with a patch clamp electrode. Using a whole cell recording amplifier (Multiclamp 700B, Axon Instruments) in voltage clamp mode, a 10 mV square pulse (50 Hz) was used to monitor tip resistance as the electrode was advanced towards the cell of interest. Once a giga-ohm seal with a cell was formed, the command voltage was set to -60 mV and gentle suction

was applied to break through the membrane to obtain a whole cell recording. Series resistance (R_s) and cell capacitance (C_m) were determined in voltage-clamp mode using the compensation features on the Multiclamp commander software (Axon Instruments). R_s was monitored throughout the course of each recording (if working in current-clamp mode we would periodically switch into voltage clamp to monitor R_s). Initial values of R_s were typically 10-15 M Ω . Recordings where R_s exceed 30 M Ω were excluded from analysis. Membrane resistance (R_m) was calculated off-line by taking the inverse slope of the linear portion of the current-voltage (I-V) relationship. In some instances, a small amount of negative bias current (10-15 pA) was required to hyperpolarize the cells (to -65 mV) to prevent spontaneous firing of action potentials. Recordings from healthy neurons could be made >6h after cutting the notch in the spinal cord. All whole cell and ENG data was digitized using an analog-digital converter (Digidata 1440A, Axon Instruments) and recorded using pClamp software (Axon Instruments) on a PC. All photomicrographs of GFP⁺ neurons during recording were taken with a monochrome CCD camera (ORCA-R2, Hamamatsu Photonics) fixed to the microscope used for recording. Following experiments in which Lucifer Yellow or Neurobiotin were included in the intracellular solution, the spinal cords were immediately fixed in 4% paraformaldehyde/PBS for 45 minutes, washed in PBS and moved to the stage of an inverted spinning-disk confocal microscope (IX81, Olympus) fitted with a camera (EM-CCD, Hamamatsu Photonics). Z-stack images and 3D reconstructions of the filled interneurons were collected using Volocity (Improvision Inc.) software and processed using both Volocity and Photoshop (Adobe Systems) software.

Data Analysis

Onsets and offsets of ENG activity were selected manually during a continuous 5-10 minute window of stable fictive locomotion using Clampfit software (Axon Instruments). Measurements of cycle period (defined as the interval between onset of burst n and burst $n+1$) and burst duration (defined as time between onset of burst n and offset of burst n) were determined by analysis of ENG activity of the second lumbar ventral root in the left side (lL2) or right side (rL2) of the spinal cord. All means are reported \pm standard deviation (SD). Student's t -tests were used to determine if means were significantly different. Circular statistics (Zar, 1974) were used to determine the coupling strength between L2 and L5 ventral roots. lL2 bursts occurring over the period of analysis were selected, and their phase values were calculated in reference to the onsets of each rL2 and lL5 burst. Phase values were determined by dividing the latency between the onset of the first lL2 burst and the following burst in rL2 (or lL5) by the cycle period. This resulted in values of 0.5 when lL2 and rL2 roots were completely out of phase (i.e. appropriate left-right alternation) and values of 1 when they were in phase (i.e. co-bursting). The phase values were imported into MATLAB (The MathWorks Inc.) and a custom script (J.Dyck) was used to generate a polar plot and provide r -values. In order to determine whether the sample r was large enough to confidently indicate a nonuniform distribution of points, Rayleigh's test ($R=nr$) was performed. The resulting value for R was compared to a critical values table (Zar, 1974).

To determine the significance of coupling between the firing behaviour of GFP⁺ interneurons and ventral root activity during fictive locomotion, the total number of action potentials fired by a cell were manually counted during 50 fictive locomotor cycles. Individual

action potentials were classified as either those that occurred during the active phase of the contralateral flexor-related ventral root (i.e. cL2) or those that occurred during the active phase of the contralateral extensor-related ventral root (i.e. cL5). The Chi-square test was then used to determine whether the interneuron preferentially fired action potentials in phase with contralateral flexor or extensor ENG activity, or whether action potential firing was evenly distributed within the two phases of fictive locomotion. A critical value of $p < 0.05$ in the Chi-square distribution was used to determine significance.

2.3 Results

In order to determine whether this preparation could be used to study neurons that comprise the locomotor CPG and the manner in which they are interconnected, it is necessary to demonstrate that after the notch is cut in the spinal cord; a) the locomotor CPG is intact and functional b) neurons located in the ventromedial region of the spinal cord are visible, can be targeted for whole cell recording and identified post-hoc in order to analyze axonal projection of those that have been filled with an intracellular tracer and c) these neurons are healthy and can fire rhythmically during fictive locomotion.

To assess whether the locomotor CPG was intact and functional, ENGs were recorded from lumbar ventral roots during pharmacologically-induced fictive locomotion in unlesioned spinal cords (n=7) as well as spinal cords in which a notch had been cut in the dorsal region of the L1-L6 segments (n=8). Coordination between the flexor and extensor related ventral roots as well as timing of fictive locomotor activity were compared. Normal fictive locomotor activity in the

neonatal mouse in vitro spinal cord preparation is characterized by rhythmic alternation of ENG activity between ipsilateral L2 (flexor related) and L5 (extensor related) ventral roots as well as alternation between contralateral L2 ventral roots and contralateral L5 ventral roots with a cycle period of approximately 4 seconds (Kullander et al. 2003; Lanuza et al. 2004; Gosgnach et al. 2006). This preparation is routinely used to study the locomotor CPG and has been shown to produce rhythmic flexor and extensor outputs similar to those underlying locomotion in the adult despite the fact that both flexor and extensor motor units course through common lumbar ventral roots (Cowley and Schmidt 1994). Lesions to the locomotor CPG result in aberrant coordination of the ENG activity and/or increases in both cycle period and burst duration (Cazalets et al. 1995; Cowley and Schmidt 1997). NMDA (5 μ M) and 5-HT (10 μ M) were applied to the bath containing both unlesioned and notched spinal cords to elicit fictive locomotor activity. In both groups, appropriate alternation of ENG activity between flexor-related ventral roots on opposite sides of the spinal cord (i.e. lL2, rL2) and between flexor and extensor-related ventral roots on the same side of the spinal cord (i.e. lL2, lL5) was observed (Figure 2-2). In addition, mean cycle period (unlesioned 4.12 ± 0.69 s n=7, notch 3.98 ± 0.71 s n=7 p<0.05, t-test) and mean burst duration (unlesioned 1.9 ± 0.56 s, n=7, notch 2.10 ± 0.32 s, n=8, p<0.05, t-test) in the notch group were not significantly different than those evoked using the same drug concentrations in the unlesioned spinal cord. These results provide evidence that this preparation can be used to assess the function of the locomotor CPG since the outputs do not differ significantly from those in the unlesioned spinal cord. This result is expected since the notch does not extend into the ventral portion of the spinal cord, the region in which the locomotor CPG resides.

The next step in demonstrating the utility of this preparation was showing that labeled neurons in the intermediate nucleus of the spinal cord were clearly visible below the notch, that these cells were healthy, and that whole cell recordings could be made from them. To this end, transgenic mice were used that expressed green fluorescent protein (GFP) in all cells that express the transcription factor Dbx1. Positioning the 40x objective over the notch that had been cut in the spinal cord allowed for identification of these neurons by GFP expression. Once a cell was confirmed to be GFP+, an IR-DIC filter was used and the neuron was targeted for patch clamp recording. Figure 2-3A illustrates the appearance of a GFP+ cell using a GFP and IR-DIC filter. In some cases, Lucifer Yellow (or Neurobiotin) was included with the intracellular solution in the recording pipette. During recording, the tracer passively diffused into the neuron and allowed for post hoc anatomical analysis (Figure 2-3A, 2-3B). In the absence of 5-HT and NMDA (r-aCSF alone), 33 neurons were recorded using the preparation described in order to assess intrinsic membrane properties. The mean membrane potential of these cells was -47.6 ± 3.6 mV, mean spike height 62.7 ± 10.2 mV. Of those in which membrane resistance was calculated (n=16) the mean value was 757.6 ± 342 M Ω . The effect of an intracellular current ramp was a linear increase and decrease of the firing rate with current injection (Figure 2-3C). Collectively, this data provides support that the neurons located under the notch in the spinal cord were healthy, as intrinsic properties did not differ substantially from ventromedially located interneurons recorded from the unlesioned mouse spinal cord (Zhong et al. 2006).

The key to this technique, and what we believe provides an advantage over previous methods, is that it enables visualization and targeting of labeled neurons for patch clamp recording

while leaving the core of the locomotor CPG intact. This allows for the identification of intrinsic cell properties in healthy neurons, and the determination of the specific activity of a neuron in relation to ipsilateral and contralateral fictive locomotor activity. An essential step in proving the utility of this technique therefore, was to demonstrate that recordings could be made simultaneously from both a labeled neuron and from lumbar ventral roots during fictive locomotion. Twenty-one GFP⁺ interneurons were recorded during fictive locomotion. A representative is illustrated in Figure 2-4. In this example, ENG recordings were made from the left L2 and L5 ventral roots while also recording from a neuron located in the L3 segment on the contralateral side of the spinal cord. The health of the locomotor CPG is illustrated by the large (10 mV) depolarizing bursts and action potentials (50 mV amplitude) recorded from the neuron after application of NMDA and 5-HT, as well as the alternation and cycle period of the ENGs recorded from the contralateral L2 and L5 ventral roots. The neuron illustrated in Figure 2-4 is clearly locomotor-related as it depolarizes and fires action potentials in synchrony with the contralateral L2 ventral root (Figure 2-4B, 2-4C). Analysis of the data using the Chi-square test demonstrates that 16 of the 21 GFP⁺ neurons recorded in the presence of 5-HT and NMDA fired rhythmic bursts of action potentials during fictive locomotion. The remaining 5 neurons fired action potentials, however they were not preferentially active during either flexion or extension (i.e. not rhythmically active). Fifteen of the 21 neurons were located in the rostral segments of the lumbar spinal cord (L2 or L3, primarily flexor-related) and six were located in the caudal segment of the lumbar spinal cord (L5, primarily extensor-related). Of the 15 rostrally located cells, 11 were rhythmically active. Nine fired preferentially out of phase, and 2 fired preferentially in phase, with contralateral flexor activity. Of the six caudally located cells, 5 were rhythmically active. Four fired preferentially out of phase, and

1 fired preferentially in phase, with contralateral extensor activity. Since V0 cells are a mixed population of interneurons that project commissurally (Pierani et al. 2002) and are primarily inhibitory (Lanuza et al. 2004) these results are consistent with previous reports suggesting that V0 neurons coordinate left-right alternation during locomotion by inhibiting contralateral motoneurons (Lanuza et al. 2004)

2.4 Discussion

This report describes a new protocol for performing whole cell patch-clamp recordings from genetically-labeled interneurons in the intermediate lamina of the embryonic/neonatal rodent spinal cord while leaving the locomotor CPG functionally intact. It is difficult to imagine any preparation enabling the visualization of interneurons located in the ventral spinal cord that allows for the study of all aspects of neurons that comprise the locomotor CPG (i.e. the effect of sensory feedback on locomotor outputs). We propose that the technique described within is the ideal method to use for analysis of neurons that comprise distributed neural circuits such as the locomotor CPG, since labeled cells are able to be visually identified and targeted with a patch clamp electrode, enabling healthy neurons to be recorded from while simultaneously monitoring robust network activity.

In the present study, the validity of this technique is demonstrated via recordings from genetically identified interneurons located in lamina VIII of the spinal cord. These cells have membrane properties (i.e. membrane potential, spike height, response to an injected current ramp) similar to those observed in the unlesioned spinal cord. In addition, cycle period and coordination of fictive locomotor activity are the same as in an unlesioned spinal cord (Figures 2-2, 2-4).

Rhythmic bursts can be recorded from labeled interneurons and are related to ENG activity recorded from ventral roots (Figure 2-4). Addition of fluorescent tracer to the recording electrode allows for the morphological study of labeled neuronal populations (Figure 2-3B) and can be used to map axonal projection patterns.

Since the initial demonstration that the mammalian CPG could be divided into interneuronal populations based on transcription factor expression, a handful of studies have investigated whether these populations are rhythmically active during locomotion and, if so, their specific role in generating locomotor outputs (Lanuza et al. 2004; Gosgnach et al. 2006; Crone et al. 2008; Zhang et al. 2008). To this point, there have been a paucity of studies investigating membrane properties and connectivity of these genetically-defined neuronal populations. It follows that a better understanding of the mechanism of function of the locomotor CPG relies on our ability to characterize the membrane properties of the cells that comprise this neural network. In addition, identification of connectivity patterns between these populations is crucial if we are to understand how these component neurons interconnect to form a functional circuit.

The studies that have been performed thus far have focused primarily on the Hb9 interneurons, which are intermingled with the V0 population, are located close to the central canal, farthest from the surface of the spinal cord and thus least accessible with a recording electrode. It has been hypothesized that this population is an integral component of the locomotor CPG that may play a role in initiating locomotor activity (Wilson et al. 2005; 2007, Brownstone and Wilson 2008). This makes examining these neurons particularly intriguing as identification of their cellular

properties and axonal projection pattern could serve as a means of identifying how components of the locomotor CPG are interconnected. The Hb9 interneurons can be visually identified in the Hb9:EGFP mouse, where EGFP expression is driven by the Hb9 promoter. Thus far, two approaches have been used to target these neurons for intracellular study. The first has employed the spinal cord slice technique where a thick (200-300 μ m) coronal section of the spinal cord is cut and cells expressing fluorescent markers close to the cut surface can be visualized using a microscope with a GFP filter and IR-DIC optics (Wilson et al. 2005). This technique was used to demonstrate that the Hb9 interneurons display endogenous bursting and led the authors to hypothesize that these cells play a role in activation of the locomotor CPG (Wilson et al. 2007). Despite these exciting experiments, testing this hypothesis directly has proven difficult due to technical limitations. Determining whether these neurons are a component of the locomotor CPG, and if so the specific role that they play, is arduous using this preparation since few, if any ventral roots are present and thus it is difficult to compare the bursting pattern of these neurons to ipsilateral and contralateral fictive locomotor activity. The spinal cord slice preparation is particularly poorly suited for the study of axonal morphology since cutting a slice from the spinal cord removes network connectivity in the rostral-caudal plane. It is therefore not possible to identify synaptic inputs to, or outputs from, these neurons if they originate or terminate more than a few hundred microns from the soma. In addition, this eliminates the possibility of determining whether this population receives synaptic input from the locomotor command centres located in the brainstem.

An alternative approach used to study the Hb9 interneurons has been to perform a

midsagittal section of the spinal cord, situate the preparation in a recording chamber with the cut region (and thus the Hb9 interneurons) exposed to the microscope objective and accessible with a recording electrode using GFP and IR-DIC optics (Hinckley et al. 2005, Hinckley et al. 2006). In this case electroneurogram (ENG) recordings of ventral root activity with a suction electrode allow an assessment of pharmacologically-evoked fictive locomotor outputs. Studies using this approach have shown the Hb9 interneurons to be rhythmically active in phase with the ipsilateral ventral root in the same segment (Hinckley et al. 2006). Like the spinal cord slice technique, however, this technique has key limitations. Perhaps most importantly hemisecting the spinal cord removes one half of the CPG and severs all commissural interneurons. This results in a fictive locomotor pattern that is aberrant, displaying extremely slow bursting in ENGs recorded from the ventral roots when compared to studies in the intact mouse spinal cord using similar concentrations of 5-HT and NMDA. Furthermore, fictive locomotion can only be evoked in hemisected spinal cords approximately 50% of the time (Ziskind-Conhaim et al. 2008). Also, as is the case with the spinal cord slice preparation, since a substantial portion of the lumbar spinal cord has been removed, it stands to reason that this technique is insufficient for an extensive assessment of connectivity, particularly any neurons with commissural axons.

The method described in this report improves on both of these techniques as it allows for the recording of intrinsic membrane properties from neurons while leaving the locomotor CPG functionally intact. In addition, since the ventral portion of the spinal cord is untouched, network connectivity remains largely undisturbed and extensive mapping of the axonal projections from labeled neuronal populations can be performed by adding neuronal tracers such as Lucifer Yellow

to the recording pipette. The preparation is particularly well suited to this task as it allows for mapping of axonal projections in the rostral-caudal, dorsal-ventral, and medial-lateral planes. Intracellular labeling experiments will allow for the identification of downstream targets of the genetically-identified neuronal populations and show promise for providing detailed information on how specific populations are interconnected to produce locomotor activity. In addition to enabling mapping of connectivity within the spinal cord, this technique can potentially be used for the study of connections between locomotor command centres in the midbrain (Matsuyama et al. 2004) and the locomotor CPG, since the descending tract in which these commands travel to the spinal cord (the ventrolateral funiculus) remains intact.

This preparation is particularly beneficial at the current time due to the plethora of recent work demonstrating that molecular strategies, in concert with classical electrophysiological and anatomical approaches provide a powerful means to analyze the structure and function of neural circuits. By varying the location and size of the notch, this method allows for easy access to neurons in all regions of the spinal cord while minimizing tissue damage. It thus provides the best way to access genetically-labeled neurons that comprise neural circuits, and enables identification of electrophysiological properties as well as neuronal connectivity. These are essential requirements if we are to understand how neural circuits, such as the locomotor CPG, are activated and how they generate rhythmic outputs.

2.5 References

Brown, T.G. The intrinsic factors in the act of progression in the mammals. Proc. Roy. Soc. 84:308. 1911.

Brownstone RM, Wilson JM. Strategies for delineating spinal locomotor rhythm-generating networks and the possible role of Hb9 interneurons in rhythmogenesis. Brain Res Rev. 57:64-76. 2008.

Cazalets JR, Borde M, and Clarac F. Localization and organization of the central pattern generator for hindlimb locomotion in newborn rat. J. Neurosci. 15:4943-4951. 1995.

Cowley KC, Schmidt BJ. Some limitations of ventral root recordings for monitoring locomotion in the in vitro neonatal rat spinal cord preparation. Neurosci Lett. 171:142-146. 1994.

Cowley KC, Schmidt BJ. Regional distribution of the locomotor pattern-generating network in the neonatal rat spinal cord. J Neurophysiol. 77:247-259. 1997.

Crone SA, Quinlan KA, Zagoraiou L, Droho S, Restrepo CE, Lundfald L, Endo T, Setlak J, Jessell TM, Kiehn O, Sharma K. Genetic ablation of V2a ipsilateral interneurons disrupts left-right locomotor coordination in mammalian spinal cord. Neuron. 60:70-83. 2008.

Gosgnach S, Lanuza GM, Butt SJ, Saueressig H, Zhang Y, Velasquez T, Riethmacher D, Callaway EM, Kiehn O, Goulding M. V1 spinal neurons regulate the speed of vertebrate locomotor outputs. *Nature*. 440:215-219. 2006.

Goulding M, Lanuza G, Sapir T, Narayan S. The formation of sensorimotor circuits. *Curr Opin Neurobiol*. 12:508-515. 2002.

Grillner S. The motor infrastructure: from ion channels to neuronal networks. *Nat Rev Neurosci*. 4:573-586. 2003.

Harris-Warrick RM. Voltage-sensitive ion channels in rhythmic motor systems. *Curr Opin Neurobiol*. 12:646-651. 2002.

Hinckley CA, Hartley R, Wu L, Todd A, Ziskind-Conhaim L. Locomotor-like rhythms in a genetically distinct cluster of interneurons in the mammalian spinal cord. *J Neurophysiol*. 93:1439-1449. 2005.

Hinckley CA, Ziskind-Conhaim L. Electrical coupling between locomotor-related excitatory interneurons in the mammalian spinal cord. *J Neurosci*. 26, 8477-8483. 2006.

Kiehn O. Locomotor circuits in the mammalian spinal cord. *Annual Rev Neurosci*. 29:279-306.

2006.

Kiehn O, Johnson BR, Raastad M. Plateau properties in mammalian spinal interneurons during transmitter-induced locomotor activity. *Neuroscience*. 75:263-273. 1996.

Kjaerulff O, Kiehn O. Distribution of networks generating and coordinating locomotor activity in the neonatal rat spinal cord in vitro: a lesion study. *J Neurosci*. 16:5777-5794. 1996.

Kudo, N. & Yamada, T. N-methyl-D,L-aspartate-induced locomotor activity in a spinal cord-hindlimb muscles preparation of the newborn rat studied in vitro. *Neurosci. Lett*. 75, 43-48. 1987.

Kullander K, Butt SJB, Le Bret JM, Lundfald, L, Restrepo CE, Rydström A, Klein R, Kiehn O. Role of EphA4 and EphrinB3 in local neuronal circuits that control walking. *Science* 299:1889-1892. 2003.

Lanuza GM, Gosgnach S, Pierani A, Jessell TM, Goulding M. Genetic identification of spinal interneurons that coordinate left-right locomotor activity necessary for walking movements. *Neuron*. 42:375-386. 2004.

Matsuyama K, Nakajima K, Mori F, Aoki M, Mori S. Lumbar commissural interneurons with reticulospinal inputs in the cat: morphology and discharge patterns during fictive locomotion. *J Comp Neurol*. 474:546-561. 2004.

Nishimaru H, Restrepo CE, Kiehn O. Activity of Renshaw cells during locomotor-like rhythmic activity in the isolated spinal cord of neonatal mice. *J Neurosci.* 26:5320-5328. 2006.

Pierani A, Moran-Rivard L, Sunshine MJ, Littman DR, Goulding M, Jessell TM. Control of interneuron fate in the developing spinal cord by the progenitor homeodomain protein Dbx1. *Neuron.* 29:367-84. 2002.

Roberts A, Soffe SR, Wolf ES, Yoshida M, Zhao FY. Central circuits controlling locomotion in young frog tadpoles. *Ann N Y Acad Sci.* 860:19-34. 1998.

Smith J.C. and Feldman J.L. In vitro brainstem-spinal cord preparations for study of motor systems for mammalian respiration and locomotion. *J Neurosci. Methods* 21, 321-333. 1987.

Srinivas S, Watanabe T, Chyuan-Sheng L, William CM, Tanabe Y, Jessell TM, Constantini, F. Cre reporter strains produced by targeted insertion of EYFP and ECFP into the ROSA26 locus. *BMC Dev Biol* 1:4 2001.

Tanabe Y, Jessell TM. Diversity and pattern in the developing spinal cord. *Science.* 274:1115-1123. 1996.

Wilson JM, Cowan AI, Brownstone RM. Heterogeneous electrotonic coupling and synchronization

of rhythmic bursting activity in mouse Hb9 interneurons. *J Neurophysiol.* 98:2370-2381. 2007.

Wilson JM, Hartley R, Maxwell DJ, Todd AJ, Lieberam I, Kaltschmidt JA, Yoshida Y, Jessell TM, Brownstone RM. Conditional rhythmicity of ventral spinal interneurons defined by expression of the Hb9 homeodomain protein. *J Neurosci.* 25:5710-5719. 2005.

Zar, J.H. Circular Distribution. In “Biostatistical Analysis”, p310-327. Prentice Hall, Engelwood Cliffs, NJ. 1974.

Zhang, Y. Narayan, S. Geiman, E. Lanuza, G.M. Velasquez, T. Shanks, B. Akay, T. Dyck, J. Pearson, K. Gosgnach, S. Fan, C.M. Goulding, M. V3 spinal neurons are essential for the robust and balanced motor rhythm that underlies walking movements. *Neuron*, 60: 1-13. 2008.

Zhong G, Díaz-Ríos M, Harris-Warrick RM. Serotonin modulates the properties of ascending commissural interneurons in the neonatal mouse spinal cord. *J Neurophysiol.* 95:1545-1555. 2006.

Ziskind-Conhaim L, Wu, L. Wiesner, E.P. Persistent sodium current contributes to induced voltage oscillations in locomotor-related Hb9 interneurons in the mouse spinal cord. *J. Neurophysiol.* 100:2254-2264. 2008

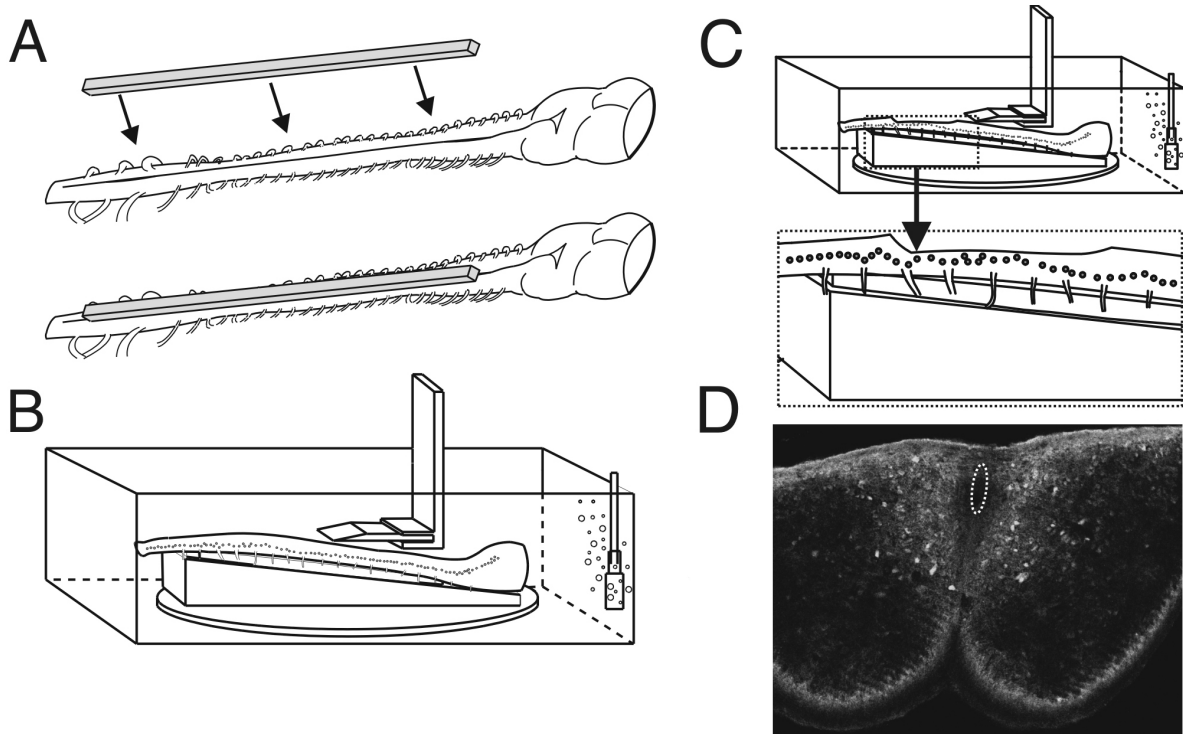


Figure 2-1. A-C Schematic of preparation. A. Thin strip of agarose is attached to ventral midline of spinal cord taking care to avoid ventral roots. B. Agarose strip is attached to angled agarose block with caudal end higher than rostral end and placed in the sectioning tray of a vibratome. Dorsal surface of the cord is exposed to vibratome blade. C. Notch is cut with vibratome and spans from L1-L6 segments. Lower panel is an enlargement of region within dashed box. Circles represent labeled neurons located near the central canal, close to the cut surface. D. Coronal cryostat section cut from notched region of spinal cord. Central canal encircled by dashed oval. GFP+ cells (white) are located in lamina VIII

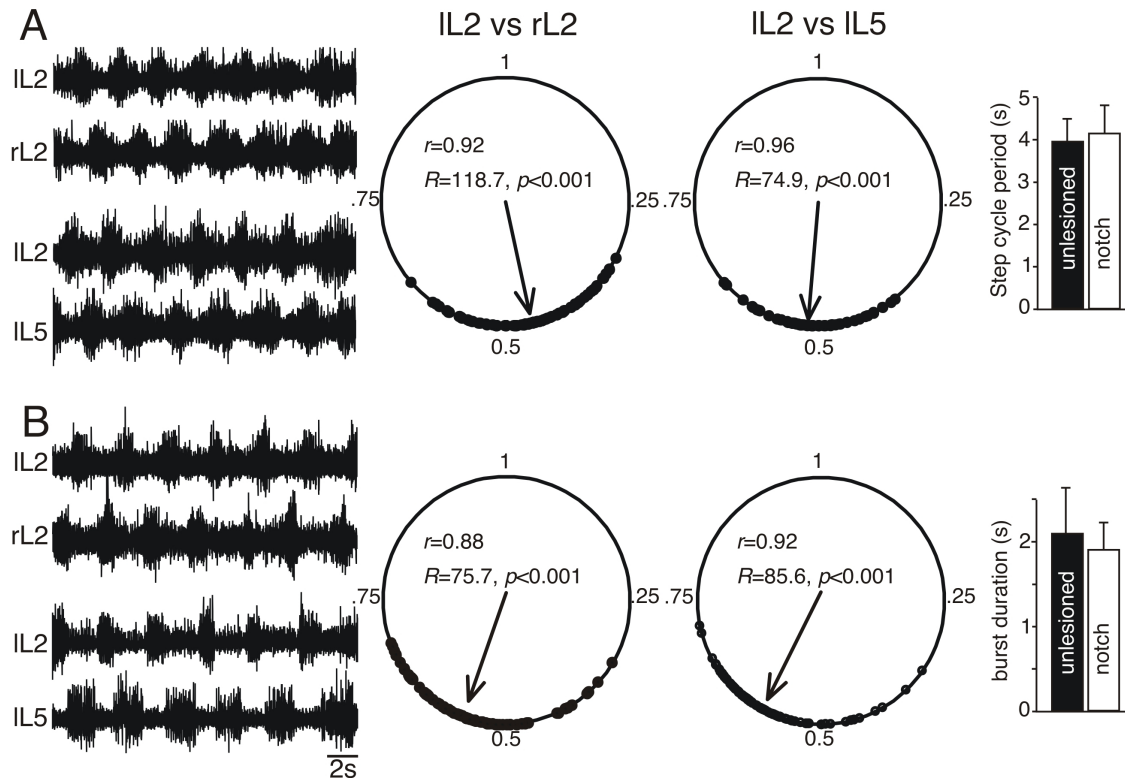


Figure 2-2. Electroneurograms (left) recorded from the L2 (flexor-related) and L5 (extensor-related) ventral roots on the left and right side of an unlesioned spinal cord (A) and a spinal cord with a notch cut on its dorsal surface (B). Ipsilateral alternation of flexor-related and extensor-related ventral roots and the contralateral flexor-related ventral roots is unchanged in the lesioned spinal cord. Appropriate coordination is illustrated in the circular plots in which points are clustered around 0.5 and r-values are close to 1. R values indicate that the points do not comprise a random distribution. Bar graphs to the right demonstrate cycle period and burst duration do not differ significantly between the unlesioned and notched preparations (Bars indicate SD).

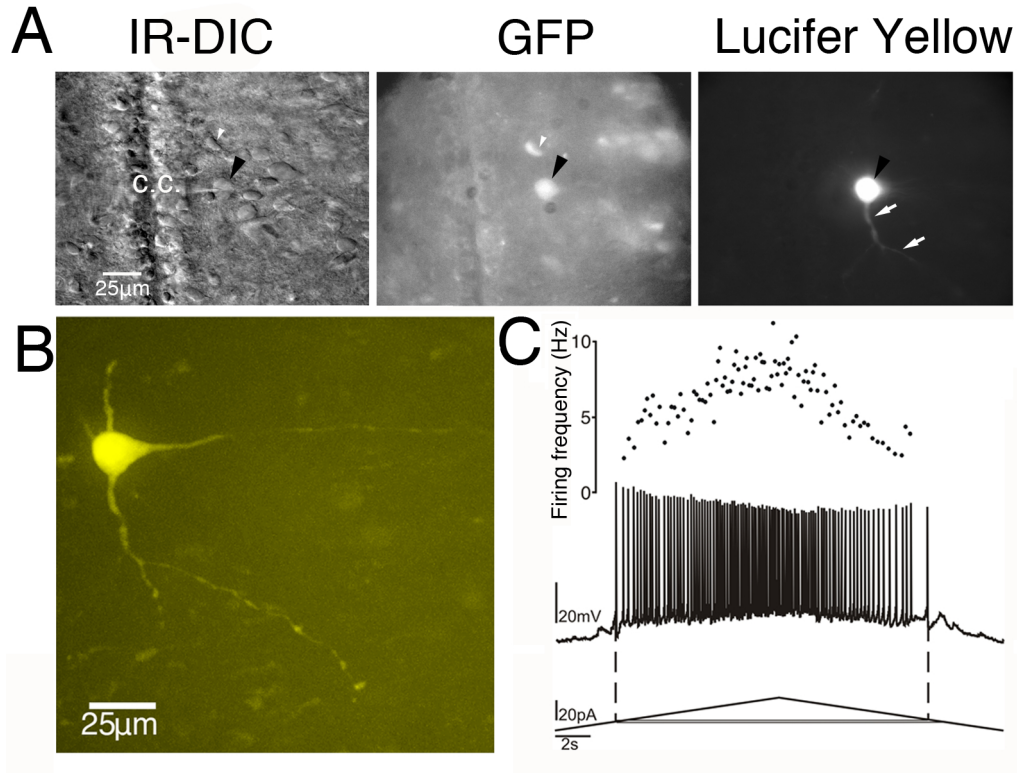


Figure 2-3. A. IR-DIC image (left), fluorescent image showing GFP expression (middle) of a recorded GFP⁺ neuron located just to the right of the central canal (c.c). Soma is indicated by black arrowhead. White arrowhead indicates another GFP⁺ neuron located close by. Right panel illustrates the same cell as it is being filled with Lucifer Yellow. Note the axon leaving the soma (white arrows) B. Collapsed Z-stack reconstruction of the neuron in panel A. C. Firing behaviour of a neuron located below the notch in response to a 40pA current ramp applied over 25s. Note the linear increase and decrease of firing frequency.

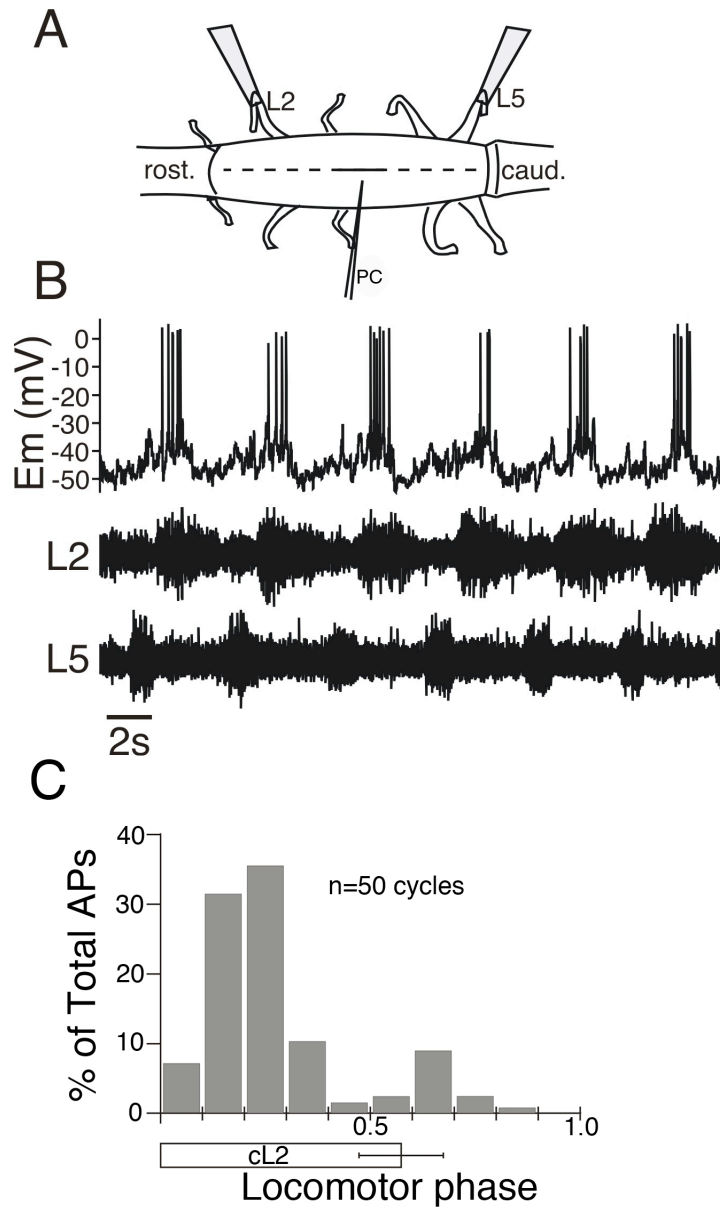


Figure 2-4. A. Suction electrodes attached to L2 and L5 ventral roots record flexor-related and extensor-related ENG signals respectively. Patch clamp electrode (PC) records from a neuron located contralaterally in lamina VIII of the L3 spinal segment. B. Fictive locomotion occurs in the presence of $5\mu\text{M}$ NMDA $10\mu\text{M}$ 5-HT. Upper trace recorded from the IC electrode shows the neuron located below the notch has a membrane potential (E_m) close to -50 mV, is rhythmically active and

fires action potentials in phase with flexor activity (L2) on the contralateral side of the spinal cord.

C. Percentage of total number of action potentials (APs) occurring in the interneuron (illustrated in panel B) during each of ten equal windows of a normalized fictive locomotor cycle period. All action potentials during 50 consecutive cycle periods were analyzed. The horizontal bar below the x-axis (average burst duration \pm SD) depicts the portion of the step cycle in which the cL2 ventral root was active.

**Chapter 3 -
Functional characterization of dI6 interneurons in the
neonatal mouse spinal cord.²**

² A version of this chapter has been submitted for Publication. Dyck et al. 2011. J Neurosci

3.1 Introduction:

Alternating rhythmic activity in hindlimb muscles during locomotion is generated by a neural network referred to as the locomotor central pattern generator (CPG), which is located in the ventro-medial regions of the lower thoracic and lumbar spinal cord. Due to the distributed nature of this neural circuit (Kjaerullf and Kiehn, 1996; Cowley and Schmidt, 1997), traditional anatomical and electrophysiological experiments have proven to be of limited use for the identification of interneuronal components of the locomotor CPG, or its detailed network structure (Kiehn, 2006). Recently a molecular approach has been used to identify five cardinal classes of interneurons that are located in the ventral spinal cord postnatally (dI6, V0-V3). Many of these can be identified by expression of a unique complement of transcription factors at early embryonic time points, and can be further subdivided into subpopulations based on downstream transcription factor expression (Goulding 2009).

Initial experiments have demonstrated that several genetically-defined cell populations play specific roles in the production of locomotor behavior. Clear deficits in the fictive locomotor pattern have been observed in the absence of the V0 (Lanuza et al. 2004) and V1 (Gosgnach et al. 2006) populations, and subsequent experiments have demonstrated a more subtle role for the V2 (Crone et al. 2008; 2009, Zhong et al. 2010) and V3 (Zhang et al. 2008) populations. Whole cell recordings of intrinsic membrane properties carried out on several populations have provided further insight into their physiological role during locomotor activity (Lundfald et al. 2007; Zhang et al. 2008; Zhong et al. 2010; Dougherty and Kiehn 2010).

One population of cells that have been suggested to play a role during locomotor activity,

but have yet to be directly investigated, are the dI6 interneurons (Lanuza et al. 2004). These cells are Lbx1-expressing neurons that originate from progenitors immediately dorsal to the p0 domain and migrate ventro-medially during embryogenesis taking up positions in laminae VII/VIII of the postnatal spinal cord (Gross et al. 2002). While the lack of a unique molecular marker for this population has hindered their characterization, preliminary studies have suggested that they are a mixed population of ipsilaterally and commissurally projecting interneurons (Goulding 2009; Rabe et al. 2009). Interestingly, these cells share many similarities with the V0 interneurons. In addition to having a similar migration pattern, both the dI6 and a subset of the V0 cells develop from Pax7 and Dbx2 progenitors. Furthermore, in the Dbx1 mutant mouse, many V0 neurons acquire characteristics of dI6 cells soon after their generation. This has led to the suggestion that the dI6 population may play a complimentary role to the V0 cells during locomotion (Lanuza et al. 2004).

In this study we utilize a transgenic mouse model that allows for identification of the dI6 cells located in the proximity of the central canal via differential expression of reporter proteins. An investigation of their intrinsic membrane properties as well as their activity during fictive locomotion demonstrates that there are two, electrophysiologically-distinct, populations of dI6 interneurons that are rhythmically active during fictive locomotion. The first have properties consistent with neurons that coordinate motoneuron output during locomotion. The second have the electrophysiological characteristics of cells that are involved in initiating rhythmicity in the locomotor CPG.

3.2 Methods:

Animals

All procedures were in accordance with the Canadian Council on Animal Care (CCAC) and approved by the Animal Welfare Committee at the University of Alberta. For generation of the Dbx1Cre transgenic mouse, sequences encoding for Cre recombinase including a nuclear localization signal and SV40 polyadenylation sequence were inserted downstream of a 5.7kb Dbx1 genomic DNA fragment (a gift from Frank Ruddle, Lu et al. 1996). The Dbx1 promoter-Cre construct was flanked by chicken β -globin insulators (Chung et al. 1993), and linearized for pronuclear injection. Potential founder mice were genotyped for Cre and crossed to Rosa26LacZ reporters to assess specific Cre-mediated recombination. All genotyping of mouse strains was performed by PCR using specific oligonucleotide primers as described previously (Lanuza et al. 2004; Gosgnach et al. 2006).

Experiments were performed on male and female neonatal (0-3 days of age) Dbx1Cre;Rosa26EGFP or Dbx1Cre;Rosa26EYFP mice (n=34; collectively referred to as Dbx1Cre;Rosa26EFP mice). In some instances, Dbx1Cre;Rosa26EFP mice were mated with Dbx1LacZ (Pierani et al. 2001) mice to generate Dbx1Cre;Rosa26EFP;Dbx1LacZ offspring, which were used for experiments (n=24).

In-vitro preparation

Mice were anesthetized via inhalation of isoflurane (4% delivered with 95% O₂ 5% CO₂). After decapitation and evisceration, the spinal cord was dissected out in a bath containing

oxygenated, ice-cold dissecting artificial cerebrospinal fluid (d-aCSF) containing (in mM) 111 NaCl, 3.08 KCl, 11 glucose, 25 NaHCO₃, 1.18 KH₂PO₄, 3.7 MgSO₄, 0.25 CaCl₂ (pH of 7.4, osmolarity 280-300 mOsm). The preparation used for targeting interneurons located close to the central canal for whole cell recording in the mouse spinal cord has been described in detail (Dyck and Gosgnach, 2009). Briefly, the spinal cord was transferred to a vibratome chamber containing oxygenated d-aCSF and glued dorsal side up to a strip of agarose. The vibratome was then used to shave away sections of the dorsal aspect of the lumbar spinal cord until the central canal was visible using a dissecting microscope. Following sectioning, the spinal cord was situated dorsal side up on a coverslip in a plexi-glass recording chamber and held in place via nylon threads stretched over a platinum wire flattened into a horseshoe shape.

Electrophysiological Recording

The preparation was constantly perfused with room temperature, oxygenated recording artificial cerebrospinal fluid (r-aCSF) composed of (in mM): 111 NaCl, 3.08 KCl, 11 glucose, 25 NaHCO₃, 1.18 KH₂PO₄, 1.25 MgSO₄, 2.52 CaCl₂ (pH of 7.4, osmolarity 280-300 mOsm). In all experiments fictive locomotor activity was induced by bath application of 10 μ M 5-hydroxytryptophan (5-HT) and 5 μ M N-Methyl-D-Aspartate (NMDA) (both from Sigma-Aldrich) and monitored via electroneurogram (ENG) activity recorded from bipolar suction electrodes (A-M Systems Inc.) positioned on the flexor-related (second lumbar i.e. L2) and extensor-related (fifth lumbar i.e. L5) ventral roots. ENG signals were amplified (20,000x) and band pass filtered (100Hz-1kHz) with custom made equipment (R&R Designs). All ENG, as well as whole cell data, was digitized (Digidata 1440A, Axon Instruments) and recorded using pClamp software (Axon Instruments) on a PC.

For whole cell recordings, patch electrodes (tip resistance: 3–5 M Ω) were pulled from borosilicate glass (Harvard Apparatus) and filled with internal solution containing (in mM): K-gluconate, 138; Hepes, 10; CaCl₂, 0.0001; GTP-Li, 0.3; ATP-Mg, 5 (pH adjusted to 7.2, osmolarity 290-305 mOsm). Liquid junction potential was calculated to be ~12mV. Em values were not corrected for the liquid junction potential since the extent to which the contents of the cells had been completely replaced with the pipette solution was unclear. A micromanipulator (MPC-385, Sutter Instruments) was used to position the electrode over the cut region of the spinal cord and lower it into the tissue. IR-DIC and GFP (bandpass 450-490 nm) filters were used to target EFP+ cells for recording. Using a whole cell recording amplifier (Multiclamp 700B, Axon Instruments) in voltage clamp mode, a 10 mV square pulse (50 Hz) was used to monitor tip resistance as the electrode was advanced towards the cell of interest. Once a giga-ohm seal with a cell was formed, the command voltage was set to -60 mV and gentle suction was applied to break through the membrane to obtain a whole cell recording. Series resistance (R_s) and cell capacitance (C_m) were determined in voltage-clamp mode using the compensation features on the Multiclamp commander software (Axon Instruments). R_s was monitored throughout the course of each recording (if working in current-clamp mode we would periodically switch into voltage clamp to monitor R_s). Initial values of R_s were typically 10-15 M Ω . Recordings where R_s exceed 30 M Ω were excluded from analysis. In some instances, a small amount of negative bias current (10-15 pA) was required to hyperpolarize the cells to prevent spontaneous firing of action potentials.

Once a stable membrane potential was reached, the amplifier was switched into voltage clamp mode and we determined whether the cell possessed a persistent inward current (PIC) by applying a triangular voltage ramp from -110 to -10mV. The speed of the voltage ramp was slow

(10sec total; 12mV/sec) to avoid activation of transient sodium channels (Tazerart et al., 2008). PIC magnitude was obtained from recordings following subtraction of the leak current, which was performed using the leak subtraction tool in Clampfit (Axon Instruments). Membrane resistance (R_m) was calculated off-line by taking the inverse slope of the linear portion of the current-voltage (I-V) relationship.

In some instances, the intrinsic bursting properties of dI6 neurons were examined by isolating these cells from network inputs. This was accomplished by either blocking fast glutamatergic transmission with CNQX (10 μ M) or by inhibiting chemical synaptic transmission with a low calcium (0.25 mM) aCSF solution. Reduction of Ca²⁺ was offset by increasing Mg²⁺ (to 3.7mM) in order to avoid changes in osmolarity. Finally, to investigate whether synaptically isolated neurons displayed voltage dependent firing frequency, small amounts of bias current were injected in a stepwise manner to change the holding potential of a cell between -70 mV and -40 mV.

Data Analysis and Statistics

In all instances in which neuronal activity was compared to fictive locomotor output, the ipsilateral ventral root in the same segment as the recorded neuron was chosen for analysis (referred to as the local ventral root). If ENG records were not available for the local ventral root, activity in a neighboring ventral root was normalized, to represent activity in the local ventral root, and used for analysis.

To create histograms of firing frequency to analyze the distribution of action potentials during fictive locomotion, a single locomotor cycle (defined as the time between the onset of two bursts of ENG activity in a given ventral root) was divided into ten equal bins, with bins 1-5

representing the period of ventral root activity and bins 6-10 representing the relatively inactive phase (i.e. the inter-burst interval). The frequency of action potentials occurring within each bin was calculated for 20 consecutive cycles and plotted as a histogram. The phase preference of a given neuron was determined by comparing the average spike frequency of the burst (i.e. bin 1-5) and inter-burst (i.e. bin 6-10) periods. In some instances, a neuron fired preferentially at the transition between the active and inactive phases. In these cases, the average spike frequency of the five consecutive bins with the highest spike frequency (e.g. bin 3-7) were compared to the remaining five consecutive bins (e.g. bin 8-2).

All means are reported \pm standard deviation (SD). Unless stated otherwise, student's t-tests were used to determine whether means were significantly different. Circular statistics (Zar, 1974) were used to determine the coupling strength between sub-threshold oscillations in membrane potential (i.e. locomotor drive potentials- LDPs) and ventral root activity. LDPs in neurons occurring over the entire period of analysis (typically 5-10 min) were selected, and their phase values were calculated in reference to the onsets of the local ventral root. Phase values were determined by dividing the latency between the onset of the LDP and the ventral root burst by the cycle period. This resulted in values close to 0.5 when LDP and ventral roots were completely out of phase, and values close to 1 when they were in phase. The phase values were imported into MATLAB (The MathWorks Inc.) and a custom script (J. Dyck) was used to generate a polar plot and provide r-values. In order to determine whether the sample r was large enough to confidently indicate a nonuniform distribution of points, Rayleigh's test ($R=nr$) was performed. The resulting value for R was compared to a critical values table.

Immunohistochemistry

Immunostaining on frozen spinal sections was performed as previously described (Gross et al., 2002; Moran-Rivard et al., 2001). Serial sections of either whole embryos or early postnatal spinal cords were cut (20 μ m) and incubated with primary antibodies. Primary antibodies were detected using species-specific secondary antibodies conjugated with Cy2, Cy3 or Cy5 (Jackson Laboratories). Images were captured using a Zeiss LSM5-Pascal confocal microscope and assembled using Adobe Photoshop.

3.3. Results

The Dbx1Cre;Rosa26EFP mouse labels V0D and dl6 interneurons.

The Dbx1LacZ mouse line has been shown to selectively mark all p0 progenitors and V0 interneurons with β -gal (Pierani et al. 2001; Lanuza et al. 2004). In order to determine whether EFP expression was limited to the V0 neuronal population in Dbx1Cre;Rosa26EFP animals, these mice were crossed with the Dbx1LacZ line. Initial inspection of the spinal cords taken from Dbx1Cre;Rosa26EFP;Dbx1LacZ mice at E11.5 indicated that rather than being expressed in all β -gal positive (i.e. Dbx1⁺-derived) cells, EFP expression was shifted dorsally beginning midway through the p0 domain and continuing slightly beyond its dorsal extent (Figure 3-1A). In order to definitively determine the cell population(s) in which the reporter protein was expressed, the transcriptional profile of the EFP expressing neurons was examined. While many EFP expressing cells co-expressed β -gal indicating that they are Dbx1-derived and belong to the V0 population (Figure 3-1A), EFP was not co-expressed with the transcription factor Evx1, a post-mitotic marker of the ventral subpopulation of V0 cells (V0V cells- Moran-Rivard et al. 2001) (Figure 3-1B)

indicating that EFP expression is limited to the dorsal subset of V0 cells (V0D). The population of EFP expressing neurons located immediately dorsal to the V0D cells was found to co-express Lbx1 (Figure 3-1C) and arise from Pax7⁺ cells (Figure 3-1D), a marker of dorsal spinal cord progenitors. In order to determine the extent of the dorsal expression of EFP in the Dbx1Cre;Rosa26EFP mouse we looked for co-localization with the transcription factor Lmx1b which is expressed in dI5 neurons. The lack of co-expression of EFP and Lmx1b (Figure 3-1E) led us to the conclusion that EFP is exclusively expressed in dI6 and V0D neurons.

The Dbx1Cre;Rosa26EFP;Dbx1LacZ line enabled these two populations to be differentiated postnatally as dI6 cells expressed EFP only while V0D cells expressed both EFP and β -gal (Figure 1F). V0V cells could be definitively identified in these mice by the expression of β -gal alone (Figure 3-1F). Initially, this mouse line was used for electrophysiological experiments, EFP cells were targeted, and post hoc β -gal staining was performed (see Kwan et al. 2009) to confirm that the cells investigated were dI6 (i.e. EFP⁺ and β -gal⁻), rather than V0D neurons. Close inspection of the location of these three cell populations revealed that 82% \pm 8% SD (n = 7 spinal cords) of all EFP⁺ neurons dorsal to the central canal were β -gal⁻, and therefore dI6 cells (Figure 3-1F, 1G). Since all electrophysiological recordings in this study were taken from cells located above the central canal and the vast majority of EFP⁺ cells in this region belonged to the dI6 population Dbx1Cre;Rosa26EFP mice were also used to target dI6 interneurons.

Dorsally located dI6 neurons oscillate during fictive locomotion

To investigate the activity of dI6 cells during locomotor like activity, fictive locomotion was evoked in spinal cords from neonatal Dbx1Cre;Rosa26EFP or Dbx1Cre;Rosa26EFP;DbxLacZ mice

in which the dorsal regions had been removed. Previous studies have shown that pharmacologically-induced fictive locomotion is not significantly altered in this preparation (Dyck and Gosgnach 2009; Dougherty and Kiehn 2010) and it allows EFP+ dI6 cells situated close to the cut surface of the spinal cord to be accessible for whole-cell patch clamp recording.

In total, whole cell patch clamp recordings were made from 79 EFP+ cells following the establishment of fictive locomotion (induced by bath application of 5 μ M NMDA, 10 μ M 5-HT). Of these, 53% (42/79) showed oscillations in their membrane potential (Figure 3-2A, 3-2B), while the remaining 47% (36/79) spiked tonically or were silent during fictive locomotion. As we were interested in examining the role of these dI6 neurons during locomotor activity we restricted our study to those cells that were rhythmically active. To determine whether activity in the oscillatory cells was directly related to fictive locomotor outputs, the firing frequency of each cell was calculated during the normalized ventral root burst cycle and plotted as a histogram (Figure 3-2C, 2D). In 86% (36/42) of the cells, the firing pattern showed a significant ($p < 0.05$ t-test) phase preference, with 40% (17/42) firing preferentially during the active phase of the ipsilateral ventral root in which the interneuron was located (i.e. the local ventral root), 33% (14/42) firing in the inactive phase of the local ventral root, and 14% (6/42) firing at the transition between the burst and inter-burst period. Even in those cases in which the phase preference of the dI6 neuron was statistically significant, a number of cells (34/42) did fire more than 20% of their action potentials in the ventral root phase in which they were primarily inactive (Figure 3-2A, 2C). These cells are referred to as loosely coupled (LC) dI6 neurons. In the remaining oscillatory GFP-neurons (8/42), oscillations were tightly coupled to ventral root output and less than 15% of action potentials were observed in the ventral root phase in which they were primarily inactive (Figure 3-2B, 3-2D). These

neurons are referred to as tightly coupled (TC) dI6 neurons.

TC and LC dI6 neurons are electrophysiologically distinct.

Initial assessment of intrinsic membrane properties recorded from dI6 interneurons that were rhythmically active during fictive locomotion revealed that LC cells (mean $R_m = 1041 \text{ M}\Omega \pm 541 \text{ M}\Omega$) were significantly smaller ($p < 0.05$ student's t-test) than TC interneurons (mean $R_m = 546 \text{ M}\Omega \pm 171 \text{ M}\Omega$). In order to characterize the dorsally-located dI6 interneurons and examine their potential function during fictive locomotion we investigated whether rhythmic oscillations in either subclass were due to intrinsic membrane properties. To this end, fictive locomotion was evoked by application of 5-HT and NMDA and whole cell recordings were made from EFP cells. Upon confirming that a cell was rhythmically active during fictive locomotion and classifying it as either a TC or LC dI6 interneuron, the preparation was synaptically isolated either by bath application of CNQX ($10 \mu\text{M}$) to block non-NMDA glutamatergic transmission, or by reducing (to 0.25 mM) the Ca^{2+} concentration of the raCSF solution. Preparations were considered to be synaptically isolated once rhythmic ventral root activity ceased.

Although the amplitude and duration of the oscillatory activity in LC dI6 neurons was altered following synaptic isolation, rhythmic activity in these cells persisted ($n=10/10$ CNQX Figure 3-3A; $n=8/8$ low Ca^{2+} , Figure 3-3B) suggesting that these cells are endogenous bursters. Oscillations in TC dI6 neurons, on the other hand, were clearly abolished when synaptically isolated ($n=4/4$ CNQX, Figure 3-3C) suggesting that oscillations in these cells are driven by other rhythmically active neurons. These results provide evidence that LC and TC dI6 neurons are electrophysiologically distinct and raises the possibility that LC neurons may be involved in driving

oscillatory activity in the locomotor CPG while TC neurons receive rhythmic input and are not involved in rhythm generation.

Based on their ability to oscillate while synaptically isolated, we were interested to determine whether the LC dI6 cells possessed other signature intrinsic properties of rhythm-generating neurons. Multiple studies have suggested that a riluzole sensitive persistent inward current (PIC) is required for locomotor rhythm generation (Rybak and McCrea, 2007; Sherwood et al. 2011; Zhong et al. 2007; Tazerat et al 2007; 2008). To determine whether LC dI6 interneurons possess this current, the current-voltage (I-V) relationship of these cells was analyzed by applying a slow voltage ramp (12mV/sec) to a cell while it was held in current clamp. In LC dI6 neurons, a clear PIC could be seen (n= 34/34; Figure 3-4A) as a region of negative slope conductance during the depolarization phase of the current ramp (Lee and Heckman, 1999; Li and Bennett, 2003). The PIC had an average leak subtracted magnitude of 29.81 ± 10.88 pA. We propose that a persistent sodium current is responsible since a low concentration of riluzole (5 μ M) successfully abolished the region of negative slope conductance in all cases in which it was applied (3/3 - Figure 3-4B). In contrast, PICs were not observed in any of the 8 TC dI6 neurons which exhibited strictly linear I-V relationships in response to the same voltage ramp (Figure 3-4C).

In addition to non-linear membrane properties, cells that generate the locomotor rhythm have also been shown to display intrinsic voltage sensitivity when synaptically isolated, such that the frequency of oscillations depends on the holding potential of the cell (Wilson et al. 2005; Tazerat et al 2008). This property is thought to be essential for driving the rhythm at various speeds (Brownstone and Wilson 2008). To determine whether LC dI6 interneurons are able to modulate oscillation frequency, the preparation was synaptically isolated, cells were held in current clamp

mode, and current steps were applied to depolarize (to -40 mV) or hyperpolarize the cell (to -70 mV). Frequency of oscillations (evoked by 5 μ M NMDA, 10 μ M 5-HT) at each holding potential was recorded. As expected, oscillations in 10/18 of LC dI6 neurons fired in a voltage dependent manner with the frequency of oscillations increasing when the cell was depolarized and decreasing when hyperpolarized (Figure 3-4D, 3-4E).

TC dI6 interneurons receive rhythmic inputs from the locomotor CPG.

Given the clear rhythmic oscillations observed in the TC dI6 cells, their inability to oscillate intrinsically and lack of a PIC, we hypothesized that rather than being involved in generating the locomotor rhythm, these cells receive outputs from the locomotor CPG and are involved in coordinating motoneuron outputs during locomotor activity. To investigate this we first compared the oscillation frequency of the TC dI6 cells to the frequency of ENG bursts recorded from the local ventral root and found that these values were almost identical in all cases (mean TC dI6 frequency = 0.350 Hz \pm 0.035 SD; mean ventral root frequency = 0.357 Hz \pm 0.035 SD; n=8). The strength of this coupling was not altered following current injection (Figure 3-5).

The strength of coupling between LDPs recorded from TC dI6 neurons and ENG activity during fictive locomotion was also analyzed by circular statistics which allowed the relationship to be represented as a data point on circular plot (Figure 3-6B). Each point in Figure 3-6B represents the phase value of the delay between the onset of LDP and the onset of the ENG burst in the local ventral root for the trial illustrated in 6A. Data points at 0.0 representing synchronous onset of LDP and ENG burst and points at 0.5 representing LDP and ENG bursts that are perfectly out of phase. The R value (which determines coupling strength of the neuron with ENG activity) for this cell was

0.89, indicating that it was tightly coupled to ventral root activity. This was representative of the entire TC population in which the mean R value was 0.893 ± 0.06 SD ($n=8$). Data points in Figure 3-6C represent the mean vector point for each individual TC dI6 cell.

Finally, if TC dI6 interneurons are involved in coordinating motoneuron activity during locomotor activity we expect that activity in these cells to mirror that of ENG activity at all times, including those in which fictive locomotor activity is aberrant. We were able to identify clear “irregularities” in five of the 8 TC dI6 interneurons from which we recorded. These included both missed steps (i.e. deletions), or additional steps (i.e. additions- see arrow in Fig 6D). As expected, in all 5 cases irregularities in the step cycle were mirrored with similar irregularities in interneuronal activity, driving home the point that ENG activity and that of TC dI6 cells are tightly coupled.

3.4 Discussion

Although it has previously been postulated that dI6 interneurons are involved in locomotor behavior (Rabe et al 2009; Goulding 2009), the lack of a unique molecular marker for these cells has hindered their study. The present work is the first to describe intrinsic electrophysiological properties of dI6 interneurons. In order to provide insight into their role during locomotor activity we utilized a preparation in which a notch is removed from the dorsal aspect of the spinal cord, allowing dI6 interneurons located dorsal to the central canal to be investigated during fictive locomotion. Our findings provide compelling evidence for the participation of dI6 neurons in the locomotor CPG by demonstrating that many are rhythmically active during locomotor activity, and that the majority of dI6 cells possess intrinsic oscillatory properties suggesting a potential role in

locomotor rhythm generation.

LC dI6 interneurons are intrinsic oscillators.

By far the most common firing pattern observed among rhythmically active dI6 interneurons (34/42) was a loose coupling to fictive locomotor activity recorded from the ventral roots. These cells are referred to as “loosely-coupled” since action potentials were often seen in the local ventral root phase in which they were primarily inactive. Several characteristics of this subclass of dI6 interneurons lead us to suggest that they may be involved in locomotor rhythm generation. First, these cells are located in lamina VII/VIII of the thoraco-lumbar spinal cord, a region that has been shown to receive monosynaptic contacts from brainstem centers responsible for generating rhythmic, locomotor activity in the spinal cord (Matsuyama et al. 2004), and is essential for the induction of fictive locomotion in the isolated preparation (Kjaerullf and Kiehn, 1996; Antri et al. 2011). Second, the LC dI6 interneurons possess intrinsic membrane properties that have been shown to be characteristic of rhythm-generating neurons. These cells are able to oscillate at multiple frequencies in synaptic isolation (Figure 3-3A, 3-3B, 3-4D, 3-4E), and exhibit a riluzole sensitive PIC (Figure 3-4A-B). While the presence of a PIC does not, in and of itself, demonstrate a role in rhythm generation (PICs are present in motoneurons which are not part of the rhythm generating network), recent work indicates a direct link between locomotor rhythm generation and the presence of persistent sodium currents in spinal interneurons (Zhong et al. 2007; Tazaret et al., 2009). Furthermore, recent computational models of the locomotor CPG suggest that neurons that generate rhythmic activity rely on a sodium-dependent PIC for intrinsic oscillations (Rybak et al., 2006; Sherwood et al. 2011).

Rhythmic bursting in TC dI6 interneurons is phase locked to motoneuron activity.

In contrast to the population of dI6 interneurons that were loosely coupled to fictive locomotion, we recorded from relatively few (8/42) dI6 interneurons that were tightly coupled to ENG activity. The phase-locked nature of oscillations in TC dI6 interneurons and the ventral roots during normal fictive locomotor activity (Figure 3-5), as well as irregular stepping (Figure 3-6D), suggest that this subclass of cells may be involved in the regulation of motoneuron activity. Although we did not have a mechanism of quantitatively measuring the medial-lateral location of these cells in our preparation, TC cells tended to be located more laterally than the LC dI6 interneurons (J.D.), in a region of the lumbar spinal cord that has been shown to contain many interneurons that make direct contact onto ipsilateral motoneurons and regulate their activity (Stepien et al. 2010). Further support for the hypothesis that TC cells regulate motoneuron firing comes from the fact that dI6 cells are closely related to the V0 population, which has been shown to make monosynaptic connections onto motoneurons and regulate their activity during fictive locomotion (Lanuza et al. 2004). Both the dorsal population of V0 cells and the dI6 population develop from similar progenitors (Pierani et al., 2001; Gross et al., 2002; Muller et al., 2002) and migrate along a similar ventromedial pathway during embryogenesis (Pierani et al., 2001; Moran-Rivard et al., 2001; Gross et al., 2002). Based on these similarities, and the previous suggestion that dI6 and V0 interneurons play an analogous role during locomotor activity (Rabe et al 2009; Goulding 2009), we were surprised that so few dI6 cells from which we recorded fit into the TC category.

It is important not to lose sight of the fact that all whole cell recordings in this study were

made from dI6 neurons located above the level of the central canal, since more ventrally located dI6 neurons were not accessible with the modified in vitro preparation used. We were therefore unable to determine whether more ventrally located dI6 neurons fit into one of the categories described here, or whether they represent a distinct subpopulation of dI6 neurons. Given that the majority of interneurons which have previously been shown to project to motoneurons are located ventral to the central canal (Lanuza et al. 2004; Zhang et al. 2008; Stepein et al, 2010), and the paucity of TC dI6 interneurons from which we recorded, we postulate that the majority of ventrally located dI6 neurons fit into the TC category and are involved in coordinating motoneuron output. Unfortunately it is difficult to test this hypothesis directly since, based on their location, it is not possible to access these cells while leaving the locomotor CPG intact and functional.

Network Implications

To date, no single genetically defined interneuronal population has been shown to be necessary and sufficient for the generation of rhythmic activity in the locomotor CPG. In fact, locomotor-like activity persists following the deletion and/or silencing of each of the V0 (Lanuza et al., 2004), V1 (Gosgnach et al., 2006), V2a (Crone et al., 2008) and V3 (Zhang et al., 2008) interneuronal populations, and the Hb9 interneuron population has been shown to have a firing pattern inconsistent with locomotor rhythm generation (Kwan et al. 2009). Based on studies that have demonstrated that the region encompassing the central canal of the thoraco-lumbar spinal cord is essential for generation of locomotor activity (Kjaerullf and Kiehn, 1996; Antri et al. 2011), and the fact that the dI6 interneurons together with the aforementioned V0, V2a, V3 and Hb9 populations make up the majority of cells located in this area, we believe that the initiation of

activity in the locomotor CPG must either be due to the dI6 interneurons alone, or is a shared role amongst several populations located in this area.

Due to the irregular rhythm seen in the LC dI6 cells when synaptically isolated (Figure 3-3A, 3B), we believe that the latter of these hypotheses is more plausible, and the LC dI6 cells work together with other interneurons, located in close proximity, to generate the locomotor rhythm. Subsets of other genetically-defined interneuron populations nearby (i.e. Hb9 and V2a) have been shown to possess many features of rhythmogenic cells (Wilson et al., 2005, Dougherty and Kiehn, 2010), however each population has been determined to be incapable of independently generating the locomotor rhythm (Kwan et al., 2009, Crone et al., 2008). We propose that subsets of each of these populations, together with the LC dI6 interneurons constitute the rhythm generating core of the locomotor CPG which drives activity in a network of so called “pattern forming” cells (Lafreniere-Roula and McCrea, 2005) that project directly onto motoneurons (Figure 7).

Support for this general organizational principle comes from experiments demonstrating that V2a interneurons (part of proposed rhythm generating core) make monosynaptic contacts onto commissural V0 interneurons (Crone et al., 2009), which are known to project to, and inhibit, contralateral motoneurons (Lanuza et al. 2004) and thus constitute part of the pattern forming network. Recent tracing studies indicate that a subset of the dI3 and V2a populations also make monosynaptic contact onto ipsilateral motoneurons (Stepien et al., 2010), suggesting that these cells, along with the TC dI6 interneurons characterized here, may comprise the pattern forming layer. Future experiments investigating detailed connectivity between each of these populations will provide valuable insight required to test this hypothesis and determine the cell populations essential for the initiation and production of locomotor behavior.

3.5 References

Antri M, Mellen N, Cazalets JR (2011). Functional organization of locomotor interneurons in the ventral lumbar spinal cord of the newborn rat. *PLoS One*. 2011 6:e20529.

Brownstone R, Wilson J. (2008). Strategies for delineating spinal locomotor rhythm-generating networks and the possible role of Hb9 interneurons in rhythmogenesis. *Brain Res. Rev.* 57:64-76.

Chung JH, Whiteley M, Felsenfeld G. (1993). A 5' element of the chicken beta-globin domain serves as an insulator in human erythroid cells and protects against position effect in *Drosophila*. *Cell* 74:505-514.

Cowley KC, Schmidt BJ. (1997). Regional distribution of the locomotor pattern-generating network in the neonatal rat spinal cord. *J. Neurophysiol.* 77:247–259

Crone SA, Quinlan KA, Zagoraiou L, Droho S, Restrepo CE, Lundfald L, Endo T, Setlak J, Jessell TM, Kiehn O, Sharma K (2008). Genetic ablation of V2a ipsilateral interneurons disrupts left-right locomotor coordination in mammalian spinal cord. *Neuron* 60:70–83.

Crone SA, Zhong G, Harris-Warrick R, Sharma K (2009). In mice lacking V2a interneurons, gait depends on speed of locomotion. *J Neurosci.* 29:7098 –7109.

Dougherty K, Kiehn, O (2010). Firing and cellular properties of V2a interneurons in the rodent spinal cord. *J Neurosci.* 30:24–37.

Dyck J, Gosgnach, S (2009). Whole cell recordings from visualized neurons in the inner laminae of the functionally intact spinal cord. *J Neurophys.* 102:590-597.

Gosgnach S, Lanuza GM, Butt SJ, Saueressig H, Zhang Y, Velasquez T, Riethmacher D, Callaway EM, Kiehn O, Goulding M (2006). V1 spinal neurons regulate the speed of vertebrate locomotor outputs. *Nature* 440:215-219.

Goulding, M (2009). Circuits controlling vertebrate locomotion: moving in a new direction. *Nat. Rev. Neurosci.* 10:507-518.

Gross, MK, Dottori, M, Goulding, M (2002). Lbx1 specifies somatosensory association interneurons in the dorsal spinal cord. *Neuron* 34:535–549.

Kiehn, O (2006). Locomotor circuits in the mammalian spinal cord. *Ann. Rev. Neurosci.* 29:279-306.

Kjaerulff O, Kiehn O (1996). Distribution of networks generating and coordinating locomotor activity in the neonatal rat spinal cord in vitro: a lesion study. *J. Neurosci.* 16:5777–5794.

Kwan AC, Dietz SB, Webb, WW, Harris-Warrick RM (2009). Activity of Hb9 interneurons during fictive locomotion in mouse spinal cord. *J Neurosci* 29:11601–11613.

Lafreniere-Roula, M, McCrea, DA (2005). Deletions of rhythmic motoneuron activity during fictive locomotion and scratch provide clues to the organization of the mammalian central pattern generator. *J. Neurophysiol.* 94:1120–1132.

Lanuza GM, Gosgnach S, Pierani A, Jessell TM, Goulding M (2004). Genetic identification of spinal interneurons that coordinate left-right locomotor activity necessary for walking movements. *Neuron* 42:375–386.

Lee RH, Heckman CJ (1999). Enhancement of bistability in spinal motoneurons in vivo by the noradrenergic alpha-1 agonist methoxamine. *J Neurophysiol.* 81: 2164-2174.

Li Y, Bennett DJ (2003). Persistent sodium and calcium currents cause plateau potentials in motoneurons of chronic spinal rats. *J Neurophysl* 90:857-869.

Lu S, Shashikant CS, Ruddle FH. (1996). Separate cis-acting elements determine the expression of mouse *Dbx* gene in multiple spatial domains of the central nervous system. *Mech. Dev.* 58:193-202.

Lundfald L, Restrepo CE, Butt SJ, Peng CY, Droho S, Endo T, Zeilhofer HU, Sharma K, Kiehn O (2007). Phenotype of V2-derived interneurons and their relationship to the axon guidance molecule

EphA4 in the developing mouse spinal cord. *Eur. J. Neurosci.* 26:2989–3002.

Matsuyama K, Nakajima K, Mori F, Aoki M, Mori S. (2004). Lumbar commissural interneurons with reticulospinal inputs in the cat: morphology and discharge patterns during fictive locomotion. *J. Comp. Neurol.* 474: 546–561.

Moran-Rivard, L, Kagawa, T, Saueressig, H, Gross, MK, Burrill, J, Goulding, M (2001). *Evx1* is a postmitotic determinant of V0 interneuron identity in the spinal cord. *Neuron* 29, 385–399.

Muller, T, Brohmann, H, Pierani, A, Heppenstall, AP, Lewin, GR, Jessell, TM, Birchmeier, C (2002). The homeodomain factor *Lbx1* distinguishes two major programs of neuronal differentiation in the dorsal spinal cord. *Neuron* 34, 551–562.

Pierani A, Moran-Rivard L, Sunshine MJ, Littman DR, Goulding M, Jessell TM (2001). Control of interneuron fate in the developing spinal cord by the progenitor homeodomain protein *Dbx1*. *Neuron* 29:367–384.

Rabe N, Gezelius H, Vallstedt A, Memic F, Kullander K (2009). Netrin-1-dependent spinal interneuron subtypes are required for the formation of left-right alternating locomotor circuitry. *J Neurosci.* 29:15642-15649.

Rybak I, Shevtsova N, Lafreniere-Roula M, McCrea D (2006). Modeling spinal circuitry involved

in locomotor pattern generation: insights from deletions during fictive locomotion. *J. Physiol.* 577:617-639.

Sherwood WE, Harris-Warrick R, Guckenheimer J (2011). Synaptic patterning of left-right alternation in a computational model of the rodent hindlimb central pattern generator. *J. Comput. Neurosci.* 30:323-360.

Stepein A, Tripodi M, Arber S (2010). Monosynaptic rabies virus reveals premotor network organization and synaptic specificity of cholinergic partition cells. *Neuron* 68:456-472.

Tazerart S, Viemari JC, Darbon P, Vinay L, Brocard F (2007). Contribution of persistent sodium current to locomotor pattern generation in neonatal rats. *J. Neurophysiol.* 98:613– 628.

Tazerart S, Vinay L, Brocard F (2008). The persistent sodium current generates pacemaker activities in the central pattern generator for locomotion and regulates the locomotor rhythm. *J. Neurosci.* 28:8577– 8589.

Wilson JM, Hartley R, Maxwell DJ, Todd AJ, Lieberam I, Kaltschmidt JA, Yoshida Y, Jessell TM, Brownstone RM (2005). Conditional rhythmicity of ventral spinal interneurons defined by expression of the Hb9 homeodomain protein. *J. Neurosci.* 25:5710–5719.

Zar, J.H. Circular Distribution. In “Biostatistical Analysis”, p310-327. Prentice Hall, Engelwood

Cliffs, NJ. 1974.

Zhang Y, Narayan S, Geiman E, Lanuza GM, Velasquez T, Shanks B, Akay T, Dyck J, Pearson K, Gosgnach S, Fan CM, Goulding M (2008). V3 spinal neurons establish a robust and balanced locomotor rhythm during walking. *Neuron* 60:84–96.

Zhong G, Masino MA, Harris-Warrick RM (2007). Persistent sodium currents participate in fictive locomotion generation in neonatal mouse spinal cord. *J. Neurosci.* 27:4507–4518.

Zhong G, Droho S, Crone S, Dietz S, Kwan AC, Webb WW, Sharma K, Harris-Warrick RM (2010). Electrophysiological characterization of the V2a interneurons and their locomotor-related activity in the neonatal mouse spinal cord. *J Neurosci* 30:170–182.

FIGURES:

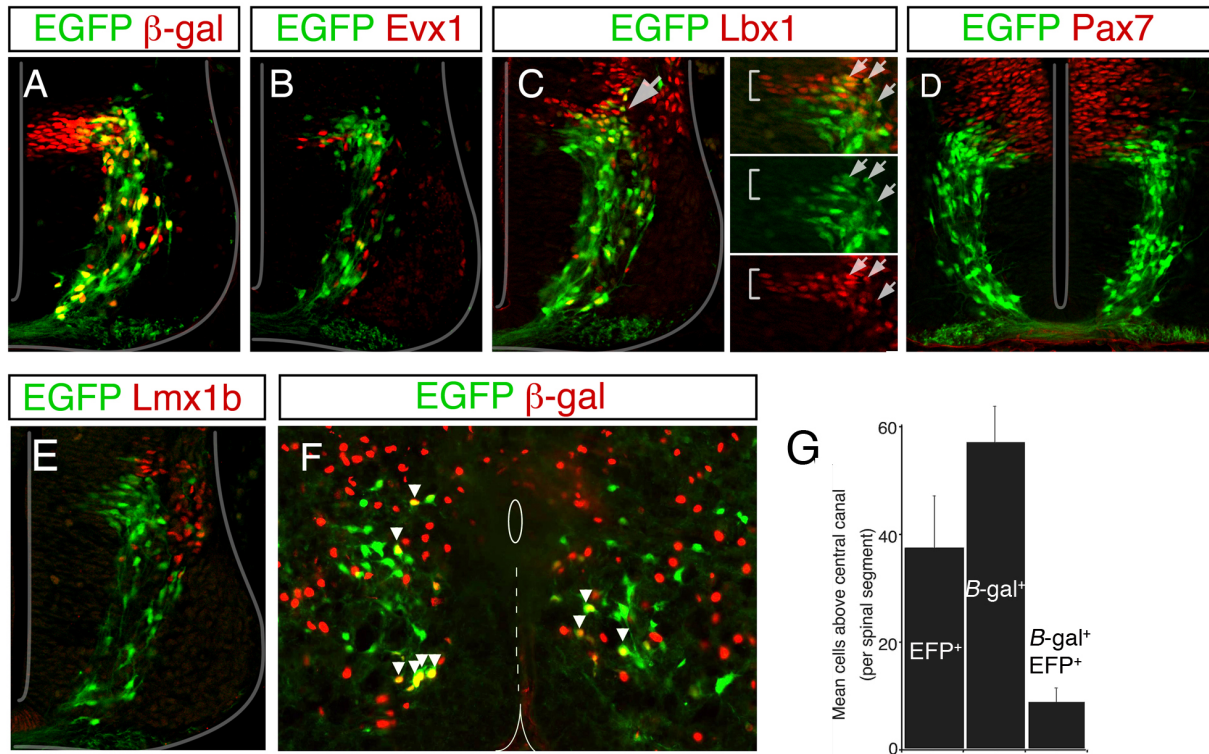


Figure 3-1. Transcriptional profile of labeled neurons in Dbx1Cre;Rosa26EGFP mouse.

(A and B). Coronal section of E11.5 neural tube from Dbx1Cre;Rosa26EGFP;Dbx1LacZ mouse illustrate that EGFP (green) is co-expressed in only a portion of β -gal⁺ cells (i.e. V0 cells - red cells panel A) and is not co-expressed with Evx1 (red cells panel B), a marker of ventral V0 neurons (V0v). (C). Cross section of an E11.5 neural tube stained with antibodies to EGFP (green) and Lbx1 (red- a marker of dorsal interneurons) indicate that some EGFP cells in the Dbx1Cre;Rosa26EGFP are dorsal spinal interneurons. Double labeled cells are indicated by white arrows in the inset panels (D). At E10.5 a portion of the EGFP marked cells (green) derived from Pax7 cells (red), indicating

that they arise from dorsal progenitors. (E). EGFP cells (green) are located ventral to neurons expressing *Lmx1b* (red), a marker of the dI5 interneuronal population. (F). A coronal section from a postnatal *Dbx1Cre;Rosa26EGFP;Dbx1LacZ* mouse in which dI6 cells express EGFP alone (green), V0D cells express EFP and β -gal (red and green i.e. yellow, marked by white arrowheads) and V0v cells express β -gal only (red). (G). Cell counts indicate that in the *Dbx1CreRosa26EFP;Dbx1LacZ* mouse the majority of cells expressing reporter protein located above the central canal are dI6 cells (i.e. EFP only).

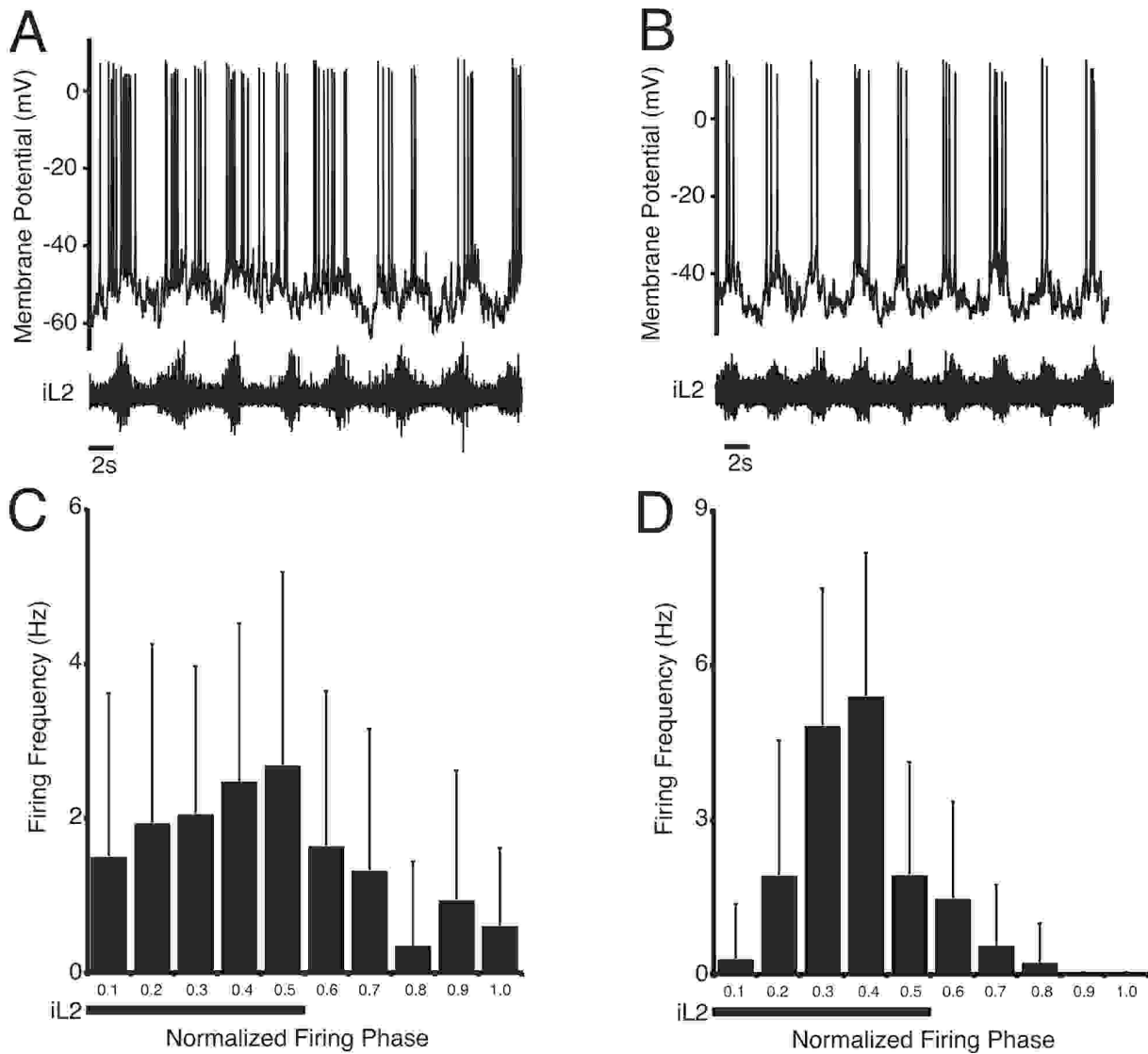


Figure 3-2. Firing patterns of oscillatory dl6 neurons during fictive locomotion.

A and B. Typical activity pattern of loosely coupled (LC; panel A) and tightly coupled (TC; panel B) dl6 neurons during fictive locomotion induced by bath application of 5-HT and NMDA. C and D. Histograms of the instantaneous firing frequency within one normalized step cycle for the LC and TC dl6 neurons shown in panels A and B. Bins 1-5 represent the period of local ventral root activity (iL2) and bins 6-10 representing the inactive phase (i.e. the inter-burst interval).

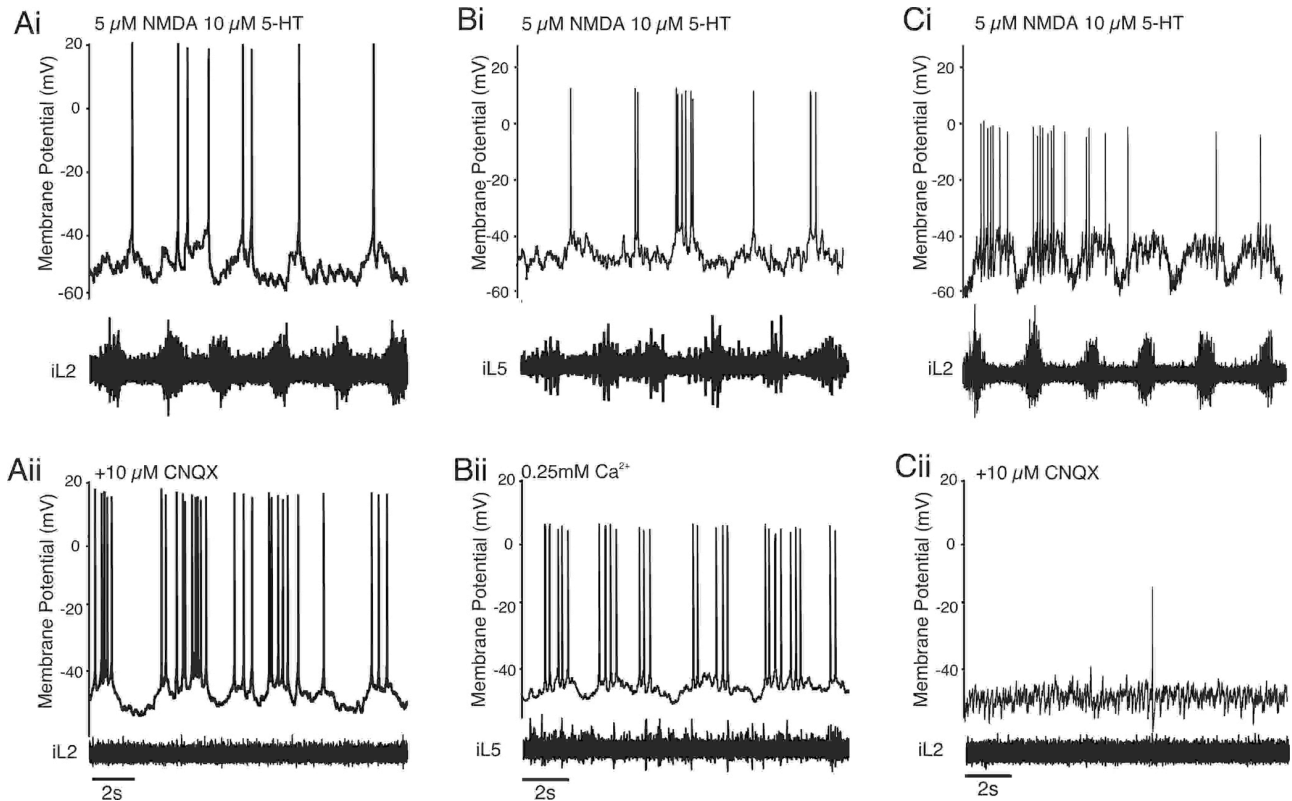


Figure 3-3. LC, but not TC, di6 neurons oscillate intrinsically.

A. Oscillations in a LC di6 neuron during fictive locomotion evoked by bath application of 5-HT and NMDA (**Ai**) persist following synaptic isolation by blockade of all fast non-NMDA glutamatergic synaptic transmission with 10 μ M CNQX (**Aii**). **B.** A similar effect is seen in another LC di6 cell (**Bi**) following synaptic isolation by application of a low calcium (0.25 mM) aCSF solution (**Bii**). Note that, in both cases, fictive locomotor activity is abolished in the ventral root following synaptic isolation (**Aii**, **Bii**). **C.** When an oscillatory TC di6 cell (**Ci**) is synaptically isolated with 10 μ M CNQX, rhythmicity is abolished in both the neuron as well as the ventral root (**Cii**) indicating that these cells are not intrinsic oscillators.

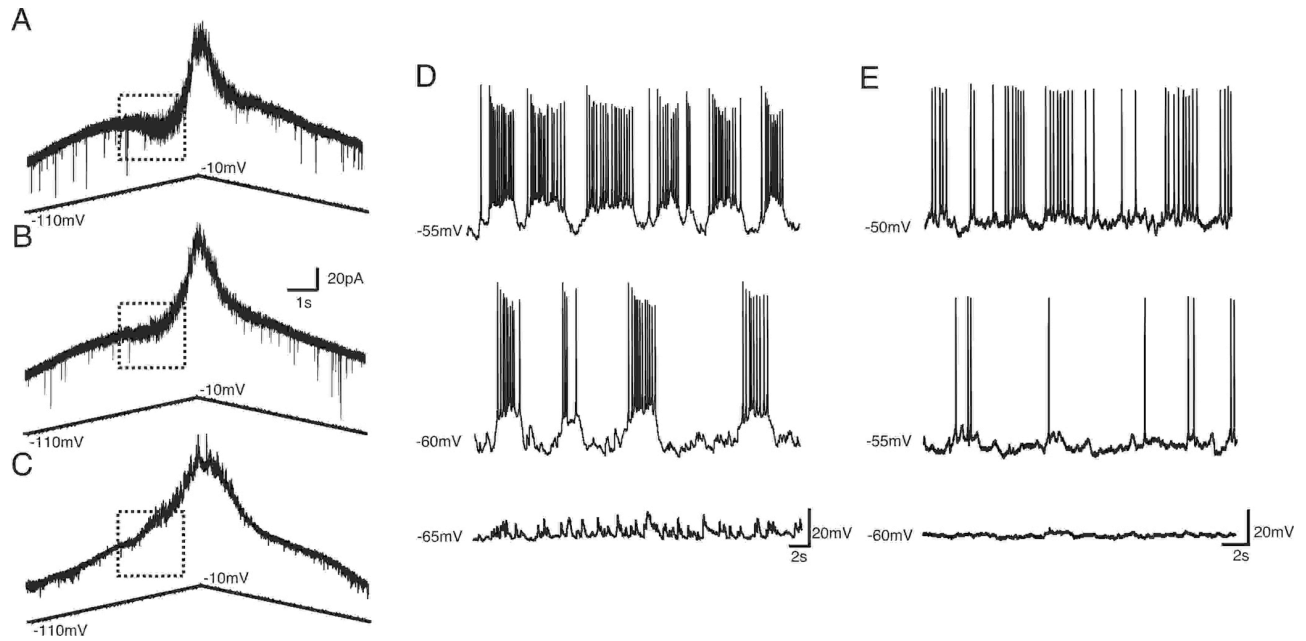


Figure 3-4. LC, but not TC dl6 neurons possess non-linear membrane properties.

A. Triangular voltage ramp reveals a persistent inward current (PIC) in LC dl6 neuron (indicated by region of negative slope conductance within dashed box). **B.** Bath application of riluzole (5 μM) inhibits the PIC in the same neuron, indicating that persistent sodium currents are the main source of the PIC. **C.** TC dl6 neurons respond linearly to the same triangular voltage ramp, no PIC is evident. **D-E.** Following synaptic isolation with 10 μM CNQX (**D**) and low calcium (0.25 mM) aCSF solution (**E**), oscillation frequency in two LC dl6 neurons increases in response to depolarization of the membrane potential at which the cell is held.

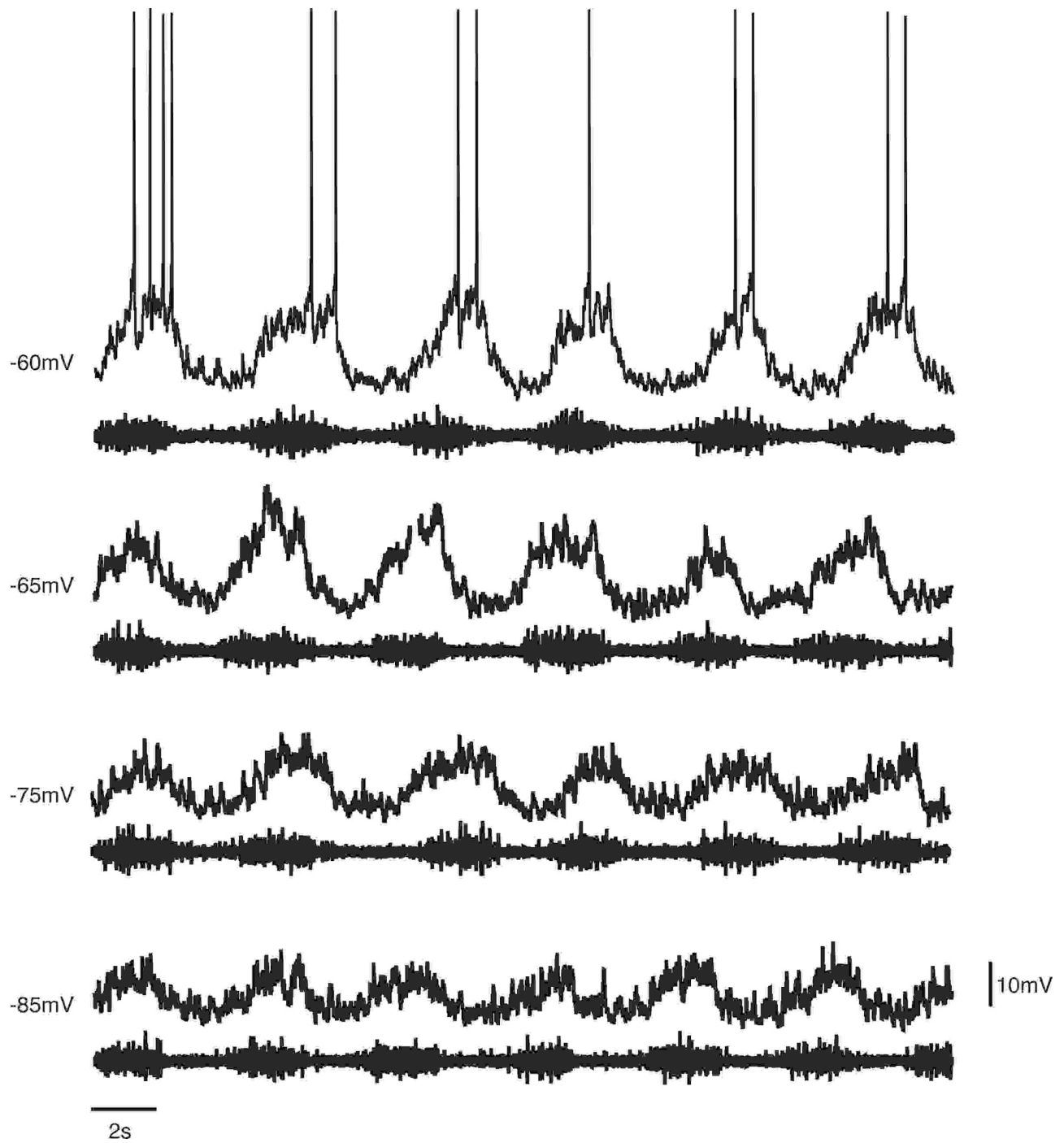


Figure 3-5. Oscillations in TC dI6 neurons are voltage insensitive.

Current clamp recording from a TC dI6 neuron during fictive locomotion in which the membrane potential is varied through intracellular current injection. At all holding potentials the cells bursts together with the local ventral root.

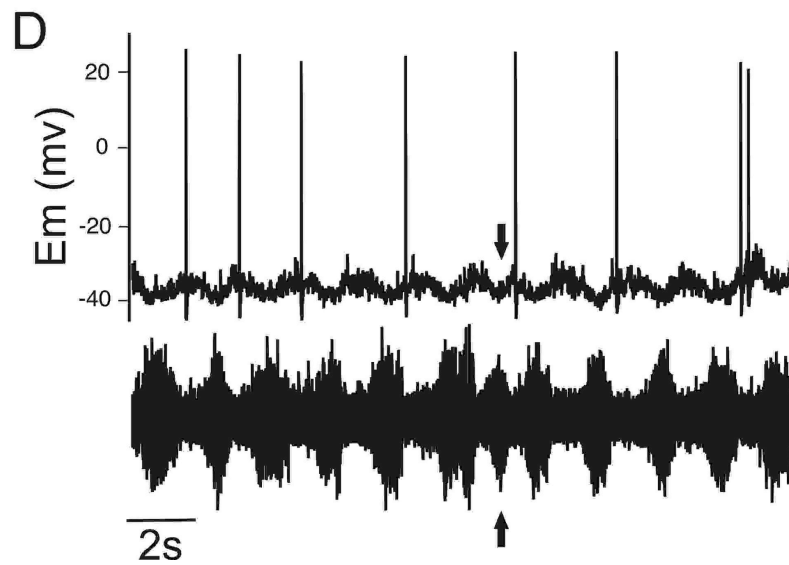
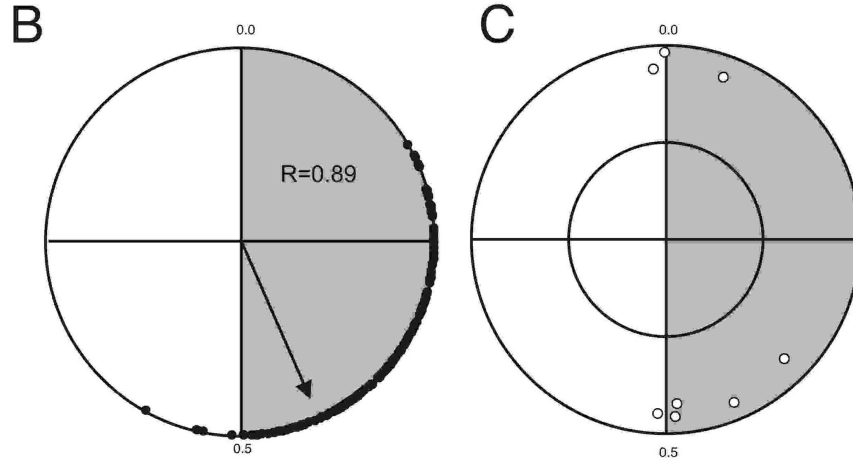
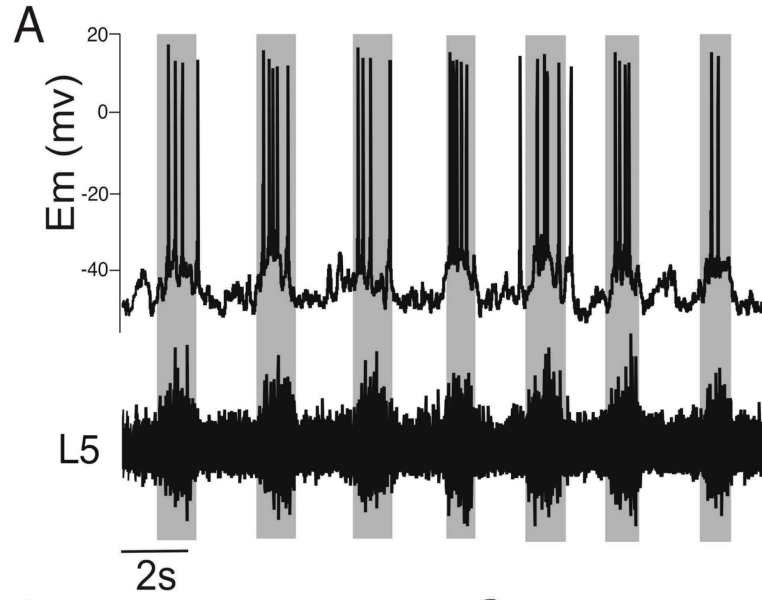


Figure 3-6. TC dI6 neurons receive highly rhythmic drive potentials.

A. Current clamp recording of an oscillatory TC dI6 interneuron that bursts in phase with the ventral root (iL5). **B.** Polar plot for the neuron is shown in panel A compares the onset of ventral root ENG activity and locomotor drive potential (LDP) onset and demonstrates that they are out of phase. **C.** Group polar plot for all TC dI6 neurons (white circles). **D.** Example of an “irregularity” seen in both TC dI6 neuron and ENG activity. During “normal” fictive locomotion neuron bursts out of phase with activity in local ventral root. When an additional small burst occurs in the ventral root (black arrow in lower panel), it is accompanied by a brief hyperpolarization in membrane potential of TC cell (black arrow in upper panel).

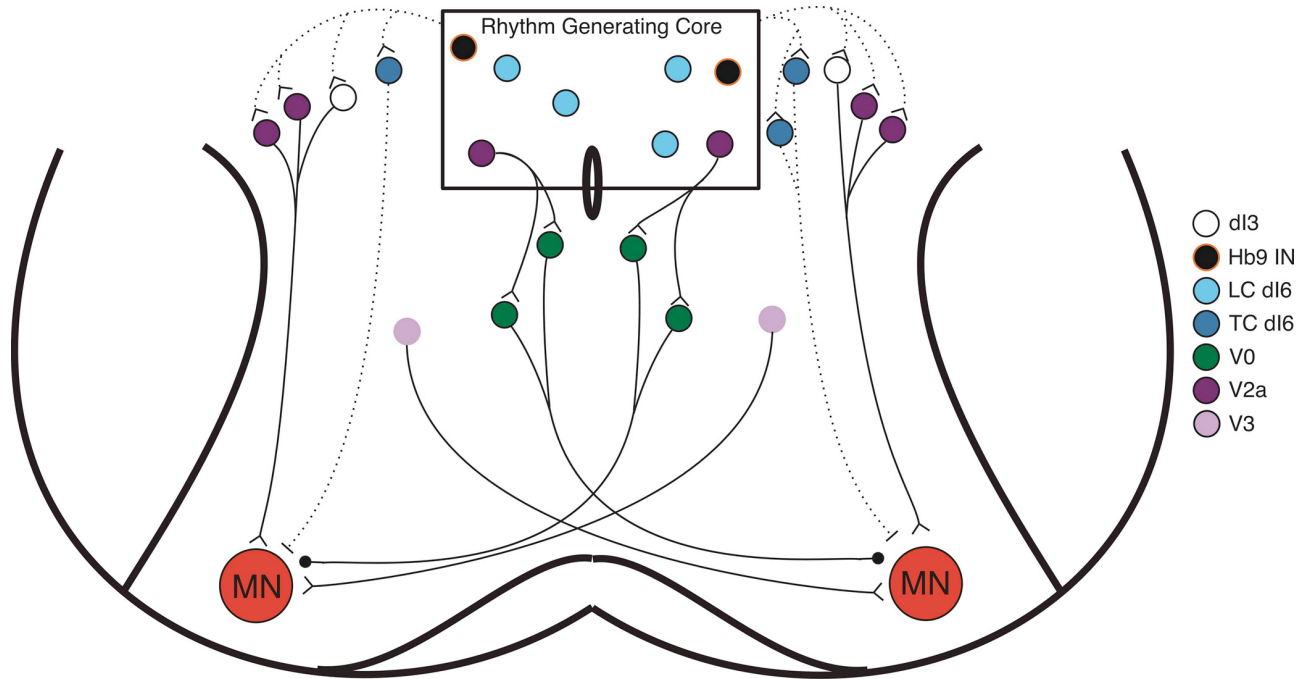


Figure 3-7. Postulated organization of locomotor CPG.

V2a, Hb9 and LC dl6 interneurons are postulated to comprise the rhythm-generating core of the locomotor CPG and receive descending input from brainstem centers known to initiate rhythmic locomotor activity in the spinal cord. We propose that these cells provide input onto the pattern forming layer which includes dI3, V2a, V0, and TC dl6 cells. Members of the pattern forming layer make direct connections onto motoneurons. Documented synaptic connectivity indicated

Chapter 4 -
Discussion and general conclusions

The experiments that comprise this thesis were designed to provide a better understanding of the structure and function of the locomotor CPG. I was able to develop a novel *in-vitro* spinal cord preparation that allows for neurons located deep within the CNS to be investigated while leaving the locomotor network functionally intact. I then used this preparation to study a previously uncharacterized, genetically-defined population of interneurons (dI6 interneurons) and demonstrate that they are an electrophysiologically diverse group of cells that may contribute to the generation of the basic locomotor rhythm. In this section I will discuss the significance as well as the limitations of this work and also comment on future experiments which should be performed to build on the results described within.

4.1 Development of a novel in-vitro preparation

In order to take full advantage of the powerful molecular tools that have recently been developed to study the structure and function of the locomotor CPG, the anatomical and electrophysiological experimental protocols that have historically been used to study this neural circuit require refinement. The necessity and benefit of the preparation described within this thesis, in which labeled neurons located close to the central canal can be targeted for whole cell recording while the locomotor CPG remains intact, is illustrated by its recent use by other groups studying the the locomotor CPG (Dougherty and Kiehn, 2010; Zhong et al. 2010; Antri et al. 2011). Initial characterization of genetically defined neuronal populations in the spinal cord relied on electrophysiological recordings from fluorescently labeled neurons in either the spinal cord slice (Wilson et al., 2005; Zhang et al. 2008) or midline hemisected preparation (Hinckley et al., 2004). While these experiments revealed basic information about certain populations, they provided little

information about the manner in which these neurons behaved in a functional network. Neurons that are physically isolated from the rest of a network (such as in a spinal cord slice) likely behave much differently than those that are embedded within a functional CPG, in which they receive a complex pattern of synaptic inputs from other elements of the neural circuit. The use of the midline hemisected preparation is a slight improvement over the spinal cord slice preparation, as connections to all ipsilateral elements of the CPG are maintained. However, inputs from all commissural connections are lost in this preparation, and as such, the speed of locomotion is drastically slowed (Hinckley et al., 2004). In contrast, using the preparation we developed, both ipsilateral and commissural connections remain intact and there is no significant slowing of the burst period or cycle duration.

While the *in vitro* preparation described here is a powerful tool for the study of neurons at the level of (or dorsal to) the central canal, it is not appropriate for the study of neurons located deeper in the ventral spinal cord (Nishimaru et al., 2006) since extension of the notch below the central canal abolishes fictive locomotor activity (Kjaerulff and Kiehn, 1996; Antri et al., 2011). Given that whole cell recordings from fluorescently labelled neurons is limited to 30-50 μm below the surface (J.Dyck, unpublished observation), the best approach to access more ventrally located neurons would involve calcium imaging. With the use of a two-photon microscope, it is possible to simultaneously visualize genetically encoded fluorescent proteins and calcium indicators (Wilson et al., 2007), and such techniques allow for the activity of cells up to 200 μm below the surface to be monitored (Kwan et al., 2009). In conjunction with the preparation we developed here, the use of such calcium imaging techniques will allow for more ventrally located interneuron populations to be investigated.

4.2 dI6 neurons contribute to rhythm generation in the locomotor CPG.

The preparation described above enabled us to be the first to electrophysiologically characterize the dI6 interneuronal population. There are several reasons why these cells had not been previously investigated. First, they originate in the dorsal neural tube and, despite the fact that they migrate ventrally to lamina VII/VIII of the postnatal spinal cord, they are not generally considered to be a population of ventral cells. Second, a unique transcription factor to this entire population has yet to be identified. In the experiments here, we take advantage of a transgenic mouse model in which we found the dI6 cells to be labeled with GFP. Our electrophysiological characterization of this population indicates that many dI6 neurons possess properties consistent with a role in rhythm generation, and as such indicates that dI6 neurons should be considered alongside other potential rhythm generating populations of neurons.

Why is it significant that dI6 neurons are candidates to generate the locomotor rhythm? It is becoming clear that no single genetically defined neuronal population is capable of acting as the sole rhythm generator in the locomotor CPG. As such, it is a distinct possibility that rhythm generation is a shared function amongst numerous populations. Along these lines, a logical next step would be to identify all populations that possess rhythm generating properties and test the hypothesis that these cells work together to generate the locomotor rhythm. Currently, there is evidence to suggest that subsets of the V2a, Hb9 and now dI6 neurons contain the required intrinsic membrane properties. If rhythm generation is indeed a shared role, it will be critical to understand how the rhythm generating neurons belonging to each of these genetically-defined populations are interconnected and how they work together to produce the locomotor rhythm. Furthermore, by

identifying the genetic identity of all rhythm generating neurons, it would then be possible to look for genetic markers which may be common to these neurons at some developmental time point.

4.3 Limitations of This Work

The work presented in this thesis indicates that dI6 neurons play a role in initiating the locomotor rhythm in the neonatal rodent spinal cord. However, precautions must be made when interpreting these results as there are limitations to the experiments performed here. One point that cannot be overlooked is that this work focuses on only a portion of the dI6 population. Recordings were limited to those cells located dorsal to the central canal in the rostral lumbar cord, as this was the only region that could be accessed without disrupting the locomotor CPG. Staining in Figure 3-1 of this thesis shows that dI6 cells are also distributed in ventral regions of the spinal cord, below the central canal. As such, we recognize that our data represents the activity of only a fraction of the dI6 population as a whole. However these experiments provide key insight into the role of dI6 interneurons within a region which has been shown to house critical components of the locomotor CPG.

Furthermore, we can not conclusively claim that LC neurons did not receive rhythmic inputs when synaptically isolated with CNQX. In Figure 3-4D, oscillations in a LC dI6 neuron are abolished when the cell is hyperpolarized to -65mV. However, in this example, the cell is still receiving synaptic inputs, as is evident by the barrage of excitatory post synaptic potentials (EPSPs). To address the possibility that rhythmic excitatory inputs to LC dI6 neurons were not blocked with CNQX, we used a low calcium aCSF solution as an alternative means to synaptically isolate these neurons. Under these conditions, EPSPs were no longer observed when the cell was

hyperpolarized, yet pacemaker-like properties were still seen in these LC dI6 neurons. The similarity of results seen under these two conditions (i.e. CNQX and low calcium aCSF) suggests that rhythmic excitatory input to these cells have been blocked. Ideally, TTX would have been used to block synaptic transmission in the spinal cord. However, given that others (Tazerart et al., 2008; Ziskind-Conhaim et al., 2008) have shown that sodium-dependent PICs are important for pacemaker-like properties in the mouse spinal cord, we would not be able to differentiate the effects of TTX on synaptically isolating the neuron versus abolishing rhythmogenic properties.

An additional limitation of these experiments is the degree to which pacemaker-like properties are expressed in LC dI6 neurons. In Chapter 3 of this thesis, examples of voltage dependent bursting are shown for both the CNQX and low calcium conditions (Figure 3-3). However, clear changes in the frequency of oscillations through current injection were difficult to produce in these neurons. We observed voltage dependent firing frequency in ~55% (10/18) of dI6 neurons tested. However, in only 4 LC dI6 neurons could stable oscillations be produced over a wide range of membrane potentials (Figure 4-1). In the remaining 6 LC dI6 neurons, oscillations which were voltage sensitive were still observed, however, these oscillations occurred over a very narrow voltage range. These neurons were silent when hyperpolarized, oscillated rhythmically with depolarizing current injection, but with further current injection the oscillations become erratic and difficult to quantify. It is unclear why only a fraction of LC dI6 neurons displayed pacemaker-like properties. One possibility is that the intracellular contents of the neurons have been washed out of the cell and into the whole cell electrode. In support of such a possibility, it has been shown previously that the contents of the intracellular solution used for whole-cell recording influences the fraction of neurons which display pacemaker-like properties (Lorier et al., 2008). Alternatively,

oscillations in these cells could be the result of activity from a very small network of cells, rather than pacemaker-like properties in a single neuron. As such, current injection into a single neuron may not always be sufficient to change the frequency of oscillations in this network.

It is also unclear how activity from rhythm generating LC dI6 neurons is transformed into the rhythmic locomotor output. The activity pattern seen in LC dI6 neurons is often more irregular and less rhythmic than that seen in both the TC dI6 neurons and ventral root bursting. If dI6 neurons do indeed play a role in rhythm generation, there must be additional populations that contribute to transforming the activity pattern of these neurons. One possibility is that an intermediate population of interneurons exists between the rhythm generating LC dI6 neurons and pre-motor interneuron populations. This intermediate population could act as a high threshold filter to ensure that only highly rhythmic periods of activity are passed on from the rhythm generating core to the rest of the locomotor CPG. Alternatively, the activity pattern seen in dI6 neurons could be an experimentally-induced artefact resulting from the whole cell recording. Ideally, alternative methods (such as calcium imaging) would be used to investigate the activity pattern of this population without disturbing the intracellular milieu of the neuron.

Lastly, the possibility that these neurons are not responsible for rhythm generation can not be ignored. Much of this thesis has centred around the assumption that pacemaker neurons are necessary for generating rhythmic activity in the spinal cord. However, work in the respiratory CPG indicates that, although they may assist, pacemaker neurons are not necessary for rhythm generation (Pace and Del Negro, 2008). If a similar situation exists in the spinal cord, LC dI6 neurons might only be involved in assisting in rhythm generation rather than playing a critical role in initiating it. Indeed, such a role has recently been suggested for Hb9 interneurons (which contain many

pacemaker-like properties) based on the observation that activity in these neurons lags behind activity in the local ventral root (Kwan et al., 2009). One piece of evidence in favour of a role in rhythm generation for dI6 neurons comes from preliminary results from knockout studies of these neurons in-vivo (Dr. Olivier Britz, unpublished data). In these experiments, dI6 (as well as some V0) neurons are ablated in the adult mouse, leading to complete paralyzation of the hindlimbs in these animals. Such experiments support the role of dI6 neurons in initiating locomotor activity in the spinal cord.

4.4 Future Directions

The work presented in this thesis has generated many potential research questions regarding the function of the dI6 population. A critical next step is to identify transcription factors that are unique to the dI6 interneuronal population, as has been done for the other genetically defined populations. This will allow for the development of a Cre recombinase transgenic mouse line, which will open to this population to investigation using the many elaborate genetic tools recently developed. These include fluorescently tagging the entire dI6 population with a single reporter protein (i.e. GFP), driving the expression of the allatostatin receptor in these cells to selectively silence them (Tan et al., 2006), or utilizing genetically based tracing systems to identify their synaptic targets (Wall et al., 2010).

In my opinion, the most critical experiments that need to be performed involve selectively silencing or ablating these neurons, which would allow the primary function of these cells during fictive locomotion to be determined. In all instances in which a genetically defined population (V0-V3) has been silenced or removed (Lanuza et al. 2004; Gosgnach et al., 2006; Crone et al., 2008;

Zhang et al. 2008), the basic locomotor rhythm has persisted. So far, dI6 neurons are the only ventral population yet to be silenced or ablated. Until such experiments are performed, it will remain uncertain whether dI6 neurons are solely responsible for driving the locomotor rhythm. If rhythmic activity is abolished when dI6 neurons are silenced, it would provide compelling evidence that these cells play a major role in generating the locomotor rhythm. Alternatively, if rhythmic activity persists in the absence of dI6 neurons, a strong case can be made that rhythm generation is a shared function amongst many populations, possibly through emergent network properties.

With the development of optical stimulation and calcium imaging, it will be particularly interesting to identify the synaptic inputs onto the dI6 cells. Given their proposed role in rhythm generation, one would expect these cells to receive inputs from descending tracts from the brainstem involved in the initiation of locomotion, such as the reticulospinal tracts. Experiments in the Gosgnach laboratory are currently underway to address this question. Based on current models of the locomotor CPG, one would expect rhythmogenic dI6 neurons to make contacts to (as well as receive inputs from) other rhythmogenic neurons. Preliminary data from our laboratory indicates that such connectivity between dI6 neurons does exist. The discovery of inputs from rhythmogenic neurons belonging to other genetically-defined populations would strengthen the argument that several populations are involved in rhythm generation.

The data in this thesis suggests that sodium-dependent PICs may be responsible for the intrinsic bursting properties of dI6 neurons. It is possible that the role of PICs in rhythm generation declines during development as alternative mechanisms emerge. This has been shown to be true for pacemaker neurons in the respiratory CPG where riluzole-sensitive neurons have been shown to be unnecessary for rhythm generation (Pace et al., 2007). Instead, the emergence of synaptically

activated latent conductances appear to be sufficient to sustain a network driven respiratory CPG (Pace and Del Negro, 2008). Testing whether a similar situation could exist in the locomotor CPG with the current pharmacological tools is challenging as the locomotor CPG is distributed over a much greater region than the respiratory CPG. As a consequence, it is difficult to block persistent sodium currents in spinal interneurons without simultaneously blocking these currents in motoneurons and disrupting locomotor output.

Further experiments should also aim to determine if currents in addition to the sodium-dependent PICs play a role in rhythm generation in dI6 neurons. Preliminary results indicate that the hyperpolarization-induced (I_h) current is present in LC dI6 neurons but not in TC dI6 neurons (Figure 4-2). It is possible that I_h current could assist in generating intrinsic oscillations in these dI6 neurons. However, recent studies have found no correlation between the rhythmicity of spinal interneurons and the presence of I_h currents (Butt et al., 2002). Therefore, the role of this current in rhythm generation remains undetermined. Alternatively, currents such as the I_{CAN} current could also be involved in rhythm generation, as was recently described in the respiratory CPG (Pace and Del Negro, 2008).

It is quite possible that the method of inducing fictive locomotion can influence the mechanisms of rhythm generation *in vitro*. Currently, the most commonly used method of inducing fictive locomotion in the *in vitro* spinal cord preparation is through bath application of neuroactive substances (i.e. 5HT and NMDA), as was used in the studies of this thesis. However, alternative means such as electrical stimulation of the brainstem (Liu and Jordan, 2005), dorsal roots (Whelan et al., 2000), or ventral roots (Mentis et al., 2005) have been shown to elicit bouts of locomotor activity. Fictive locomotion induced by electrical stimulation (particularly brainstem stimulation) is

generally seen as a more physiological means to elicit fictive locomotion, as pharmacological induced locomotion non-selectively activates all neurons in the spinal cord. Recently, the activity of one genetically-defined population (Hb9 neurons) has been shown to respond differently depending to the method used to elicit locomotion (Kwan et al. 2009). These authors found that Hb9 neurons were highly rhythmic with drug-induced locomotion yet non-rhythmic with electrically-induced locomotion. It would thus be interesting to investigate the activity of dI6 interneurons in response to locomotor activity evoked by various forms of brainstem, or peripheral nerve stimulation and determine if the intrinsic properties seen here, persist.

4.5 Where do dI6 neurons fit into the current model of the locomotor CPG?

Conceptual models of the locomotor CPG were reviewed in the introductory chapter of this thesis. Among these were the two-layer model, which proposes the separation of rhythm generating and pattern forming layers. Whole cell recordings from dI6 neurons indicate that many of these cells possess rhythmogenic properties, and as such, potentially constitute part of the rhythm generating core in the two-layer model. Furthermore, we occasionally observed instances where LC dI6 neurons respond to irregularities in the fictive locomotor pattern (Figure 4-3, see also Chapter 3-6). Due to the fact that such irregularities occur very infrequently while recording from a LC dI6 neuron, such results are still quite preliminary. Nonetheless, such observations support the notion that LC dI6 neurons constitute part of the rhythm generating core. Our data also indicates that another subset of highly rhythmic dI6 neurons (i.e. TC dI6) comprise part of the pattern forming layer. Unfortunately, no examples of deletions have been observed while recording from a TC dI6 neuron.

Recent results suggest that several genetically defined populations have intrinsic properties of rhythm generating cells (Dougherty and Kiehn, 2010; Hinkley et al., 2005) and several have properties of pattern forming interneurons (Stepain et al., 2010). We provide evidence that dI6 neurons contribute to rhythm generation, but postulate that this function is a shared role amongst several populations. Based on the locations of cells shown to possess rhythm generating properties, it is likely that anatomical position in the postnatal spinal cord (as well as genetic origin) is a key factor in determining the functional role of a neuron. Here we propose a model of the locomotor CPG in which functional populations of neurons tend to aggregate together and are comprised of neurons with diverse genetic origins (Figure 4-4).

According to this model, interneurons that make up the locomotor CPG can be classified into one of four groups; rhythm generating interneurons (RG), pre-motor interneurons (PMI), flexor-extensor interneurons (FE), and commissural interneurons (CIN). As mentioned previously, rhythm generating neurons have been shown to be localized to lamina VII and VIII, an area in which V0, V2a, V3, dI6 and Hb9 neurons reside. Interneurons belonging to the V2a, Hb9, and dI6 populations have all been shown to fire rhythmically during fictive locomotion and possess non-linear membrane properties (Dougherty and Kiehn, 2010, Ziskind-Conhaim et al., 2008, this thesis), while these characteristics have not been fully addressed for both the V0 and V3 populations. These properties, in conjunction with their anatomical position in the spinal cord, make these cells likely candidates to contribute to rhythm generation. In regards to PMI, anatomical tracing techniques were used to determine that V2a (Stepain et al., 2010) and V3 (Zhang et al., 2008) interneurons make direct contacts onto motoneurons, and we provide evidence here that dI6 neurons behave in a manner consistent with this role. The possibility exists, however, that additional populations also

act as PMI. Studies are currently underway to identify the populations of interneurons which control ipsilateral flexion-extension (i.e. FE interneurons). Prime candidates potentially responsible for this role include the V2b and V1 interneuron populations, as both are located outside key rhythmogenic regions, are exclusively inhibitory, and project axons ipsilaterally (Lundfald et al., 2007; Sapir et al., 2004). In contrast to F-E interneurons, the identify of CINs is fairly well established as being comprised of the inhibitory V0 population (Pierani et al., 2001) and the excitatory V3 population (Zhang et al., 2009).

There are obviously additional classes of interneuron which are not part of the locomotor CPG, but instead play a key role in modulation of this rhythm (such as Renshaw cells, and 1a inhibitory interneurons) that have not been included in this model. While there remain many aspects of this model that require further investigation for confirmation, this is a first attempt to combine classical electrophysiological data with more recent genetic-based experiments. This model holds that no specific function during locomotion is the result of a single genetically-defined interneuron population, and that each genetically based population likely contributes to multiple aspects of locomotion.

4.6 References:

Antri M, Mellen N, Cazalet J (2011) Functional organization of locomotor interneurons in the ventral lumbar spinal cord of the newborn rat. *PLoS One*. 6:e20529

Bracci E, Ballerini L, Nistri A (1996) Spontaneous rhythmic bursts induced by pharmacological block of inhibition in lumbar motoneurons of the neonatal rat spinal cord. *J Neurophysiol* 75:640–7.

Butt S, Harriss-Warrick R, Kiehn O (2002) Firing properties of identified interneuron populations in the mammalian hindlimb central pattern generator. *J Neurosci*. 15:9961-71.

Crone SA, Quinlan KA, Zagoraiou L, Droho S, Restrepo CE, Lundfald L, Endo T, Setlak J, Jessell TM, Kiehn O, Sharma K (2008) Genetic ablation of V2a ipsilateral interneurons disrupts left-right locomotor coordination in mammalian spinal cord. *Neuron* 60:70–83.

Dougherty K, Kiehn O (2010) Firing and cellular properties of V2a interneurons in the rodent spinal cord. *J Neurosci* 30:24 –37.

Hinckley CA, Hartley R, Wu L, Todd A, Ziskind-Conhaim L (2005) Locomotor-like rhythms in a genetically distinct cluster of interneurons in the mammalian spinal cord. *J. Neurophysiol.* 93:1439–49

Goulding M (2009) Circuits controlling vertebrate locomotion: moving in a new direction. *Nat Rev Neurosci* 10:507-518

Gosgnach S, Lanuza GM, Butt SJ, Saueressig H, Zhang Y, Velasquez T, Riethmacher D, Callaway EM, Kiehn O, Goulding M (2006) V1 spinal neurons regulate the speed of vertebrate locomotor outputs. *Nature* 440:215-219.

Kjaerulff O, Kiehn O (1996) Distribution of networks generating and coordinating locomotor activity in the neonatal rat spinal cord in vitro: a lesion study. *J. Neurosci.* 16:5777–94

Kwan AC, Dietz SB, Webb WW, Harris-Warrick RM (2009) Activity of Hb9 interneurons during fictive locomotion in mouse spinal cord. *J Neurosci* 29:11601–11613.

Lanuza GM, Gosgnach S, Pierani A, Jessell TM, Goulding M (2004) Genetic identification of spinal interneurons that coordinate left-right locomotor activity necessary for walking movements. *Neuron* 42:375–386.

Liu J, Jordan LM. (2005) Stimulation of the parapyramidal region of the neonatal rat brainstem produces locomotor-like activity involving spinal 5-HT₇ and 5-HT_{2A} receptors. *J. Neurophysiol.* 94:1392–404

Lorier AR, Lipski J, Housley GD, Greer J, and Funk GD (2008). ATP sensitivity of preBötzinger complex neurones in neonatal rat in vitro: mechanism underlying a P2 receptor-mediated increase in inspiratory frequency. *J Physiol.* 586:1429-46.

Lundfald L, Restrepo CE, Butt SJ, Peng CY, Droho S, Endo T, Zeilhofer HU, Sharma K, Kiehn O (2007) Phenotype of V2-derived interneurons and their relationship to the axon guidance molecule EphA4 in the developing mouse spinal cord. *Eur J Neurosci* 26:2989 –3002.

Mentis G, Alvarez F, Bonnot A, Richards D, Gonzalez-Forero D, Zerda R, O'Donovan MJ (2005) Non- cholinergic excitatory actions of motoneurons in the neonatal mammalian spinal cord. *Proc. Natl. Acad. Sci.*102: 7344–7349

Nishimaru H, Restrepo C, Kiehn O (2006) Activity of Renshaw Cells during Locomotor-Like Rhythmic Activity in the Isolated Spinal Cord of Neonatal Mice. *J Neurosci.* 26:5320-5328

Pace RW, Del Negro CA (2008) AMPA and metabotropic glutamate receptors cooperatively generate inspiratory-like depolarization in mouse respiratory neurons in vitro. *Eur J Neurosci* 28:2434–2442.

Pace, R.W., Mackay, D.D., Feldman, J.L. & Del Negro, C.A. (2007) Role of persistent sodium current in mouse preBotzinger complex neurons and respiratory rhythm generation. *J. Physiol.* 580:485–496.

Pierani A, Moran-Rivard L, Sunshine MJ, Littman DR, Goulding M, Jessell TM (2001) Control of interneuron fate in the developing spinal cord by the progenitor homeodomain protein Dbx1. *Neuron* 29:367–384.

Sapir. Pax6 and Engrailed 1 Regulate Two Distinct Aspects of Renshaw Cell Development. *J Neurosci* (2004) vol. 24 (5) pp. 1255-1264

Stepein A, Tripodi M, Arber S (2010) Monosynaptic rabies virus reveals premotor network organization and synaptic specificity of cholinergic partition cells. *Neuron* 68:456-72.

Tan E, Yamaguchi Y, Horwitz G, Gosgnach S, Lein E, Goulding M, Albright T, Callaway E (2006) Selective and quickly reversible inactivation of mammalian neurons in vivo using the *Drosophila* allatostatin receptor. *Neuron*. 51:157-170.

Tazerart S, Vinay L, Brocard F (2008) The persistent sodium current generates pacemaker activities in the central pattern generator for locomotion and regulates the locomotor rhythm. *J Neurosci* 28:8577– 8589.

Whelan P, Bonnot A, O'Donovan M (2000) Properties of Rhythmic Activity Generated by the Isolated Spinal Cord of the Neonatal Mouse. *J Neurophys.* 84:2821-2833

Wall N, Wickersham I, Cetin A, De La Parra M, Callaway E (2010). Monosynaptic circuit tracing in vivo through Cre-dependent targeting and complementation of modified rabies virus. PNAS. 107:21848-53

Wilson J, Dombeck D, Diaz-Rios M, Harris-Warrick R, Brownstone R (2007) Two-photon calcium imaging of network activity in XFP-expressing neurons in the mouse. J Neurophys 97:3118-25

Wilson JM, Hartley R, Maxwell DJ, Todd AJ, Lieberam I, Kaltschmidt JA, Yoshida Y, Jessell TM, Brownstone RM (2005) Conditional rhythmicity of ventral spinal interneurons defined by expression of the Hb9 homeodomain protein. J Neurosci 25: 5710–5719

Zhang Y, Narayan S, Geiman E, Lanuza GM, Velasquez T, Shanks B, Akay T, Dyck J, Pearson K, Gosgnach S, Fan CM, Goulding M (2008) V3 spinal neurons establish a robust and balanced locomotor rhythm during walking. Neuron 60:84 –96.

Zhong G, Droho S, Crone S, Dietz S, Kwan AC, Webb WW, Sharma K, Harris-Warrick RM (2010) Electrophysiological characterization of the V2a interneurons and their locomotor-related activity in the neonatal mouse spinal cord. J Neurosci 30:170 –182.

Ziskind-conhaim L, Wu L, Wisener EP (2008) Persistent sodium current contributes to induced voltage oscillations in locomotor-related hb9 interneurons in the mouse spinal cord. J Neurophys. 100:2254-64

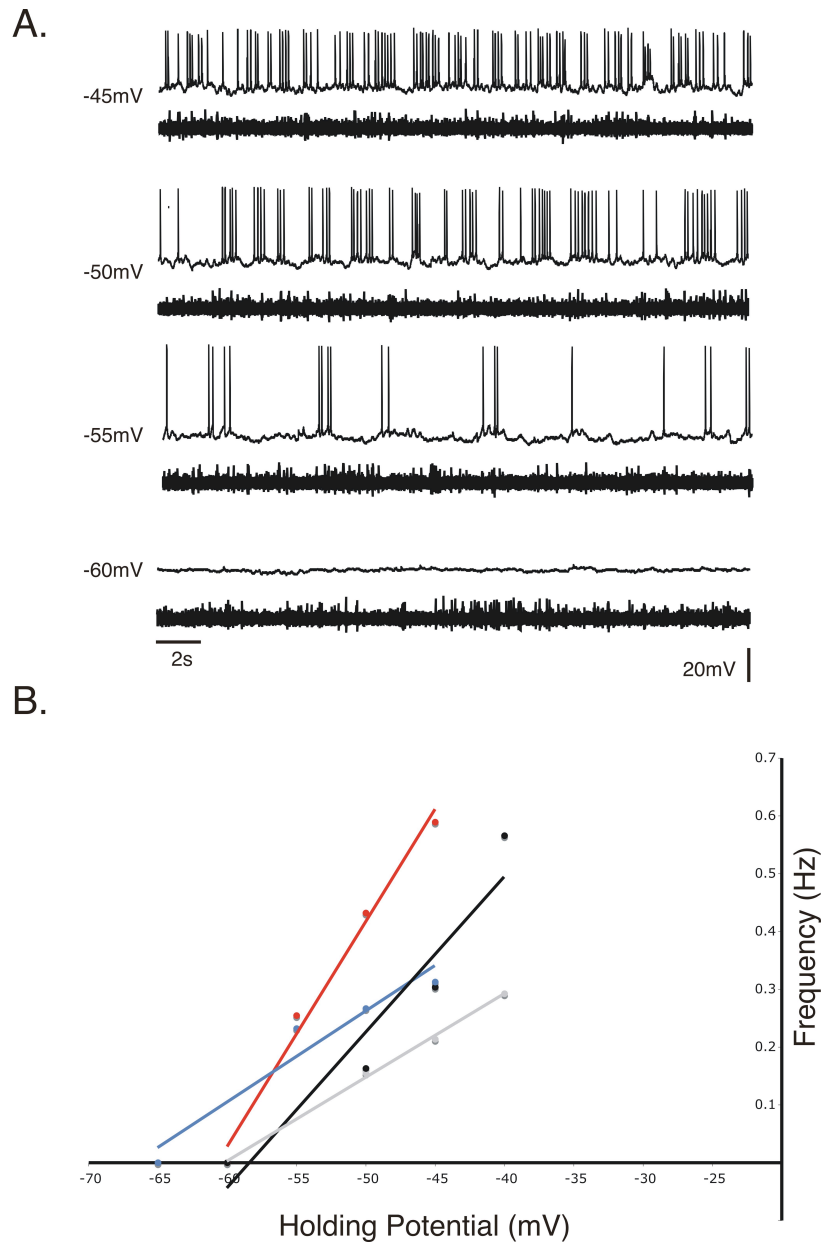


Figure 4-1. LC dI6 neurons display voltage dependent firing frequency activity patterns. A. Traces of a single LC dI6 neuron at different holding potentials when synaptically isolated using a low-calcium aCSF solution. B). Plot of the frequency (Hz) of oscillations versus the holding potential (Vm) for four synaptically isolated LC dI6 neurons.

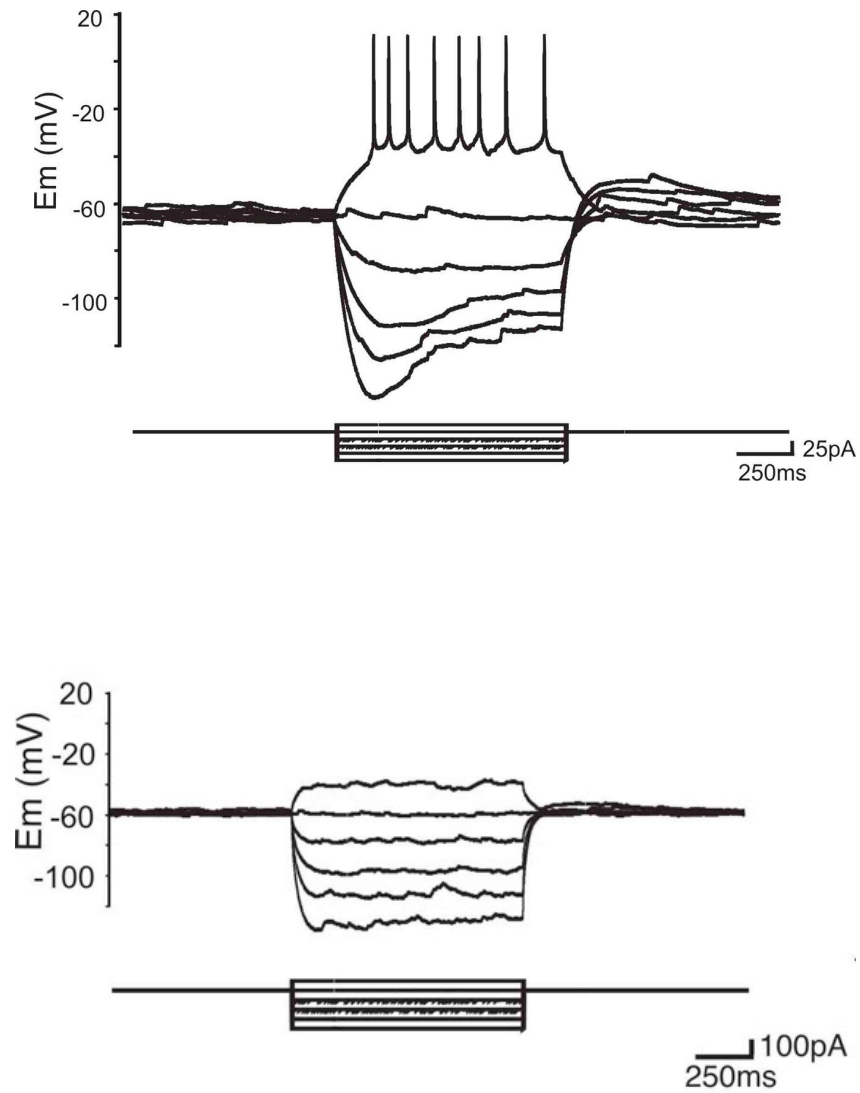


Figure 4-2. LC, but not TC, dI6 neurons display hyperpolarizing induced (I_h) currents. Example of a post-inhibitory rebound and depolarizing sag current in a LC dI6 neuron (top trace), but not in a TC dI6 neuron (bottom trace).

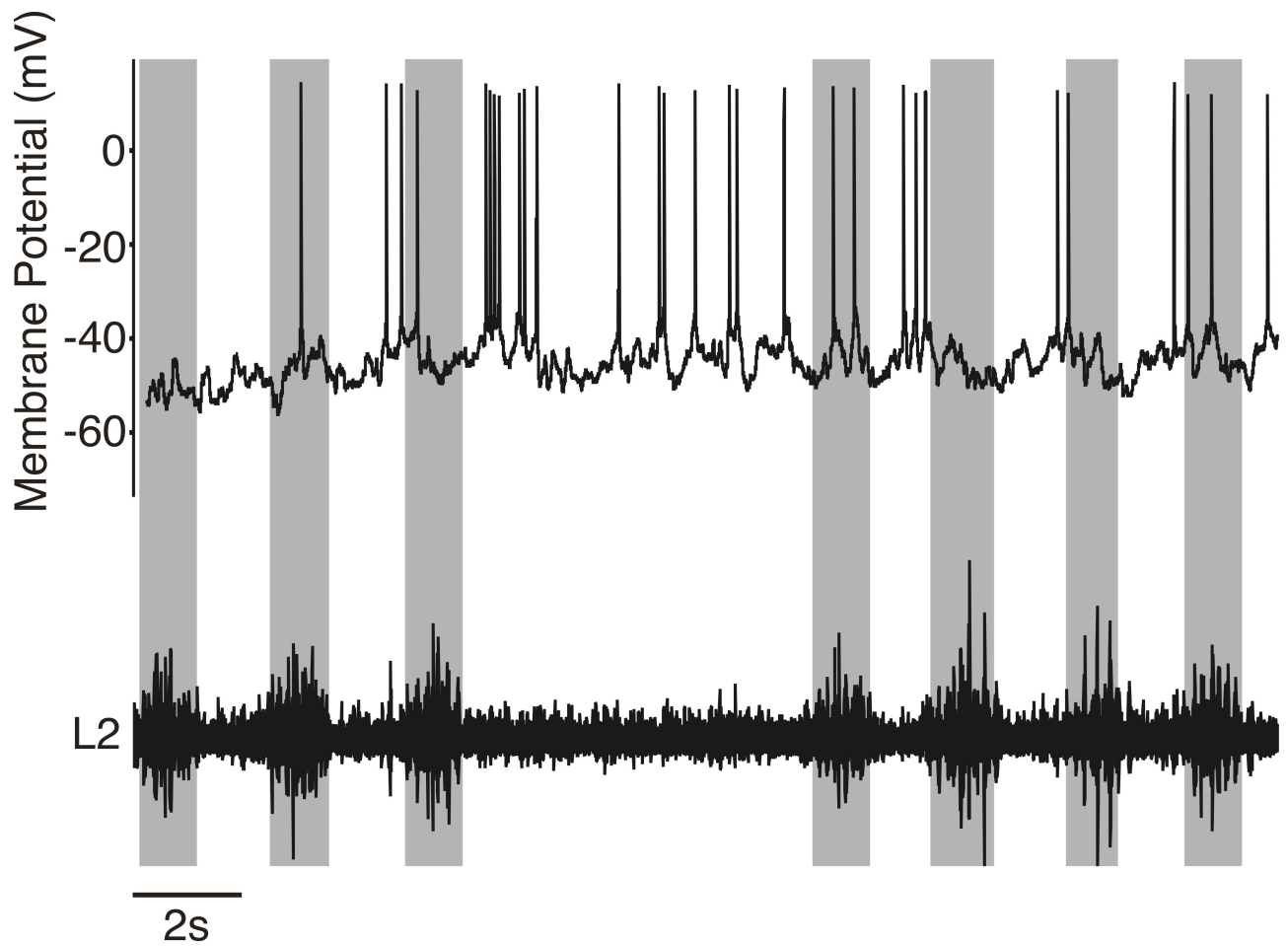


Figure 4-3. Activity pattern of LC dl6 neuron during deletion in fictive locomotion. A rhythmically active LC dl6 neuron (top) continues to oscillate during a resetting deletion in the L2 ventral root (below).

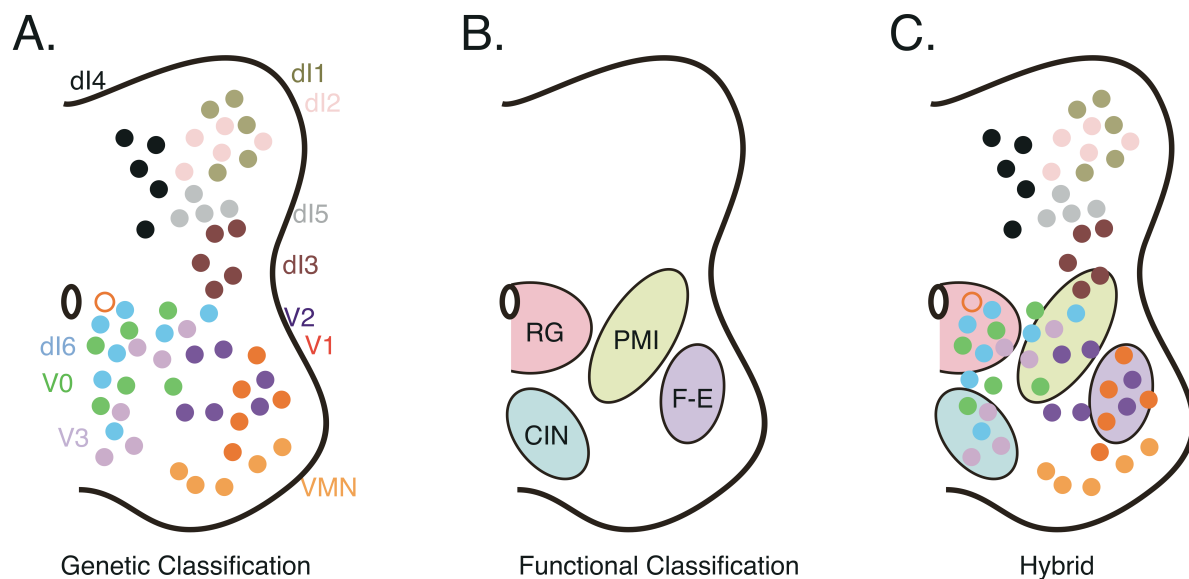


Figure 4-4. Hybrid model of the locomotor CPG. A. Post-natal distribution of genetically defined (dl1 - V3) interneuron populations in the lumbar spinal cord. B. Functional classification of interneurons based on roles in generating the basic locomotor pattern. Neurons are classified as either being rhythm generating (RG), commissural interneurons (CIN), pre-motor interneurons (PMI), or flexor-extensor related (F-E) neurons.